A stable and convergent O-method for general moving hypersurfaces

EINDHOVEN UNIVERSITY OF TECHNOLOGY
Department of Mathematics and Computer Science

CASA-Report 14-21
July 2014

A stable and convergent O-method for general moving hypersurfaces

by

S.F. Nemadjieu

Centre for Analysis, Scientific computing and Applications
Department of Mathematics and Computer Science
Eindhoven University of Technology
P.O. Box 513
5600 MB Eindhoven, The Netherlands
ISSN: 0926-4507

Noname manuscript No.
(will be inserted by the editor)

A stable and convergent O-method for general moving hypersurfaces

Simplice Firmin Nemadjieu

Received: date / Accepted: date

Abstract We present a finite volume method for transport, diffusion and reaction problems on evolving hyper-surfaces. The surface motion is assumed to be given. The numerical scheme is built on a sequence of general polygonal hyper-surfaces approximating the continuous hyper-surface and whose nodes propagate with the actual velocity field. Our approach consists of using a dual strategy to approximate the solution of our partial differential equation (PDE). First we use a suitable interpretation of the flux continuity condition on a dual mesh and a proper minimization strategy to construct an adequate operator dependent piece-wise linear interpolant around nodal points. The interpolant builds from discrete points around nodes a piece-wise linear function whose the piece-wise constant gradient satisfies an appropriate flux continuity condition on the sub-cells induced by the space discretization on the dual mesh. Next we integrate the PDE on cells using the Gauss formula and the gradients of the above introduced functions. The diffusion operators as well as the reaction operators are approximated implicitly while the advection operators are approximated explicitly using the upwind procedure and an adapted min-mode strategy. The obtained semi-implicit scheme is a cell center finite volume which is second order convergent in spacial $\mathbb{L}^2$ norm and first order in spacial $\mathbb{H}^1$ norm. Finally, we provide several examples to support the theory.

Keywords
Finite volume method, O-method, evolving surfaces, transport diffusion equations

Mathematics Subject Classification (2000) 35K05 35K57 35L65 41A10 41A29 65D05 65N12 65N08 65N15 58J35 76R05 76R50

1 Introduction

In [1], we have defined a consistent and convergent finite volume scheme for the simulation of diffusion and advection processes on moving surfaces. Although the proposed

Simplice Firmin Nemadjieu
Technical University of Eindhoven, The netherlands, Tel.: +31 402475857,
E-mail: s.f.nemadjieu@tue.nl

scheme is stable and convergent, it is subject to strong constraints on the mesh, namely the orthogonality condition which is related to the diffusion tensor. This makes the mesh used in the algorithm problem-dependent and it becomes difficult to couple inter-dependent phenomena involving many spatially varying anisotropic diffusion tensors on the same mesh. Also, even on fixed surfaces, it would be difficult using this algorithm to simulate problems with time and space dependent diffusion tensors when variations on eigenvectors of diffusion tensors become important as time evolves. In this case one is obliged to remesh the substrate often as needed. This might introduce some inaccuracy in the result depending on the remeshing method and the approximation method used to reallocate values on cells. In the last two decades, researchers have invested a lot of effort in developing finite volume schemes for anisotropic diffusion problems on unstructured meshes which tackle the best these issues. Unfortunately, focus has been put on planar 2-dimensional and on 3-dimensional problems. We refer to the benchmark parts of [2] and [3], Proceedings of Finite Volumes for Complex Applications V and VI, for the state of art on research in this domain. Nevertheless, the methods developed in the context of finite volumes rely on a suitable approximation of fluxes across edges of control volumes. One constructs fluxes either using only the two unknowns across interfaces or a set of unknowns around edges. The first strategy is referred to as the two-point flux approximation method while the second is known as the multi-point flux approximation method. The method defined in [1] is an example of the two-point flux approximation method on curved surfaces and one will find in [4] a more extended description and analysis of the method applied on various problems on flat surfaces. As already said above, it is unfortunately very restrictive in terms of meshes and problems on which it can be applied. The multi-point flux approximation is the up-to-date strategy in the finite volume simulation and is much more flexible. It can be divided into two main groups:

• The Discrete Duality Finite Volumes: In this class of methods, one interplays simultaneously between two meshes; the primal mesh and the dual mesh. The computation is done here on the two nested meshes and the degrees of freedom include the center points of the primal mesh as well as its vertices which are in fact the center points of the dual mesh. We refer to [5; 6; 7; 8] for more insight in the methodology.

• The Mixed or Hybrid Finite Volumes: Here, the degrees of freedom are maintained at the cell centers and one explicitly constructs the gradient operators using different strategies: O-Method [9; 10; 11], L-Method [9], scheme using stabilization and hybrid interfaces [12], finite element strategy [13], least square reconstruction [14] among others.

Since most of these schemes use properties valid only in Cartesian geometry, they cannot be directly transferred to curved surfaces. Also, the fact that a general curved geometry can only be approximated requires a special treatment of schemes on curved surfaces since one should combine the accuracy of the geometric approximation and the accuracy of the scheme. Nevertheless, the methodology in [13] has been analyzed on curved surfaces in [15; 16]. We should also mention the finite volume approach on logically rectangular grids studied in [17] for diffusion and advection in circular and spherical domains. As in these few papers, the few works devoted to finite volumes on curved surfaces encountered in the literature rely either on a good triangulation of the domain or on a special partitioning of the curved geometry; this restricts their domain of application. In this paper, we present a finite volume type O-method for general polygonal meshes on curved and moving surfaces. Our method is close to the ones developed by Le Potier in [10] and K. Lipnikov, M. Shashkov and I. Yotov in [11]. Similar

to these authors, we first partition each cell of the given discrete domain into subcells attached to cells vertices; this implies a partition of each edge into two subedges and a virtually refined domain where the subcells are effectively the new cells and are grouped around vertices. Next around each vertex, we construct an approximate constant gradient of our solution on surrounding subcells using surrounding cell center unknowns and the continuity of fluxes on subedges. We also take into account worse situations that can occur when the diffusion coefficients become almost degenerate, by using a suitable minimization process which controls the norm of the chosen solution gradients around vertices. These gradients are latter included properly in the flux formulation of the diffusion operator to obtain its discretization. Finally, we use the approximate gradients issued from the identity operator on surfaces to construct a slope limited gradient of the solution function on each control volume. These last gradients approximation are used to develop a second order upwind scheme for the advection part of our model equation. Since the stencil of our slope limited gradients remains unchanged during the process, we experimentally have a second order space convergence of the whole scheme. We should mention that our method is identical to the methods developed in [10; 11] for diffusion on flat surfaces and to the method discussed in [16] for diffusion on curved surfaces when applied with the same parameters, but the scope of meshes that we can handle in those cases is wider. Nevertheless, we would like to emphasize that we primarily deal with moving curved surfaces. This includes surfaces whose evolution is implicitly defined through partial differential equations and surfaces whose evolution is explicitly given among others. Let us also mention that this method can be reduced to the method discussed in [1] for appropriate meshes designed for this purpose. In the following, we explicitly introduce the model problem discussed in this chapter, next we present the method and give a possible implementation algorithm. Furthermore, we prove some stability results and the convergence of the scheme and finally we present some numerical results to validate the theory. For the purpose of self containment, we will reproduce some proofs from [1].

2 Problem setting

We consider a family of compact hypersurfaces $\Gamma(t) \subset \mathbb{R}^n$ $(n = 2, 3, \cdots)$ for $t \in [0, t_{max}]$ generated by a time-dependent function $\Phi : [0, t_{max}] \times \Gamma^0 \longrightarrow \mathbb{R}^n$ defined on a reference frame Γ^0 with $\Phi(t, \Gamma^0) = \Gamma(t)$. We assume $\Phi(t, \cdot)$ to be the restriction of a function that we abusively call $\Phi(t, \cdot) : \mathcal{N}_0 = \mathcal{N}(0) \longrightarrow \mathcal{N}(t)$, where $\mathcal{N}_0$ and $\mathcal{N}(t)$ are neighborhoods of Γ^0 and $\Gamma(t)$ in $\mathbb{R}^n$, respectively. We also take Γ^0 to be C^3 smooth and $\Phi \in \mathrm{C}^1\left([0, t_{max}], \mathrm{C}^3\left(\mathcal{N}_0\right)\right)$. For simplicity, we assume the reference surface Γ^0 to coincide with the initial surface $\Gamma(0)$. We denote by $v = \partial_t \Phi$ the velocity of material points and assume the decomposition $v = v_n \nu + v_{tan}$ into a scalar normal velocity v_n in the direction of the surface normal ν and a tangential velocity v_{tan}. The evolution of a conservative material quantity u with $u(t, \cdot) : \Gamma(t) \longrightarrow \mathbb{R}$, which is propagated with the surface and, at the same time, undergoes a linear diffusion on the surface, is governed by the parabolic equation

$$\dot{u} + u \nabla_\Gamma \cdot v - \nabla_\Gamma \cdot (\mathcal{D} \nabla_\Gamma u) = g \text{ on } \Gamma(t), \tag{1}$$

where $\dot{u} = \frac{d}{dt} u(t, x(t))$ is the (advective) material derivative of u, $\nabla_\Gamma \cdot v$ the surface divergence of the vector field v, $\nabla_\Gamma u$ the surface gradient of the scalar field u, g a source

term with $g(t,\cdot) : \Gamma(t) \longrightarrow \mathbb{R}$, and $\mathcal{D}$ the diffusion tensor on the tangent bundle. Here we assume a symmetric, uniformly coercive C^2 diffusion tensor field on whole $\mathbb{R}^n$ to be given, whose restriction on the tangent plane is then effectively incorporated in the model. With slight misuse of notation, we denote this global tensor also by $\mathcal{D}$. Furthermore, we impose an initial condition $u(0,\cdot) = u_0$ at time $t = 0$. We also consider here a surface with boundary and impose a Dirichlet boundary condition. A remark on how to treat the Neuman boundary condition and the mixed Dirichlet-Neumann boundary condition will be made too. We should notice that the case of surfaces without boundary falls into this setup since they are merely surfaces with empty boundary. Finaly, we assume that the mappings $(t,x) \longrightarrow u\left(t,\Phi(t,x)\right)$, $v(t,\Phi\left(t,x\right))$ and $g(t,\Phi(t,x))$ are $\mathrm{C}^1\left([0,t_{max}],\mathrm{C}^3(\Gamma^0)\right)$, $\mathrm{C}^0\left([0,t_{max}],\left(\mathrm{C}^3(\Gamma^0)\right)^3\right)$, and $\mathrm{C}^1\left([0,t_{max}],\mathrm{C}^1(\Gamma^0)\right)$, respectively. For the discussion on existence, uniqueness and regularity, we refer to [18] and references therein.

3 Surface approximation

We introduce in this part a more general notion of surface approximation.

Definition 31 *(Cell, cell center and vertices) Let* $(\mathcal{p}_1,\mathcal{p}_2,\cdots,\mathcal{p}_{n_S})$ *and* X_S *be* (n_S+1) *distinct points in* $\mathbb{R}^3$. *We call cell* S *the closed fan of triangles* $S_{\{i,j\}} = [X_S,\mathcal{p}_i,\mathcal{p}_j]$ $(j = (i \mod n_S)+1)$ *where* X_S *is the shared vertex. The point* X_S *is called cell center or center point while the points* $\mathcal{p}_i$ *are called vertices of the cell and are not necessarily coplanar. Figure 1 shows an example of a cell.*

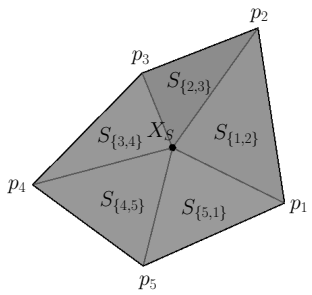

Fig. 1 Cell S made of subtriangles $S_{\{i,i+1\}}$.

In the following, we adopt the notation $j = i+1$ for the cyclic addition ($j = (i \mod n_S)+1$) if there is no confusion.

Definition 32 *(Admissible cell)*
Let S *be a cell,* X_S *its center point and* $\mathcal{p}_i$ $(i = 1,\cdots,n_S)$ *its* n_S *vertices. For a given vertex* $\mathcal{p}_i$ *we define* $r_i := \overrightarrow{X_S\mathcal{p}_i}$ *and denote by* $\nu_{S_{\{i,i+1\}}} = r_i \wedge r_{i+1}/\|r_i \wedge r_{i+1}\|$ *the oriented normal of the triangle* $[X_S,\mathcal{p}_i,\mathcal{p}_{i+1}]$ *if the triangle has a nonzero measure. We also define a pseudo-normal to the cell by*
$\nu_S = \left(\sum_i r_i \wedge r_{i+1}\right)/\|\sum_i r_i \wedge r_{i+1}\|$. *We will then call the cell* admissible *if for any*

i, j and $m \in \{1, 2, \cdots, n_S\}$, $\|r_i\| \leq \max_{j,m} \|\overrightarrow{p_j p_m}\|$ and $\nu_{S_{\{i,i+1\}}} \cdot \nu_S > 0$ for well defined normals.

Remark 33 *The vector ν_S depends only on the vertices and not on X_S.*

Definition 34 *(admissible polygonal surface)*
We define an admissible polygonal surface as a union of admissible cells which form a partition of a C^0 surface Γ_h. Also, the normals ν_{S_i} and ν_{S_j} of two different cells S_i, $S_j \subset \Gamma_h$ with $S_i \cap S_j \neq \emptyset$, must satisfy $\nu_{S_i} \cdot \nu_{S_j} > 0$. We refer to Figure 2 for an example of admissible mesh (polygonal surface). The index h in Γ_h represents the maximum distance between two points in a given cell $S \subset \Gamma_h$.

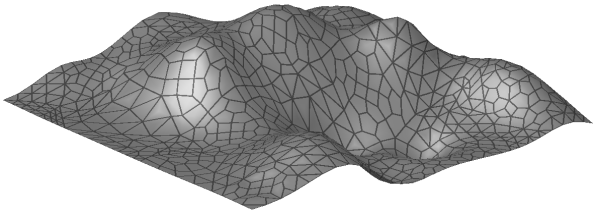

Fig. 2 Admissible polygonal surface

In the sequel, we assume for surfaces with nonempty boundary a piecewise C^2 boundary. In that case, we assume Γ^0 to be part of a larger surface $\Omega_0 \subset \mathcal{N}_0$ with the same properties as Γ^0. Ω_0 is transformed to $\Omega(t, \cdot)$ by the map $\Phi(\cdot, \cdot)$ as time evolves. We also denote by $\mathcal{C}$ a generic constant.

Definition 35 *($(m,h)-$polygonal approximation of a surface)*
We will say that the polygonal surface Γ_h^0 is an (m, h) − approximation ($m \geq 2$) of the surface Γ^0 if and only if Γ_h^0 is admissible and there exists a neighborhood $\mathcal{N}_{\delta,0} := \{x \,|\, d(x, \Omega_0) = \inf_{p \in \Omega_0} \|\overrightarrow{px}\| \leq \delta\}$ ($\delta \leq \mathcal{C}h^2$) of $\Omega_0 \supset \Gamma^0$ which satisfies the following conditions:

- *i) $\Gamma_h^0 \subset \mathcal{N}_{\delta,0}$.*
- *ii) The perpendicular lines to Ω_0 at two different points do not intersect within $\mathcal{N}_{\delta,0}$.*
- *iii) The orthogonal projection $\mathcal{P}\Gamma_h^0$ of Γ_h^0 onto Ω_0 is a bijection between Γ_h^0 and its image.*
- *iv) The orthogonal projection of any cell of Γ_h^0 onto Ω_0 intersects Γ^0.*
- *v) There exists $\Gamma_{rest}^0 \subset \Gamma^0$ and $\Gamma_{ext}^0 \supset \Gamma^0$ satisfying $\Gamma_{rest}^0 \subset \mathcal{P}\Gamma_h^0 \subset \Gamma_{ext}^0 \subset \Omega_0$ (cf. Figure 3) and $m(\Gamma_{ext}^0 \backslash \Gamma_{rest}^0) \leq \mathcal{C}h^2$ where $m(\cdot)$ represents the $(n-1)-$dimensional Hausdorff measure.*
- *vi) Let us denote by $\mathcal{P}_{\partial\Gamma^0} : x \mapsto y = \operatorname{argmin} d(x, \partial\Gamma^0)$ the map that projects points orthogonally on the boundary $\partial\Gamma^0$ of Γ^0. This map should be well defined in a neighborhood of $\partial\Gamma^0$ containing $(\Gamma_{ext}^0 \backslash \Gamma_{rest}^0)$, and its restriction on $\mathcal{P}(\partial\Gamma_h^0)$ should be bijective. Furthermore, we assume that the reverse image of a vertex of Γ^0 onto $\mathcal{P}(\partial\Gamma_h^0)$ is the projection of a vertex of Γ_h^0 onto Γ_{ext}^0 (cf. Figure 3).*
- *vii) For two different vertices p_i and p_j of the same cell S, we have $\mathcal{C}h \leq \|\overrightarrow{p_i p_j}\| \leq h$.*

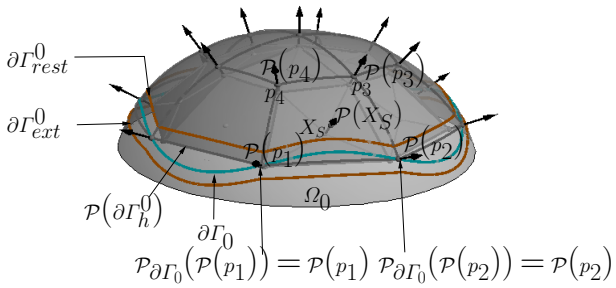

Fig. 3 Representation of $\Gamma^0 \subset \Omega_0$, Γ^0_h, $\mathcal{P}(\Gamma^0_h)$, Γ^0_{rest} and Γ^0_{ext} delimited respectively by $\partial\Gamma^0$ (green line), $\partial\Gamma^0_h$ (hidden behind the surface), $\partial\mathcal{P}(\Gamma^0_h)$ (gray line), $\partial\Gamma^0_{rest}$ (inner brown line) and $\partial\Gamma^0_{ext}$ (outer brown line).

viii) For any cell S, there exists a point $p_S \in S$ and a vector $\overrightarrow{b}_S$ such that the trace on S of the cylinder with principal axis $(p_S, \overrightarrow{b}_S)$ and the radius Ch do not intersect the boundary of S.

ix) The distance between a vertex and its projection on Γ^0_{ext} is less than Ch^m.

Remark 36 *In the above definition,*

- *v) expresses the convergence of $\mathcal{P}\Gamma^0_h$ toward Γ^0 as h tends to 0.*
- *i), iii) and v) ensure the convergence of the discrete surface Γ^0_h toward Γ^0 as h tends to 0.*
- *ii) will allow for an extension of functions defined on the reference surface Γ^0 onto a narrow band around Γ^0 which includes Γ^0_h.*
- *vii) ensures the nondegeneracy of sides while viii) ensures the nondegeneracy of cells. For usual triangular meshes, viii) is expressed as $\mathcal{C}_1 h^2 \leq m_S \leq \mathcal{C}_2 h^2 \ \forall\ S \subset \Gamma^0_h$ where $\mathcal{C}_1$, $\mathcal{C}_2$ are some fixed constants and m_S is the $(n-1)-$dimensional measure of S.*
- *iv) ensures that there is no unnecessary cell.*
- *ix) allows us to see that the best paraboloid that can be fitted to a closed set of points will be an $m-$order approximation of the original surface. In fact, if some intrinsic properties have to be computed, we will need a good approximation of vertices. This is for example the case in the fourth example considered in this paper, where we have to discretize an additional advection term which involves the curvature tensor. To evaluate the curvature tensor at center points, the best method in the literature to do such a computation at a desired order on a parametric surface is the least square fitting. Of course the consistency of the fitting is at most the consistency of points used, which should be $m \geq 3$ in this case. Furthermore, this general setting is much closer to the real world application than considering vertices bound to the original surface. Most often, the movement of surfaces is described by another partial differential equation; the mean curvature motion considered in the fourth example of this paper is an illustration. In this case, there is no way to tackle the exact position of the surface points; hence the importance of introducing some inaccuracy on points used to approximate the surface.*

4 Derivation of the finite volume scheme

4.1 General setting

We consider a family of admissible polygonal surfaces $\{\Gamma_h^k\}_{k=0,\cdots,\ k_{max}}$, with Γ_h^k approximating $\Gamma(t_k) \subset \Omega^k \subset \mathcal{N}(t_k)$ for $t_k = k\tau$ and $k_{max}\tau = t_{max}$. Here $\Omega^k := \Omega(t_k) = \Phi(t_k, \Omega_0)$ is a sequence of two dimensional surfaces as defined above in Section 3 and, as in [1], h denotes the maximum diameter of a cell on the whole family of polygonizations, τ the time step size and k the index of a time step. Successive polygonizations share the same grid topology and given the set of vertices p_j^k on the polygonal surface Γ_h^k, the vertices of Γ_h^{k+1} lie on motion trajectories; thus they are evaluated based on the flux function Φ, i.e., $p_j^{k+1} = \Phi\left(t_{k+1}, \Phi^{-1}\left(p_j^k, t_k\right)\right)$. Upper indices denote the time steps and foot indices "j" are vertex indices. Let us for the moment merely assume the center points being chosen at each time step such that the discrete surfaces remain uniformly admissible $(2,h)-$polygonizations of the original surfaces; i.e., the constants in Definition 35 remain the same for all time steps. In Section 5, we will give more detailed precisions for their choice. Next, at each time step t_k, we consider a virtual subdivision of each cell S^k into n_S subcells (virtual cells) $S_{p_i}^k$ $(i = 1, \cdots, n_S)$ which share the common vertex X_S^k as depicted on Figure 4. We

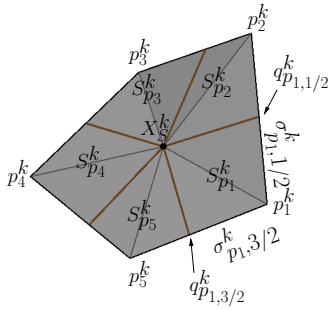

Fig. 4 Subdivision of the cell S^k into polygonal subcells $S_{p_i}^k$ and subedges $\sigma_{p_1,1/2}^k := [q_{p_1,1/2}^k, p_1^k]$, $\sigma_{p_1,3/2}^k := [q_{p_1,3/2}^k, p_1^k]$ induced by $S_{p_1}^k$ around p_1^k.

recall that n_S denotes the number of vertices of the cell S^k. This subdivision, as we can notice again on Figure 4, induces a partition of each edge $\sigma = [p_i^k, p_{i+1}^k] \subset \partial S^k$ into two subedges $\sigma_{p_i,l-1/2}^k := [q_{p_i,l-1/2}^k, p_i^k]$ and $\sigma_{p_{i+1},m+1/2}^k := [q_{p_{i+1},m+1/2}^k, p_{i+1}^k]$; $q_{p_i,l-1/2}^k = q_{p_{i+1},m+1/2}^k := S_{p_i}^k \cap S_{p_{i+1}}^k \cap [p_i, p_{i+1}]$, l and m are subindices used to reference the cell S^k around the vertices p_i^k and p_{i+1}^k, respectively. We will come back on how these indices are built in Section 4.2. We furthermore assume that two virtual cells $S_{p_i}^k$ and $L_{p_i}^k$ of two different cells S^k and L^k, which have the vertex p_i^k in common, share either a common subedge or the only vertex p_i^k as depicted on Figure 5. For later comparison of discrete quantities on polygonal surfaces Γ_h^k and continuous surfaces $\Gamma^k = \Gamma(t_k)$, we first extend functions defined on Γ^k or Γ_h^k in their neighborhood $\mathcal{N}(t_k)$. The resulting functions still bear their original names and will

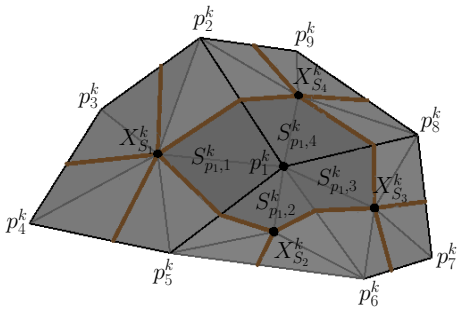

Fig. 5 Cells and subcells around a vertex.

be understood from the context. A function $u(t_k,\cdot)$ defined on Γ^k is then extended by requiring $\nabla u(t_k,\cdot)\cdot\nabla d(\cdot,\Gamma^k)\equiv 0$; $d(\cdot,\Gamma^k)$ being a signed distance function from Γ^k. This means in other words that, given a point $x\in\mathcal{N}(t_k)$, the extended function $u(t_k,\cdot)$ is constant along the shortest line segment from x to the surface Γ^k. The restriction of this new function on Γ_h^k will be denoted $u^{-l}(t_k,\cdot)$ or shortly $u^{-l,k}$. On the other hand, the extension of a function $u_h(t_k,\cdot)$ defined on Γ_h^k is done in two steps. We first extend as constant along the normal ν to $\mathcal{P}^k(\Gamma_h^k)$; $\mathcal{P}^k(\cdot)$ being the orthogonal projection operator onto Ω^k. The resulting function, still called $u_h(t_k,\cdot)$, is finally extended by requirering $\nabla u_h(t_k,\cdot)\cdot\nabla d(\cdot,\mathcal{P}^k(\Gamma_h^k))\equiv 0$. The restriction of the final extended function on Γ^k will be termed $u_h^l(t_k,\cdot)$ or simply $u^{l,k}$ and the operation which transforms $u_h(t_k,\cdot)$ to $u_h^l(t_k,\cdot)$ will be called " lift " operator. These extension operations are by definition well defined in a neighborhood of $\Gamma(t_k)$ in which Γ_h^k lies, thus the lift operator is well defined. We will also refer to the orthogonal projection as a lift operator; and therefore lift operators will be understood from the context. We denote by $S^{l,k}:=\mathcal{P}^kS^k$ the orthogonal projection of S^k onto Ω^k, by $S^{l,k}(t)=\Phi\left(t,\Phi^{-1}\left(t_k,S^{l,k}\right)\right)$ the temporal evolution of $S^{l,k}$ and by m_S^k the area of S^k. We should mention here that the symbol " l " written as upper index is meant for the " lift " operator; therefore $x^{l,k}$ will literally mean lift of x^k onto the surface Ω^k. Along the same line, we will call $S_{p_i}^{l,k}:=\mathcal{P}^kS_{p_i}^k$ the orthogonal projection of $S_{p_i}^k$ onto Ω^k. So defined, the subcells $S_{p_i}^{l,k}$ form a curved mesh on $S^{l,k}$.
The key of our approach will be to define on these subcells a reasonable approximation of the surface gradient operators $\nabla_\Gamma u$, and deduce a suitable numerical integration of $\nabla_\Gamma\cdot(\mathcal{D}_\Gamma\nabla_\Gamma u)$ in the cells S^k. Our algorithm can be identified as a hybrid algorithm between mixed finite volume and the usual finite volume procedure. The mixed finite volume defines fluxes or even $w=\mathcal{D}_\Gamma\nabla_\Gamma u$ as unknowns which have to be found together with the solution u. This often leads to a system of equations that has to be stabilized via some restriction on meshes and some appropriate techniques. In our case we define an approximate gradient $\nabla_h^k u$ of $\nabla_\Gamma u(t_k,\cdot)$ as a piecewise constant gradient $\left\{\nabla^k_{p_i,\mathcal{J}(p_i,S)}u\right\}_{p_i,S}$ on subcells $\left\{S_{p_i}^k\right\}_{p_i,S}$; $\mathcal{J}(p_i,S)$ being the local index of subcell $S_{p_i}^k$ around p_i. The construction of $\nabla_h^k u$ is done locally around vertices p_i via a proper use of the flux continuity condition on subedges, as will be explained below. This procedure leads to a local system of equations which in a worse case senario (very bad mesh and highly anisotropic tensor) is underdetermined. In that case, a suitable minimization procedure is used to stabilize the system which is thereafter partially solved

and introduced into the global system of equations that represents (1) to obtain a cell center scheme. The procedure of restricting oneself to cells around vertices to construct subfluxes in the finite volume procedure has already been used in [9; 10; 11] for finite volumes on flat surfaces. Restricting oneself to that case, the method developed in [10] is a particular case of the present one. Unfortunately, it loses consistency for polygonal meshes with very deformed quadrangles or nonconvex starshaped cells (flat version of admissible cells which are not convex), while the present method produces good results in those cases. Let us now introduce the construction of the piecewise gradient operator.

4.2 The discrete gradient operator

Let us first consider a vertex p_i. We locally reorder the cells S_j^k, the subcells $S_{p_i,j}^k$ and the subedges $\sigma_{p_i,j-1/2}^k$ counterclockwise around the continuous surface normal at $\mathcal{P}^k p_i^k$. The subedges are reordered in a way that $\sigma_{p_i,j-1/2}^k$ and $\sigma_{p_i,j+1/2}^k$ are subedges of the cell S_j^k and edges of the subcell $S_{p_i,j}^k$. We also locally rename by $X_{p_i,j}^k$ the center point of S_j^k. We refer to Figure 4 and Figure 5 for the illustration of this setup. Next, we define on each subedge $\sigma_{p_i,j-1/2}^k$ the virtual point $X_{p_i,j-1/2}^k$, and on each subcell $S_{p_i,j}^k$, we define the covariant vectors $e_{p_i,j|j-1/2}^k := X_{p_i,j-1/2}^k - X_{p_i,j}^k$ and $e_{p_i,j|j+1/2}^k := X_{p_i,j+1/2}^k - X_{p_i,j}^k$ which are used to define the local approximate tangent plane $T_{p_i,j}^k := \mathrm{Span}\left\{e_{p_i,j|j-1/2}^k, e_{p_i,j|j+1/2}^k\right\}$ to points of the subcell $S_{p_i,j}^{l,k}$. We also define on $T_{p_i,j}^k$ the contravariant (dual) basis $(\mu_{p_i,j|j-1/2}^k, \mu_{p_i,j|j+1/2}^k)$ such that $e_{p_i,j|j-1/2}^k \cdot \mu_{p_i,j|j-1/2}^k = 1$, $e_{p_i,j|j-1/2}^k \cdot \mu_{p_i,j|j+1/2}^k = 0$, $e_{p_i,j|j+1/2}^k \cdot \mu_{p_i,j|j-1/2}^k = 0$ and $e_{p_i,j|j+1/2}^k \cdot \mu_{p_i,j|j+1/2}^k = 1$. Figure 6 illustrates this setup.

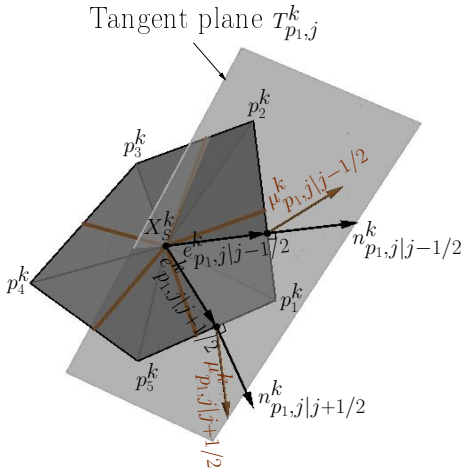

Fig. 6 Approximate tangent plane $T_{p_i,j}^k$ to $S_{p_i,j}^{l,k}$.

Using this dual system of vectors, we define for a continuous and derivable scalar

function $u(t_k,\cdot)$ on Γ^k, constant gradients $\nabla^k_{p_i,j}u$ which approximate $\nabla u(t_k,\cdot)|_{S^{l,k}_{p_i,j}}$, restrictions of $\nabla u(t_k,\cdot)$ on $S^{l,k}_{p_i,j}\cap\Gamma^k$.

$$\nabla^k_{p_i,j}u := \left(U^k_{p_i,j-1/2}-U^k_{p_i,j}\right)\mu^k_{p_i,j|j-1/2}+\left(U^k_{p_i,j+1/2}-U^k_{p_i,j}\right)\mu^k_{p_i,j|j+1/2} \quad (2)$$

where $U^k_{p_i,j-1/2}$, $U^k_{p_i,j+1/2}$, $U^k_{p_i,j}$, are appropriate approximations of $u\left(t_k,\mathcal{P}^k(X^k_{p_i,j-1/2})\right)$, $u\left(t_k,\mathcal{P}^k(X^k_{p_i,j+1/2})\right)$ and $u\left(t_k,\mathcal{P}^k(X^k_{p_i,j})\right)$, respectively. In this notation, if a point X^k is on the boundary of Γ^k_h, $u\left(t_k,\mathcal{P}^k(X^k)\right)$ will be taken to be the value of u at the closest point of Γ^k to $\mathcal{P}^k(X^k)$. The definition of our piecewise constant gradient will be completed if we give the explicit expression of the virtual unknowns $U^k_{p_i,j-1/2}$. For this purpose, let us introduce without proof the following proposition.

Proposition 41 *Let Ω be an open and bounded set in $\Gamma(t)$, made up of two disjoint open sets Ω_1 and Ω_2 which share a curved segment $\sigma^l := \partial\Omega_1\cap\partial\Omega_2$ as border. Let w be a tangential vector function which is C^1 on Ω_1 and Ω_2. w has a weak tangential divergence in $\mathbb{L}^2(\Omega)$ if and only if its normal component through σ^l is continuous.*

The prerequisites in this proposition can also be weakened by assuming w being $\mathbb{H}^1$ on Ω_1 and Ω_2. In that case, the continuity in the conclusion becomes a continuity almost everywhere.
Also, for a line segment $\sigma^k\subset\Gamma^k_h$ we define

$$\sigma^{l,k} := \{y = x - d(x,\Gamma(t))\nabla d^T(x,\Gamma(t_k)), x\in\sigma^k\}.$$

It is worth mentioning here that $\sigma^{l,k}$ can be different from $\mathcal{P}^k(\sigma^k)$ in some cases. For example, considering the line segment $\sigma^k := [p_1,p_2]$ on Figure 3, $\sigma^{l,k}$ is the blue curve joining $\mathcal{P}(p_1)$ and $\mathcal{P}(p_2)$. Let us now consider a subcell $S^{l,k}_{p_i,j}$ of a cell $S^{l,k}_j$. We approximate the diffusion tensor $\mathcal{D}$ in (1) on $S^{l,k}_{p_i,j}$ by

$$\mathcal{D}^k_{p_i,j} := \left(\mathrm{Id}-\nu^k_{p_i,j}\otimes\nu^k_{p_i,j}\right)\left(\frac{1}{m(S^{l,k}_j)}\int_{S^{l,k}_j}\mathcal{D}\,dS^{l,k}_j\right)\left(\mathrm{Id}-\nu^k_{p_i,j}\otimes\nu^k_{p_i,j}\right),$$

where $\nu^k_{p_i,j} := \left(e^k_{p_i,j|j+1/2}\wedge e^k_{p_i,j|j-1/2}\right)/\|e^k_{p_i,j|j+1/2}\wedge e^k_{p_i,j|j-1/2}\|$ is the normal to $T^k_{p_i,j}$ that we take as the approximation of the oriented normal ν to $S^{l,k}_{p_i,j}$. We also approximate the unit outer conormals to $\sigma^{l,k}_{p_i,j-1/2} := \left(\sigma^k_{p_i,j-1/2}\right)^l$ and $\sigma^{l,k}_{p_i,j+1/2} := \left(\sigma^k_{p_i,j+1/2}\right)^l$ by $n^k_{p_i,j|j-1/2}$ and $n^k_{p_i,j|j+1/2}$, respectively. These are vectors of $T^k_{p_i,j}$ which are respectively normal to $\sigma^k_{p_i,j-1/2}$ and $\sigma^k_{p_i,j+1/2}$ (cf. Figure 6) and which point outward from the projection in the direction of ν of $S^{l,k}_{p_i,j}$ onto $T^k_{p_i,j}$. Finally, we approximate $m^{l,k}_{p_i,j-1/2}$, the measure of $\sigma^{l,k}_{p_i,j-1/2}$, by $m^k_{p_i,j-1/2}$, the measure of $\sigma^k_{p_i,j-1/2}$. Since $\mathcal{D}\nabla_\Gamma u$ has a weak divergence in $\mathbb{L}^2(\Gamma)$, we apply a discrete version of Proposition 41 on subcells surrounding vertices p^k_i; namely,

$$\begin{aligned} &m^k_{p_i,j-1/2}\mathcal{D}^k_{p_i,j-1}\nabla^k_{p_i,j-1}u\cdot n^k_{p_i,j-1|j-1/2}\\ &+ m^k_{p_i,j-1/2}\mathcal{D}^k_{p_i,j}\nabla^k_{p_i,j}u\cdot n^k_{p_i,j|j-1/2} = 0 \end{aligned} \quad (3)$$

for the subedge $\sigma^k_{p_i,j-1/2}$. Rewriting the system of equations given by (3) around p^k_i in the matrix form gives

$$M^k_{p_i}\widetilde{U}^k_{p_i,\sigma} = N^k_{p_i}\widetilde{U}^k_{p_i}, \tag{4}$$

where $\widetilde{U}^k_{p_i,\sigma} := (U^k_{p_i,1/2}, U^k_{p_i,3/2}, \cdots)^\top$, $\widetilde{U}^k_{p_i} := (U^k_{p_i,1}, U^k_{p_i,2}, \cdots)^\top$, and the entries of $M^k_{p_i}$ and $N^k_{p_i}$ are

$$\begin{aligned}
\left(M^k_{p_i}\right)_{j,j-1} &= m^k_{p_i,j-1/2}\lambda^k_{p_i,j-3/2|j-1|j-1/2},\\
\left(M^k_{p_i}\right)_{j,j} &= m^k_{p_i,j-1/2}(\lambda^k_{p_i,j-1|j-1/2} + \lambda^k_{p_i,j|j-1/2}),\\
\left(M^k_{p_i}\right)_{j,j+1} &= m^k_{p_i,j-1/2}\lambda^k_{p_i,j+1/2|j|j-1/2},
\end{aligned}$$

$$\begin{aligned}
\left(N^k_{p_i}\right)_{j,j-1} &= m^k_{p_i,j-1/2}(\lambda^k_{p_i,j-1|j-1/2} + \lambda^k_{p_i,j-3/2|j-1|j-1/2}),\\
\left(N^k_{p_i}\right)_{j,j} &= m^k_{p_i,j-1/2}(\lambda^k_{p_i,j|j-1/2} + \lambda^k_{p_i,j+1/2|j|j-1/2}),
\end{aligned}$$

and 0 elsewhere; with

$$\begin{aligned}
\lambda^k_{p_i,j|j-1/2} &= n^k_{p_i,j|j-1/2}\cdot\mathcal{D}^k_{p_i,j}\mu^k_{p_i,j|j-1/2},\\
\lambda^k_{p_i,j+1/2|j|j-1/2} &= n^k_{p_i,j|j-1/2}\cdot\mathcal{D}^k_{p_i,j}\mu^k_{p_i,j|j+1/2},\\
\lambda^k_{p_i,j-1/2|j|j+1/2} &= n^k_{p_i,j|j+1/2}\cdot\mathcal{D}^k_{p_i,j}\mu^k_{p_i,j|j-1/2},\\
\lambda^k_{p_i,j|j+1/2} &= n^k_{p_i,j|j+1/2}\cdot\mathcal{D}^k_{p_i,j}\mu^k_{p_i,j|j+1/2}.
\end{aligned}$$

If p^k_i is a boundary point, making use of the Dirichlet boundary condition, we rewrite (4) using the same notation $M^k_{p_i}\widetilde{U}^k_{p_i,\sigma} = N^k_{p_i}\widetilde{U}^k_{p_i}$ with $\widetilde{U}^k_{p_i,\sigma} := (U^k_{p_i,3/2}, \cdots, U^k_{p_i,n_{p_i}-1/2})^\top$, $\widetilde{U}^k_{p_i} := (U^k_{p_i,1/2}, U^k_{p_i,1}, \cdots, U^k_{p_i,n_{p_i}}, U^k_{p_i,n_{p_i}+1/2})^\top$.
n_{p_i} denotes the number of cells around p^k_i and $U^k_{p_i,1/2} := u(t_k, \mathcal{P}^k(X^k_{p_i,1/2}))$, $U^k_{p_i,n_{p_i}+1/2} := u(t_k, \mathcal{P}^k(X^k_{p_i,n_{p_i}+1/2}))$ at the boundary. The matrix $M^k_{p_i}$ is then a square matrix whose dimension is the number of subedges around p^k_i on which we have unknowns while the matrix $N^k_{p_i}$ is a square matrix for interior vertices (vertices which do not belong to the boundary) and a rectangular matrix for boundary vertices. We should mention here that for consistency reasons, the subedge points $X^k_{p_i,j-1/2}$ should be chosen in such a way that the angle $\theta^k_{p_i,j} := \sphericalangle(X^k_{p_i,j-1/2}\ X^k_j\ X^k_{p_i,j+1/2})$ between $e^k_{p_i,j|j+1/2}$ and $e^k_{p_i,j|j-1/2}$ is always greater than a threshold angle θ during the entire process. This condition also leads to the invertibility of $M^k_{p_i}$ when the diffusion tensors $\mathcal{D}^k_{p_i,j}$ involved in the system are uniformly elliptic on corresponding tangent plane, with the elliptic constant far from 0, and the incident angles at p^k_i acute and far from 0 and π ($0 << \sphericalangle(X^k_{p_i,j+1/2}\ p^k_i\ X^k_{p_i,j-1/2}) << \pi$). In that case, equation (4) will be transformed to

$$\widetilde{U}^k_{p_i,\sigma} = \left(M^k_{p_i}\right)^{-1} N^k_{p_i}\widetilde{U}^k_{p_i}. \tag{5}$$

If there exist a subcell $S^{l,k}_{p_i,j}$ in which $\mathcal{D}^k_{p_i,j}$ is almost one dimensional, for example $\mathcal{D}^k_{p_i,j} := (\mathrm{Id} - \nu^k_{p_i,j}\otimes\nu^k_{p_i,j})\begin{pmatrix}1&0&0\\0&\alpha&0\\0&0&\alpha\end{pmatrix}(\mathrm{Id} - \nu^k_{p_i,j}\otimes\nu^k_{p_i,j})$, $\alpha = 1/10000$, $M^k_{p_i}$ can

become noninvertible if the mesh is not aligned with the anisotropy and the virtual points $X^k_{p_i,j-1/2}$ as well as the center points X^k_j chosen consequently. Simulation of strong anisotropic flow on such a general moving mesh will often encounter this problem if we did not take care from the beginning by trying to produce an adequate mesh near to what has been described in [1] for the triangular case. By doing so, we limit a lot the possibilities of the actual scheme. Then if $M^k_{p_i}$ is singular, we will first make sure that the choice of the virtual points on subedges guarantees that the range of $N^k_{p_i}$ is a subset of the range of $M^k_{p_i}$; i.e $Im(N^k_{p_i}) \subset Im(M^k_{p_i})$. Thereafter, we choose $\widetilde{U}^k_{p_i,\sigma}$ as the solution of (4) whose the induced discrete gradient around p^k_i has the minimum $\mathbb{H}^1_0$-norm. The problem of finding $\widetilde{U}^k_{p_i,\sigma}$ is then stated numerically as follows:

$$\left\{\begin{array}{l} \text{Find } \widetilde{U}^k_{p_i,\sigma} \text{ in } \mathcal{B}^k_{p_i} := \left\{\widetilde{V}^k_{p_i,\sigma} := (V^k_{p_i,1/2}, V^k_{p_i,3/2}, \cdots)^\top \mid M^k_{p_i}\widetilde{V}^k_{p_i,\sigma} = N^k_{p_i}\widetilde{U}^k_{p_i}\right\} \\ \text{such that} \quad \widetilde{U}^k_{p_i,\sigma} = \underset{\widetilde{V}^k_{p_i,\sigma}\in\mathcal{B}^k_{p_i}}{\operatorname{argmin}} \sum_j m^k_{p_i,j}\Big\| \left[V^k_{p_i,j-1/2} - U^k_{p_i,j}\right]\mu^k_{p_i,j|j-1/2} \\ \qquad\qquad + \left[V^k_{p_i,j+1/2} - U^k_{p_i,j}\right]\mu^k_{p_i,j|j+1/2}\Big\|^2, \end{array}\right. \tag{6}$$

where $m^k_{p_i,j} := m(S^k_{p_i,j})$ approximates $m(S^{l,k}_{p_i,j})$. One easily verifies that this problem is equivalent to the following least square problem

$$\left\{\begin{array}{l} \text{Find } \widetilde{U}^k_{p_i,\sigma} \text{ in } \mathcal{B}^k_{p_i} := \left\{\widetilde{V}^k_{p_i,\sigma} := (V^k_{p_i,1/2}, V^k_{p_i,3/2}, \cdots)^\top \mid M^k_{p_i}\widetilde{V}^k_{p_i,\sigma} = N^k_{p_i}\widetilde{U}^k_{p_i}\right\} \\ \text{such that} \quad \widetilde{U}^k_{p_i,\sigma} = \underset{\widetilde{V}^k_{p_i,\sigma}\in\mathcal{B}^k_{p_i}}{\operatorname{argmin}} \left\|\sqrt{\mathbf{B}^k_{p_i}}\,\widetilde{V}^k_{p_i,\sigma} - \left(\sqrt{\mathbf{B}^k_{p_i}}\right)^{-1}\mathbf{C}^k_{p_i}\widetilde{U}^k_{p_i}\right\|^2, \end{array}\right.$$

where $\sqrt{\mathbf{B}^k_{p_i}}$ is the square root of the symmetric positive definite matrix $\mathbf{B}^k_{p_i}$ (i.e. $\sqrt{\mathbf{B}^k_{p_i}}\sqrt{\mathbf{B}^k_{p_i}} = \mathbf{B}^k_{p_i}$) defined by

$$\begin{aligned} \left(\mathbf{B}^k_{p_i}\right)_{j,j} &= m^k_{p_i,j-1}\|\mu^k_{p_i,j-1|j-1/2}\|^2 + m^k_{p_i,j}\|\mu^k_{p_i,j|j-1/2}\|^2, \\ \left(\mathbf{B}^k_{p_i}\right)_{j+1,j} &= \left(\mathbf{B}^k_{p_i}\right)_{j,j+1} = m^k_{p_i,j}\mu^k_{p_i,j|j-1/2}\cdot\mu^k_{p_i,j|j+1/2}; \end{aligned}$$

and $\mathbf{C}^k_{p_i}$ the matrix defined by

$$\begin{aligned} \left(\mathbf{C}^k_{p_i}\right)_{j,j} &= m^k_{p_i,j}\left(\|\mu^k_{p_i,j|j-1/2}\|^2 + \mu^k_{j|j-1/2}\cdot\mu^k_{p_i,j|j+1/2}\right), \\ \left(\mathbf{C}^k_{p_i}\right)_{j+1,j} &= m^k_{p_i,j}\left(\|\mu^k_{p_ij|j+1/2}\|^2 + \mu^k_{j|j-1/2}\cdot\mu^k_{p_i,j|j+1/2}\right). \end{aligned}$$

Our aim here is not to solve this least square problem at this stage but to build a relation between the solution $\widetilde{U}^k_{p_i,\sigma}$ and the cell center values $\widetilde{U}^k_{p_i}$. Lars Eldén discussed the solution of this class of problems extensively in [19] and it turns out that this problem has a unique solution if the intersection of the null space of $\sqrt{\mathbf{B}^k_{p_i}}$ and the null space of $M^k_{p_i}$ is the null vector. This is the case here since $\sqrt{\mathbf{B}^k_{p_i}}$ is invertible. The use of

the new variable $\widetilde{W}^k_{p_i,\sigma} := \sqrt{\mathbf{B}^k_{p_i}}\,\widetilde{V}^k_{p_i,\sigma} - \left(\sqrt{\mathbf{B}^k_{p_i}}\right)^{-1}\mathbf{C}^k_{p_i}\widetilde{U}^k_{p_i}$ reduces the problem to

$$\left\{\begin{array}{l} \text{Find } \widetilde{W}^k_{p_i,\sigma} \text{ in } \bar{\mathcal{B}}^k_{p_i} := \left\{\widetilde{V}^k_{p_i,\sigma} := (V^k_{p_i,1/2}, V^k_{p_i,3/2}, \cdots)^\top \,|\right. \\ \left. M^k_{p_i}\left(\sqrt{\mathbf{B}^k_{p_i}}\right)^{-1}\widetilde{V}^k_{p_i,\sigma} = \left(N^k_{p_i} - M^k_{p_i}\left(\mathbf{B}^k_{p_i}\right)^{-1}\mathbf{C}^k_{p_i}\right)\widetilde{U}^k_{p_i}\right\} \\ \text{such that } \widetilde{W}^k_{p_i,\sigma} = \underset{\widetilde{V}^k_{p_i,\sigma}\in\bar{\mathcal{B}}^k_{p_i}}{\operatorname{argmin}} \left\|\widetilde{V}^k_{p_i,\sigma}\right\|^2. \end{array}\right.$$

From the solution of this last problem, one easily deduces the solution to the original problem

$$\widetilde{U}^k_{p_i,\sigma} = \mathbf{Coef}^k_{p_i}\widetilde{U}^k_{p_i}, \tag{7}$$

$$\begin{aligned} \text{where } \mathbf{Coef}^k_{p_i} = &\left(\sqrt{\mathbf{B}^k_{p_i}}\right)^{-1}\left(M^k_{p_i}\left(\sqrt{\mathbf{B}^k_{p_i}}\right)^{-1}\right)^\dagger\left(N^k_{p_i} - M^k_{p_i}\left(\mathbf{B}^k_{p_i}\right)^{-1}\mathbf{C}^k_{p_i}\right) \\ &+ \left(\mathbf{B}^k_{p_i}\right)^{-1}\mathbf{C}^k_{p_i} \end{aligned} \tag{8}$$

$\left(M^k_{p_i}\left(\sqrt{\mathbf{B}^k_{p_i}}\right)^{-1}\right)^\dagger$ is the Moore-Penrose inverse of $M^k_{p_i}\left(\sqrt{\mathbf{B}^k_{p_i}}\right)^{-1}$. We recall that the Moore-Penrose inverse of a matrix $\mathbf{A}$ is the unique matrix $\mathbf{A}^\dagger$ that satisfies

$$\mathbf{A}\mathbf{A}^\dagger\mathbf{A} = \mathbf{A}, \qquad \mathbf{A}^\dagger\mathbf{A}\mathbf{A}^\dagger = \mathbf{A}^\dagger,$$
$$\left(\mathbf{A}\mathbf{A}^\dagger\right)^\top = \mathbf{A}\mathbf{A}^\dagger, \qquad \left(\mathbf{A}^\dagger\mathbf{A}\right)^\top = \mathbf{A}^\dagger\mathbf{A}.$$

The Moore-Penrose inverse coincides with the usual inverse of an invertible matrix; thus (5) is recovered in (7) and we can consider the least square problem as being the problem to be solve to find the virtual unknowns. We refer to [20; 21; 22; 23; 19; 24; 25; 26] for details on the general topic of generalized inverse of matrices. Let us remark that the sum of line element of the matrix $\mathbf{Coef}^k_{p_i}$ is 1, i.e $\mathbf{Coef}^k_{p_i}\mathbf{1}_{p_i} = \mathbf{1}_{p_i,\sigma}$ where $\mathbf{1}_{p_i} := (1,1,\cdots)^\top$, $\mathbf{1}_{p_i,\sigma} := (1,1,\cdots)^\top$ are respectively vector of ones with the same length as $\widetilde{U}^k_{p_i}$ and $\widetilde{U}^k_{p_i,\sigma}$.In fact, $\mathbf{1}_{p_i,\sigma}$ is the unique solution of the above least square problem for $\widetilde{U}^k_{p_i} = \mathbf{1}_{p_i}$. Therefore $U^k_{p_i,j+1/2}$ can be seen as a barycenter of the values $U^k_{p_i}$. Such an idea to introduce the barycenter of values at cell centers to approximate values on edges in the finite volume context was already used by Eymard, Gallouët and Herbin in [12]. Unfortunately, due to the random choice of the barycentric coefficients, their resulting fluxes were poorly approximated, did not respect the flux continuity in the usual sense of finite volume methods and therefore needed extra treatment to guarantee good accuracy of the simulation result. This is a reason of our special treatment of virtual unknowns. Also, by minimizing the gradient, we try to avoid extra extrema on edges which would cause oscillations while keeping the consistency of the approximations. This enforces the monotonicity whenever possible. On the other hand, (2), (7) and (8) define a special quadrature rule to construct the gradient of a function on subcells around a vertex p^k_i knowing the surrounding cell center values. In one dimension, this is exactly the usual finite volume procedure. One can easily extend the procedure to three dimensions.

Remark 42

a) Let us point out some trivial setup on triangular meshes.

i) First we assume the center points at the isobarycenter of triangles and subcells constructed such that the edges are divided exactely in the middle. We assume the virtual subedge points $X^k_{p_i,j-1/2}$ *being placed such that* $\|\overrightarrow{p^k_i\, X^k_{p_i,j-1/2}}\| = (2/3)m^k_{p_i,j-1/2}$ *(cf. Figure 7); then (7) reduces to (5).*

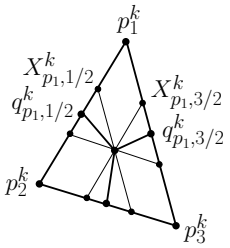

Fig. 7 Subdivision of a triangle cell using its isobarycenter and the middle of edges.

ii) Secondly, we assume the setup defined in [1]; namely, the center points X^k_S *and the subcells are constructed such that the boundary points* $q^k_{p_i,j-1/2}$ *on* $\sigma^k_{p_i,j-1/2}$ *with* $\|\overrightarrow{p^k_i\, q^k_{p_i,j-1/2}}\| = m^k_{p_i,j-1/2}$ *satisfy the orthogonality conditions* $\Big[\big(\mathcal{D}^k_{p_i,j-1}\big)^{-1}\,(\overrightarrow{X^k_{p_i,j-1}\; q^k_{p_i,j-1/2}})\Big]\cdot\overrightarrow{p^k_i\; q^k_{p_i,j-1/2}} = 0$ *and* $\Big[\big(\mathcal{D}^k_{p_i,j}\big)^{-1}\,(\overrightarrow{X^k_{p_i,j}\; q^k_{p_i,j-1/2}})\Big]\cdot\overrightarrow{p^k_i\; q^k_{p_i,j-1/2}} = 0$ *(cf. Figure 8). If we choose* $X^k_{p_i,j-1/2} = q^k_{p_i,j-1/2}$*, (7) reduces to (5). Here, (3) links the virtual unknown* $U^k_{p_i,j-1/2}$ *only to the cells*

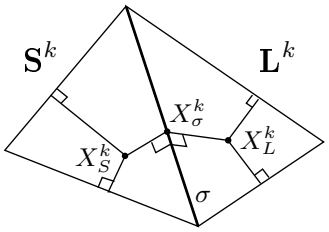

Fig. 8 A sketch of the local configuration of center points and subedge points satisfying the orthogonality condition. The two neighboring cells are not always coplanar.

unknowns $U^k_{p_i,j-1}$ *and* $U^k_{p_i,j}$ *across the subedge* $\sigma^k_{p_i,j-1/2}$*; thus the local matrices* $M^k_{p_i}$ *are diagonal.*

iii) We could also define $\mathcal{D}^k_{p_i,j}$ *as being constant around vertices* p^k_i*; for instance*

$$\mathcal{D}^k_{p_i,j} = \mathcal{D}^k_{p_i} := \left(1/\sum_j m^k_{p_i,j}\right)\sum_j \int_{S^{l,k}_j} \mathcal{D}\, dS^{l,k}_{p_i,j}.$$

i.e., The summation is done on subcells around p^k_i*. Let us restrict ourselves to triangular meshes on flat surfaces. We consider the dual mesh obtained by first*

joining the center points of triangles sharing a common edge, secondly join the middle of triangle edges σ^k that belong to the mesh boundary ($\sigma^k \subset \partial\Gamma_h^k$) to the center of the coresponding triangles. This setup is depicted on Figure 9. We adopt the vertices of the previous mesh as the center points of this new mesh. Each interior vertex of the dual mesh is surrounded by exactly three subcells

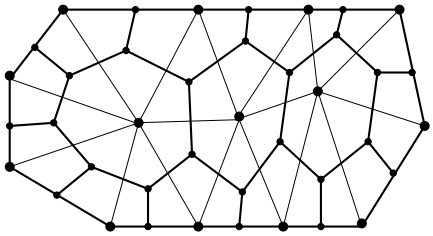

Fig. 9 A sketch of a triangular mesh (delimited by thin line) and its dual (delimited by thick line).

and (7) reduces to (5) since there is only one way to build a gradient from three noncolinear points.

b) If we had to treat the case of Neumann boundary condition or mixed boundary condition (Dirichlet-Neumann), then for any subedge $\sigma_{p_i,j}^k \subset \Gamma_h^k$, only one type of boundary condition should be defined on $\sigma_{p_i,j}^{l,k}$. We obtain (4) by adding extra equations to (3) which correspond to the realization of the Neumann boundary condition at corresponding subedge virtual points.

Based on these preliminaries, we can now introduce the finite volume discretization.

4.3 Finite Volumes discretization

Let us integrate (1) on $\left\{(t,x)|t \in [t_k, t_{k+1}], x \in S^{l,k}(t) \cap \Gamma(t)\right\}$, where $S^{l,k}(t) := \Phi(t, \Phi^{-1}(t_k, S^{l,k}))$.

$$\int_{t_k}^{t_{k+1}} \int_{S^{l,k}(t)\cap\Gamma(t)} g \,\mathrm{d}a \,\mathrm{d}t \approx \tau\, m_S^{k+1} G_S^{k+1}, \tag{9}$$

where $G_S^{k+1} := g\left(t, \mathcal{P}^{k+1} X_S^{k+1}\right)$. As in [1], the use of the Leibniz formula leads to the following approximation of the material derivative

$$\begin{aligned} &\int_{t_k}^{t_{k+1}} \int_{S^{l,k}(t)\cap\Gamma(t)} (\dot{u} + u\nabla_\Gamma v)\, \mathrm{d}a \,\mathrm{d}t \\ &= \int_{S^{l,k}(t_{k+1})\cap\Gamma(t_{k+1})} u \,\mathrm{d}a - \int_{S^{l,k}(t_k)\cap\Gamma(t_k)} u \,\mathrm{d}a \;\approx\; m_S^{k+1} U_S^{k+1} - m_S^k U_S^k, \end{aligned} \tag{10}$$

where we recall that the discrete quantities U_S^k and U_S^{k+1} approximate $u\left(t_k, \mathcal{P}^k X_S^k\right)$ and $u\left(t_{k+1}, \mathcal{P}^{k+1} X_S^{k+1}\right)$, respectively. Integrating the elliptic term

again over the temporal evolution of a lifted cell and applying the Gauss' theorem, leads to the following approximation

$$
\begin{aligned}
&\int_{t_k}^{t_{k+1}} \int_{S^{l,k}(t)\cap\Gamma(t)} \nabla_\Gamma \cdot (\mathcal{D}\nabla_\Gamma u)\, \mathrm{d}a\, \mathrm{d}t \\
&= \int_{t_k}^{t_{k+1}} \int_{\partial\left(S^{l,k}(t)\cap\Gamma(t)\right)} (\mathcal{D}\nabla_\Gamma u)\cdot n_{\partial\left(S^{l,k}(t)\cap\Gamma(t)\right)} dl\, \mathrm{d}t \\
&\approx \tau \sum_{p_i\in\partial S^k} \Big(m^{k+1}_{p_i,\mathcal{J}(p_i,S)-1/2} \mathcal{D}^k_{p_i,\mathcal{J}(p_i,S)} \nabla^{k+1}_{p_i,\mathcal{J}(p_i,S)} u \cdot n^{k+1}_{p_i,\mathcal{J}(p_i,S)|\mathcal{J}(p_i,S)-1/2} \\
&+ m^{k+1}_{p_i,\mathcal{J}(p_i,S)+1/2} \mathcal{D}^k_{p_i,\mathcal{J}(p_i,S)} \nabla^{k+1}_{p_i,\mathcal{J}(p_i,S)} u \cdot n^{k+1}_{p_i,\mathcal{J}(p_i,S)|\mathcal{J}(p_i,S)+1/2} \Big).
\end{aligned} \tag{11}
$$

where $n_{\partial\left(S^{l,k}(t)\cap\Gamma(t)\right)}$ is the unit outer conormal to the curved boundary $\partial\left(S^{l,k}(t)\cap\Gamma(t)\right)$ of $\left(S^{l,k}(t)\cap\Gamma(t)\right)$. We recall that $\mathcal{J}(p_i,S^k)$ denotes the local number of the cell S^k around p_i^k. Combining (2), (9), (10) and (11) gives the finite volume scheme

$$
\begin{aligned}
&m_S^{k+1}U_S^{k+1} - m_S^k U_S^k \\
&- \tau \sum_{p_i\in\partial S^k} \Big[m^{k+1}_{p_i,\mathcal{J}(p_i,S)-1/2} \left(U^{k+1}_{p_i,\mathcal{J}(p_i,S)-1/2} - U^{k+1}_{p_i,\mathcal{J}(p_i,S)} \right) \lambda^{k+1}_{p_i,\mathcal{J}(p_i,S)|\mathcal{J}(p_i,S)-1/2} \\
&+ m^{k+1}_{p_i,\mathcal{J}(p_i,S)-1/2} \left(U^{k+1}_{p_i,\mathcal{J}(p_i,S)+1/2} - U^{k+1}_{p_i,\mathcal{J}(p_i,S)} \right) \lambda^{k+1}_{p_i,\mathcal{J}(p_i,S)+1/2|\mathcal{J}(p_i,S)|\mathcal{J}(p_i,S)-1/2} \\
&+ m^{k+1}_{p_i,\mathcal{J}(p_i,S)+1/2} \left(U^{k+1}_{p_i,\mathcal{J}(p_i,S)-1/2} - U^{k+1}_{p_i,\mathcal{J}(p_i,S)} \right) \lambda^{k+1}_{p_i,\mathcal{J}(p_i,S)-1/2|\mathcal{J}(p_i,S)|\mathcal{J}(p_i,S)+1/2} \\
&+ m^{k+1}_{p_i,\mathcal{J}(p_i,S)+1/2} \left(U^{k+1}_{p_i,\mathcal{J}(p_i,S)+1/2} - U^{k+1}_{p_i,\mathcal{J}(p_i,S)} \right) \lambda^{k+1}_{p_i,\mathcal{J}(p_i,S)|\mathcal{J}(p_i,S)+1/2} \Big] \\
&= \tau\, m_S^{k+1} G_S^{k+1}.
\end{aligned} \tag{12}
$$

where the subedge virtual unknowns $U^{k+1}_{p_i,\mathcal{J}(p_i,S)-1/2}$ and $U^{k+1}_{p_i,\mathcal{J}(p_i,S)+1/2}$ are given by equation (7) in terms of cells unknowns $U^{k+1}_{p_i,\mathcal{J}(p_i,S)}$. The system of equations (12) is completely determined by the initial data $U_S^0 := u(t_0,\mathcal{P}^0(X_S^0))$. Let us now associate to cells unknowns and subedges virtual unknowns the piecewise constant functions U^k defined on Γ_h^k with $U^k|_S = U_S^k$, and $U^k_{\partial\Gamma}$ defined on $\partial\Gamma_h^k$ with $U^k_{\partial\Gamma}|_{\sigma^k_{p_i,1/2}} = U^k_{p_i,1/2}$, $U^k_{\partial\Gamma}|_{\sigma^k_{p_i,n_{p_i}+1/2}} = U^k_{p_i,n_{p_i}+1/2}$ for any boundary vertex p_i and its surrounding boundary subedges $\sigma^k_{p_i,1/2}$ and $\sigma^k_{p_i,n_{p_i}+1/2}$. We denote by

$$
\mathcal{V}_h^k := \left\{ U^k : \Gamma_h^k \to \mathbb{R} \mid \forall\, S^k \subset \Gamma_h^k,\ U^k|_{S^k} = \text{const} \right\} \tag{13}
$$

$$
\begin{aligned}
\mathcal{V}^k_{\partial\Gamma} := \Big\{ U^k_{\partial\Gamma} : \partial\Gamma_h^k \to \mathbb{R} \mid \forall\, p_i^k \in \partial\Gamma_h^k,\ U^k_{\partial\Gamma}|_{\sigma^k_{p_i,1/2}} = \text{const}, \\
U^k_{\partial\Gamma}|_{\sigma^k_{p_i,n_{p_i}+1/2}} = \text{const} \Big\}
\end{aligned} \tag{14}
$$

the sets of such functions. (2) can be considered as a quadrature rule that builds an approximate gradient of a continuous function on Γ^k out of its projection (representant)

in $\mathcal{V}_h^k \cup \mathcal{V}_{\partial\Gamma}^k$. We wish to build a seminorm on $\mathcal{V}_h^k$. For this sake, we first denote by

$$\begin{aligned}\mathfrak{I}\mathfrak{D}_S^k := \frac{1}{m_S^k} \sum_{p_i \in \partial S^k} \Big[& m^k_{p_i,\mathcal{J}(p_i,S)-1/2} \Big(\mathcal{D}^k_{p_i,\mathcal{J}(p_i,S)} \nabla^k_{p_i,\mathcal{J}(p_i,S)} u \Big) \cdot n^k_{p_i,\mathcal{J}(p_i,S)|\mathcal{J}(p_i,S)-1/2} \\ & + m^k_{p_i,\mathcal{J}(p_i,S)+1/2} \Big(\mathcal{D}^k_{p_i,\mathcal{J}(p_i,S)} \nabla^k_{p_i,\mathcal{J}(p_i,S)} u \Big) \cdot n^k_{p_i,\mathcal{J}(p_i,S)|\mathcal{J}(p_i,S)+1/2} \Big] \end{aligned} \tag{15}$$

the approximation of $\int_{S^{l,k}(t_k)\cap\Gamma(t_k)} \nabla_\Gamma \cdot (\mathcal{D}\nabla_\Gamma u)\, \mathrm{d}a$. We thereafter multiply each equation of (15) by the corresponding cell center value $-U_S^k$, and each equation of (3) by the corresponding subedge virtual unknown $U^k_{p_i,j-1/2}$. Finally, we sum the resulting equations over all cells and subedges and obtain

$$\begin{aligned} & -\sum_{S^k} m_S^k\, U_S^k\, \mathfrak{I}\mathfrak{D}_S^k \\ = & \sum_{S^k} \sum_{p_i^k \in S^k} \Big[(U^k_{p_i,\mathcal{J}(p_i,S^k)+1/2} - U_S^k), \Big(U^k_{p_i,\mathcal{J}(p_i,S^k)-1/2} - U_S^k \Big) \Big] \\ & Q^k_{p_i,\mathcal{J}(p_i,S^k),sym} \Big[(U^k_{p_i,\mathcal{J}(p_i,S^k)+1/2} - U_S^k), \Big(U^k_{p_i,\mathcal{J}(p_i,S^k)-1/2} - U_S^k \Big) \Big]^\top \\ & - \sum_{p_i^k \in \partial\Gamma_h^k} \Big(m^k_{p_i,1/2}\, U^k_{p_i,1/2}\, \mathcal{D}^k_{p_i,1} \nabla^k_{p_i,1} u \cdot n^k_{p_i,1|1/2} \\ & \quad + \; m^k_{p_i,n_{p_i}+1/2}\, U^k_{p_i,n_{p_i}+1/2}\, \mathcal{D}^k_{p_i,n_{p_i}} \nabla^k_{p_i,n_{p_i}} u \cdot n^k_{p_i,n_{p_i}|n_{p_i}+1/2} \Big), \end{aligned} \tag{16}$$

where $Q^k_{p_i,\mathcal{J}(p_i,S^k),sym} = \Big(Q^k_{p_i,\mathcal{J}(p_i,S^k)} + (Q^k_{p_i,\mathcal{J}(p_i,S^k)})^\top \Big)/2$ with

$$\begin{aligned} \Big(Q^k_{p_i,\mathcal{J}(p_i,S^k)} \Big)_{11} &:= m^k_{p_i,\mathcal{J}(p_i,S^k)-1/2} \lambda^k_{p_i,\mathcal{J}(p_i,S^k)|\mathcal{J}(p_i,S^k)-1/2}, \\ \Big(Q^k_{p_i,\mathcal{J}(p_i,S^k)} \Big)_{12} &:= m^k_{p_i,\mathcal{J}(p_i,S^k)-1/2} \lambda^k_{p_i,\mathcal{J}(p_i,S^k)+1/2|\mathcal{J}(p_i,S^k)|\mathcal{J}(p_i,S^k)-1/2}, \\ \Big(Q^k_{p_i,\mathcal{J}(p_i,S^k)} \Big)_{21} &:= m^k_{p_i,\mathcal{J}(p_i,S^k)+1/2} \lambda^k_{p_i,\mathcal{J}(p_i,S^k)-1/2|\mathcal{J}(p_i,S^k)|\mathcal{J}(p_i,S^k)+1/2}, \\ \Big(Q^k_{p_i,\mathcal{J}(p_i,S^k)} \Big)_{22} &:= m^k_{p_i,\mathcal{J}(p_i,S^k)+1/2} \lambda^k_{p_i,\mathcal{J}(p_i,S^k)|\mathcal{J}(p_i,S^k)+1/2}. \end{aligned}$$

We rewrite (16) in a matrix form using (7) as follows

$$\begin{aligned} & -\sum_{S^k} m_S^k\, U_S^k\, \mathfrak{I}\mathfrak{D}_S^k \\ = & \sum_{p_i \in \Gamma_h^k} \Big(\widetilde{U}^k_{p_i} \Big)^\top A^k_{p_i}\, \widetilde{U}^k_{p_i} - \sum_{p_i^k \in \partial\Gamma_h^k} \Big(m^k_{p_i,1/2}\, U^k_{p_i,1/2}\, \mathcal{D}^k_{p_i,1} \nabla^k_{p_i,1} u \cdot n^k_{p_i,1|1/2} \\ & \quad + \; m^k_{p_i,n_{p_i}+1/2}\, U^k_{p_i,n_{p_i}+1/2}\, \mathcal{D}^k_{p_i,n_{p_i}} \nabla^k_{p_i,n_{p_i}} u \cdot n^k_{p_i,n_{p_i}|n_{p_i}+1/2} \Big), \end{aligned} \tag{17}$$

where $A^k_{p_i}$ is defined by:
$A^k_{p_i} := A^k_{p_i,c} - A^k_{p_i,\sigma} \mathbf{Coef}^k_{p_i}$ with $A^k_{p_i,c}$ being a diagonal matrix and $A^k_{p_i,\sigma}$ a sparse matrix whose nonzero elements are given by

$$
\begin{aligned}
(A^k_{p_i,c})_{j,j} &:= m^k_{p_i,j-1/2}(\lambda^k_{p_i,j|j-1/2} + \lambda^k_{p_i,j+1/2|j|j-1/2}) \\
&\quad + \ m^k_{p_i,j+1/2}(\lambda^k_{p_i,j|j+1/2} + \lambda^k_{p_i,j-1/2|j|j+1/2}),\\
(A^k_{p_i,\sigma})_{j,j} &:= m^k_{p_i,j-1/2}\lambda^k_{p_i,j|j-1/2} + m^k_{p_i,j+1/2}\lambda^k_{p_i,j-1/2|j|j+1/2},\\
(A^k_{p_i,\sigma})_{j,j+1} &:= m^k_{p_i,j-1/2}\lambda^k_{p_i,j+1/2|j|j-1/2} + m^k_{p_i,j+1/2}\lambda^k_{p_i,j|j+1/2},
\end{aligned}
$$

for interior points. For boundary points,
$A^k_{p_i} := A^k_{p_i,c} - A^k_{p_i,\sigma}\mathbf{Coef}^k_{p_i}$ with $A^k_{p_i,c}$ being a sparse square matrix and $A^k_{p_i,\sigma}$ a sparse rectangular matrix whose nonzero elements are given by

$$
\begin{aligned}
(A^k_{p_i,c})_{1,1} &:= m^k_{p_i,1/2}\,\lambda^k_{p_i,1|1/2},\\
(A^k_{p_i,c})_{1,2} &:= -m^k_{p_i,1/2}\,(\lambda^k_{p_i,1|1/2} + \lambda^k_{p_i,3/2|1|1/2}),\\
(A^k_{p_i,c})_{2,1} &:= -(m^k_{p_i,1/2}\,\lambda^k_{p_i,1|1/2} + m^k_{p_i,3/2}\,\lambda^k_{p_i,1/2|1|3/2}),\\
(A^k_{p_i,c})_{j,j} &:= m^k_{p_i,j-1/2}(\lambda^k_{p_i,j|j-1/2} + \lambda^k_{p_i,j+1/2|j|j-1/2})\\
&\quad + \ m^k_{p_i,j+1/2}\,(\lambda^k_{p_i,j|j+1/2} + \lambda^k_{p_i,j-1/2|j|j+1/2}),\\
&\quad \forall\ j = 2,3,\cdots,n_{p_i}+1,\\
(A^k_{p_i,c})_{n_{p_i}+1,n_{p_i}+2} &:= -\Big(m^k_{p_i,n_{p_i}-1/2}\,\lambda^k_{p_i,n_{p_i}+1/2|n_{p_i}|n_{p_i}-1/2}\\
&\quad + \ m^k_{p_i,n_{p_i}+1/2}\,\lambda^k_{p_i,n_{p_i}|n_{p_i}+1/2}\Big),\\
(A^k_{p_i,c})_{n_{p_i}+2,n_{p_i}+1} &:= -m^k_{p_i,n_{p_i}+1/2}\,(\lambda^k_{p_i,n_{p_i}-1/2|n_{p_i}|n_{p_i}+1/2} + \lambda^k_{p_i,n_{p_i}|n_{p_i}+1/2}),\\
(A^k_{p_i,c})_{n_{p_i}+2,n_{p_i}+2} &:= m^k_{p_i,n_{p_i}+1/2}\,\lambda^k_{p_i,n_{p_i}|n_{p_i}+1/2},
\end{aligned}
$$

$$
\begin{aligned}
(A^k_{p_i,\sigma})_{1,1} &:= -m^k_{p_i,1/2}\,\lambda^k_{p_i,3/2|1|1/2},\\
(A^k_{p_i,\sigma})_{2,1} &:= m^k_{p_i,1/2}\,\lambda^k_{p_i,3/2|1|1/2} + m^k_{p_i,3/2}\,\lambda^k_{p_i,1|3/2},\\
(A^k_{p_i,\sigma})_{j+2,j} &:= m^k_{p_i,j-1/2}\,\lambda^k_{p_i,j|j-1/2}, + m^k_{p_i,j+1/2}\,\lambda^k_{p_i,j-1/2|j|j+1/2},\\
(A^k_{p_i,\sigma})_{j+2,j+1} &:= m^k_{p_i,j-1/2}\,\lambda^k_{p_i,j+1/2|j|j-1/2}, + m^k_{p_i,j+1/2}\,\lambda^k_{p_i,j|j+1/2},\\
&\quad \forall\ j = 1,2,\cdots,n_{p_i}-2,\\
(A^k_{p_i,\sigma})_{n_{p_i}+1,n_{p_i}-1} &:= m^k_{p_i,n_{p_i}-1/2}\,\lambda^k_{p_i,n_{p_i}|n_{p_i}-1/2}\\
&\quad + \ m^k_{p_i,n_{p_i}+1/2}\,\lambda^k_{p_i,n_{p_i}-1/2|n_{p_i}|n_{p_i}+1/2},\\
(A^k_{p_i,\sigma})_{n_{p_i}+2,n_{p_i}-1} &:= -m^k_{p_i,n_{p_i}+1/2}\,\lambda^k_{p_i,n_{p_i}-1/2|n_{p_i}|n_{p_i}+1/2}.
\end{aligned}
$$

Since $\mathbf{Coef}^k_{p_i}$ is not defined for $n_{p_i} = 1$, $A^k_{p_i} := A^k_{p_i,c}$ in that case.
The submatrices $A^k_{p_i}$ satisfy $A^k_{p_i}\mathbf{1}_{p_i} = \mathbf{0}_{p_i}$, where $\mathbf{1}_{p_i} := (1,1,\cdots)^\top$ and $\mathbf{0}_{p_i} := (0,0,\cdots)^\top$. This is due to the minimization procedure introduced in the interpolation of the virtual values on subedges. The procedure forces the system to pick the solution of minimum gradient norm. Let us also remark that if the submatrices $A^k_{p_i} + (\mathbf{1}_{p_i}\otimes\mathbf{1}_{p_i})/n_{p_i}$ are positive semi-definite for all vertices, $\sum_{p_i\in\Gamma^k_h}\left(\widetilde{U}^k_{p_i}\right)^\top A^k_{p_i}\,\widetilde{U}^k_{p_i}$ defines a seminorm on $\mathcal{V}^k_h\cup\mathcal{V}^k_{\partial\Gamma}$. Also, if the submatrices $A^k_{p_i} + (\mathbf{1}_{p_i}\otimes\mathbf{1}_{p_i})/n_{p_i}$ are strictly

positive definite for all vertices, $\sum_{p_i \in \Gamma_h^k} \left(\widetilde{U}_{p_i}^k\right)^\top A_{p_i}^k \widetilde{U}_{p_i}^k$ will define a norm on $\mathcal{V}_h^k \cup \{0_{\mathcal{V}_{\partial\Gamma}^k}\}$, where $0_{\mathcal{V}_{\partial\Gamma}^k} = (0, 0, \cdots, 0)$ is the zero element of $\mathcal{V}_{\partial\Gamma}^k$. Since the submatrices $A_{p_i}^k$ basically depend on the choice of the subedges virtual points and the discrete cell tensor $\mathcal{D}_{p_i,j}^k$ around p_i^k, we can assume the virtual points being chosen such that the submatrices $A_{p_i}^k + (\mathbf{1}_{p_i} \otimes \mathbf{1}_{p_i})/n_{p_i}$ are strictly positive definite as the diffusion tensors are supposed to be strictly positive definite. Although this assumption is reasonable, it is not useful to require its realization for all the vertices. In case a highly anisotropic tensor is involved in the computation and the mesh very distorted too, the condition might not be satisfied. We will then weaken the assumption by introducing a slight modification of the algorithm. Let us assume the center points being chosen in advance.

Definition 43 *(Regular vertex and uniformly regular vertex)*
We will say that a vertex p_i^k is regular if the following is satisfied:

i) It is possible to choose the virtual subcells $S_{p_i,j}^k$ and the subedge virtual points $X_{p_i,j-1/2}^k$ around p_i^k such that $A_{p_i}^k + (\mathbf{1}_{p_i} \otimes \mathbf{1}_{p_i})/n_{p_i}$ is strictly elliptic,
ii) If p_i^k is an interior vertex, then it is surrounded by at least three cells.

Any vertex which does not fulfill these requirements will be called nonregular.
A vertex will be called uniformly regular if it is regular for any time step k.

Definition 44 *(Regular polygonisation and uniformly regular polygonisation)*
We will say that an admissible polygonal surface Γ_h^k is regular if any of its nonregular vertex is surrounded by regular vertices.
Γ_h^k will be called uniformly regular if it is regular and any of its regular vertex is uniformly regular.

In the sequel we assume our polygonal surfaces to be uniformly regular. We now introduce a slight modification of the scheme. For any nonregular vertex p_i, we assume that the surrounding subcells have zero measure; which means that the subedges $\sigma_{p_i,j-1/2}^k$ around p_i^k have zero measure. Thus there is no equation written around that vertex. We will also assume the submatrices
$A_{p_i}^k + (\mathbf{1}_{p_i} \otimes \mathbf{1}_{p_i})/n_{p_i}$ to be uniformly strictly elliptic for all regular points (i.e. $\exists\, \alpha > 0 | \forall\, p_i^k, \forall\, U_{p_i}^k, \left(U_{p_i}^k\right)^\top \left(A_{p_i}^k + (\mathbf{1}_{p_i} \otimes \mathbf{1}_{p_i})/n_{p_i}\right) U_{p_i}^k \geq \alpha \|U_{p_i}^k\|^2$). The resulting scheme remains the same, except that the summation over vertices will be done over regular vertices. From now on, any summation over vertices will simply mean summation over regular vertices unless specified otherwise. A straightforward example of meshes needing this setup can be found on Figure 5, when we consider the dual mesh to our primary mesh. Let us mention here that the dual mesh of a primal mesh is the mesh whose cells are the union of virtual subcells around vertices and center points the vertices of the primal mesh. Here the points $q_{p_i,j-1/2}^k$ on edges which limit the virtual subcells of the primal mesh (*cf.* Figure 4) are nonregular vertices of the dual mesh and therefore will be subject to this treatment. We then define a discrete energy seminorm on $\mathcal{V}_h^k \cup \mathcal{V}_{\partial\Gamma}^k$.

Definition 45 *(Discrete $\mathbb{H}_0^1$ seminorm) For $U^k \in \mathcal{V}^k$ and $U_{\partial\Gamma}^k \in \mathcal{V}_{\partial\Gamma}^k$, we define*

$$\|U^k\|_{1,\Gamma_h^k}^2 = \sum_{p_i} \left(\widetilde{U}_{p_i}^k\right)^\top A_{p_i}^k \widetilde{U}_{p_i}^k \tag{18}$$

We also define the discrete $\mathbb{L}^2$ norm as follows

Definition 46 *(Discrete $\mathbb{L}^2$ norm) For $U^k \in \mathcal{V}^k$ we define*

$$\|U^k\|^2_{\mathbb{L}^2(\Gamma_h^k)} = \sum_S m_S^k \left(U_S^k\right)^2 \tag{19}$$

Proposition 47 *(Existence and uniqueness) The discrete problem (12) has a unique solution.*

Proof The system (12) has a unique solution $U^k \in \mathcal{V}^k$ if the kernel of the corresponding linear operator is trivial. To prove this, we consider the homogeneous system obtained by assuming $U^k \equiv 0$, $G^k \equiv 0$ and the homogeneous Dirichlet boundary condition $U_{\partial\Gamma}^{k+1} \equiv 0$. Next, we multiply each equation of (12) by the corresponding cell center unknown U_S^{k+1} and sum over all cells. Taking into account (17), we obtain

$$\|U^{k+1}\|^2_{\mathbb{L}^2(\Gamma_h^k)} + \tau \|U^{k+1}\|^2_{1,\Gamma_h^k} = 0,$$

from which $U^{k+1} \equiv 0$ follows.

□

4.4 Maximum principle

Let us consider around each uniformly regular vertex p_i^k, the matrix $\mathbf{W}_{p_i}^k$ whose entries are defined by

$$\left(\mathbf{W}_{p_i}^k\right)_{j,j} := m^k_{p_i,j-1/2}\lambda^k_{j|j-1/2} + m^k_{p_i,j+1/2}\lambda^k_{j-1/2|j|j+1/2},$$
$$\left(\mathbf{W}_{p_i}^k\right)_{j,j+1} := m^k_{p_i,j-1/2}\lambda^k_{j+1/2|j|j-1/2} + m^k_{p_i,j+1/2}\lambda^k_{j|j+1/2},$$

and 0 elsewhere. We also consider the column vector $\mathbf{e}_{p_i,j}$ of length the number of columns of $\mathbf{Coef}_{p_i}^k$ with components $(\mathbf{e}_{p_i,j})_j := 1$ and 0 elsewhere (i.e. $\mathbf{e}_{p_i,j} := (0,\cdots,0,1,0,\cdots,0)^\top$) and the augmented matrix of coefficients $\mathbf{ACoef}_{p_i}^k$ defined by $\mathbf{ACoef}_{p_i}^k := \mathbf{Coef}_{p_i}^k$ if p_i^k is an interior uniformly regular point. For boundary points, $\mathbf{ACoef}_{p_i}^k := \left[(\mathbf{e}_{p_i,1})^\top; \mathbf{Coef}_{p_i}^k; \left(\mathbf{e}_{p_i,n_{p_i}+1}\right)^\top\right]$, concatenation of the vector $(\mathbf{e}_{p_i,1})^\top$, the matrix $\mathbf{Coef}_{p_i}^k$, and the vector $\left(\mathbf{e}_{p_i,n_{p_i}+1}\right)^\top$.

Proposition 48 *If $\forall\, S$, $U_S^0 \geq 0$ and at any time step t_k, $\left(U_{\partial\Gamma}^k\right)_i \geq 0\ \forall\, i$, $G_S^k \geq 0\ \forall\, S$, and the matrices $\mathbf{W}_{p_i}^k\mathbf{ACoef}_{p_i}^k$ are positive $\left(\left(\mathbf{W}_{p_i}^k\mathbf{ACoef}_{p_i}^k\right)_{i,j} \geq 0\ \forall\, i,j\right)$, then $U_S^k \geq 0\ \forall\, k,\ \forall\, S$.*

Proof Let us first assume the uniformly regular vertices p_i of a given cell S being numbered by $s(p_i)$. We define for the cell S the column vectors $\mathbf{e}_{S,j}$ of length the number of subcells on S, with components $(\mathbf{e}_{S,j})_j := 1$ and 0 elsewhere (i.e. $\mathbf{e}_{S,j} := (0,\cdots,0,1,0,\cdots,0)^\top$). The system (12) can be rewritten as

$$m_S^{k+1}U_S^{k+1} - m_S^k U_S^k - \tau \sum_{p_i \in \partial S^k} \left(\mathbf{e}_{S,s(p_i)}\right)^\top \left(\mathbf{W}_{p_i}^{k+1}\mathbf{ACoef}_{p_i}^{k+1}\right)\left(U_{p_i}^{k+1} - U_S^{k+1}\mathbf{1}_{p_i}\right)$$
$$= \tau\, m_S^{k+1}G_S^{k+1}. \tag{20}$$

Let us assume that $U_S^k \geq 0 \; \forall \; S^k$, the minimum of U^{k+1} $(min_S \; U_S^{k+1})$ is reached in a cell S_0^{k+1}, and that $U_{S_0}^{k+1} := min_S \; U_S^{k+1} < 0$; then (20) cannot be satisfied for the cell S_0^{k+1} since all components of the vector $\left(U_{p_i}^{k+1} - U_S^{k+1}\mathbf{1}_{p_i}\right)$ are nonnegative. Hence, we conclude that $U_{S_0}^{k+1} \geq 0$.

□

This proposition will be of great importance in the next paragraph, especially when one of our aim will be to satisfy the maximum principle.

4.5 Implementation

Let us first consider the setups defined for triangular meshes in Remark 42 a) part *i*) and *ii*). For these setups, the submatrices $Q_{p_i,j}^k$ defined for equation (16) are symmetric and strictly positive definite; thus the vertices p_i^k are uniformly regular. Hence the scheme works for any triangular mesh as long as cells do not degenerate. Restricting to the flat case and using the setup in Remark 42 a) part *i*), the present scheme coincides exactly with the scheme proposed by K. Lipnikov, M. Shashkov and I. Yotov in [11] and as already said, is identical to the one presented by Le Potier in [10]. We should also mention that for the setup presented in Remark 42 a) part *ii*), we obtain exactly the scheme presented in [1]; moreover, the hypotheses of Proposition 48 are satisfied and the resulting matrix is a M–matrix. This last property is not evident for all meshes. We can nevertheless enforce it whenever possible. This will be one of our goals when trying to build on a given mesh, a setup on which the present scheme can be applied. Next, we consider a dual mesh of a triangular mesh. As defined above, this is constructed from the primal mesh and its virtual subcells by grouping the virtual subcells around each vertex p_i^k to form the cells of the dual mesh. We refer again to Figure 9 for an example of a triangular dual mesh in a flat case. We should nevertheless mention that in the curved case, virtual subcells around the vertices are not coplanar. For these meshes, virtual subcells of primal meshes are also considered as virtual subcells of dual meshes. As already mentioned in Remark 42 a) part *iii*), each new vertex X_S^k, center of the triangle S^k, is surrounded by exactly three virtual subcells and therefore the construction of the gradient does not need any regularization. Also, the points X_S^k are uniformly regular points; consequently, any mesh which is the dual of a triangular mesh is suitable for the scheme. If we restrict ourselves to fixed surfaces, this last setup gives exactly the scheme presented by Lili Ju and Qiang Du in [16] when the diffusion tensor is taken to be constant on triangles. As already reported there, if the triangles edge points $q_{p_i,j-1/2}^k$ that limit the subcells are taken to be the middle of triangles edges and the diffusion tensor taken to be constant on triangles, the resulting matrix is a symmetric $M-$matrix. In some cases it can be advantageous to use the dual mesh since one can reduce the number of variables.

Except in the trivial case of triangular meshes where one has some trivial choices of discrete points, we do need a good algorithm which always delivers the discrete points in such a way that the polygonal surface remains a uniformly regular polygonisation and the angle condition in Section 4.2 is satisfied for appropriate virtual points $X_{p_i,j-1/2}^k$ around vertices. Also, for some problems, especially in the field of chemistry, one needs to have additionally the maximum principle satisfied by the scheme. We give in the sequel an algorithm to construct the discrete points such that the maximum principle

is satisfied if possible. To begin with, we chose the center points in such a way that the surface of our cell is minimal. This is done by minimizing for each cell S^k the energy functional

$$E_S^k := \sum_{i=1:n_S} \frac{1}{2} \| \left(X - p_i^k\right) \wedge \left(p_{i+1}^k - p_i^k\right) \|^2$$

over X. This energy is in fact the sum of the square measure of the triangles $[X, p_i^k, p_{i+1}^k]$; p_i^k and p_{i+1}^k being two consecutive vertices of S^k. The resulting $X_S^k := \text{argmin}_{X \in \mathbb{R}^3} E_S^k$ guarantees the status of admissible cell to S^k and when the vertices are coplanar, X_S^k is the isobarycenter for triangular cells, rectangular cells and regular polygonal cells. Next, we define the edge points X_σ^k that limit the subcells on cell's boundary σ as the mid point of σ; but if an interior vertex p_i^k is surrounded by less than three cells, then all the points X_σ^k around the given vertex are set to p_i^k. We refer to Figure 10 for more illustration. We shall now fix the subedge virtual points. From Proposition 48, the

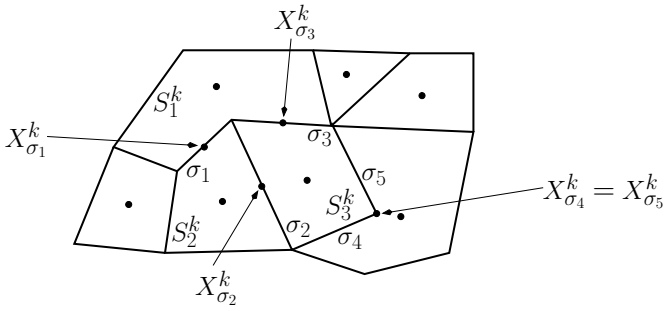

Fig. 10 Representation of edge points $X_{\sigma_j}^k$ and center points in cells.

scheme will satisfy the maximum principle if the submatrices $W_{p_i}^{k+1}\mathbf{ACoef}_{p_i}^{k+1}$ defined around uniformly regular points are positive. To enforce this, we find the virtual points by minimizing the energy

$$E_3^k := \text{tr}\left[\left(W_{p_i}^{k+1}\mathbf{ACoef}_{p_i}^{k+1} - \alpha\, \mathbf{1}_{p_i,S} \otimes \mathbf{1}_{p_i}\right)\left(W_{p_i}^{k+1}\mathbf{ACoef}_{p_i}^{k+1} - \alpha\, \mathbf{1}_{p_i,S} \otimes \mathbf{1}_{p_i}\right)^\top\right]$$

under the constraints that $A_{p_i}^k + (\mathbf{1}_{p_i} \otimes \mathbf{1}_{p_i})/n_{p_i}$ is strictly elliptic and the angles $\theta_{p_i,j}^k := \sphericalangle(X_{p_i,j-1/2}^k\ X_j^k\ X_{p_i,j+1/2}^k)$ between the covariant vectors $e_{p_i,j|j+1/2}^k$ and $e_{p_i,j|j-1/2}^k$ are greater than a threshold angle θ as requested in Section 4.2. Here, α is a positive constant, $\text{tr}\,(\cdot)$ the trace operator and $\mathbf{1}_{p_i,S} = (1, 1, \cdots)^\top$ a vector of ones with length n_{p_i}. This process tries to pull the coefficients of the submatrices $W_{p_i}^{k+1}\mathbf{ACoef}_{p_i}^{k+1}$ near α as possible. Finally, if the symmetric property of the global matrix is important, one can impose it here by setting the symmetry of the submatrices $Q_{p_i,j}^k$ as a constraint in this last minimization problem.

5 A priori estimates

We will now give the discrete counterparts of continuous a-priori estimates. They obviously depend on the behavior of the mesh during the evolution and a proper, in particular time coherent choice of center points X_S^k, subedge points $X_{p_i,j-1/2}^k$ and edge points X_σ^k. Let us assume that the center points X_S^k describe a time continuous C^1 curve $\gamma(t, X_S^0)$ (i.e. $X_S^k(t) := \gamma(t, \gamma^{-1}(t_k, X_S^k))$) during the time evolution. The algorithm described in Section 4.5 provides such a curve. We refer to [27; 28] for reading about the regularity of the solution of parametric minimization problems. One can also imagine X_S^k being transported by Φ (i.e. $X_S^k(t) := \Phi(t, \Phi^{-1}(t_k, X_S^k))$); of course, with the resulting $X_S^k(t)$ satisfying the necessary condition for the scheme to be applied. Let us identify a point x on the triangle $[X_S^k, p_i^k, p_{i+1}^k] \subset S^k$ by its barycentric coordinates $\beta_S^k(x)$, $\beta_{S,i}^k(x)$, $\beta_{S,i+1}^k(x)$ with respect to X_S^k, p_i^k, and p_{i+1}^k, respectively. (i.e. $x = \beta_S^k(x)X_S^k + \beta_{S,i}^k(x)p_i^k + \beta_{S,i+1}^k(x)p_{i+1}^k$). We construct the following map that transforms the cells during the time evolution:

$$\begin{aligned} \Upsilon^k(t,\cdot) : S^k &\longrightarrow \mathbb{R}^3, \\ x &\longmapsto x(t) := \beta_S^k(x)X_S^k(t) + \beta_{S,i}^k(x)p_i^k(t) + \beta_{S,i+1}^k(x)p_{i+1}^k(t), \end{aligned} \tag{21}$$

where $p_i^k(t) := \Phi(t, \Phi^{-1}(t_k, p_i^k)$. We also assume

$$\|\Upsilon^k(t_{k+1}, X_{j+1/2}^{k,i}) - X_{j+1/2}^{k+1,i}\| \le Ch\tau \tag{22}$$

$$|m_{p_i,j+1/2}^{k+1} - m_{p_i,j+1/2}^k| \le Ch\tau. \tag{23}$$

These conditions are obviously satisfied for the setups described in Section 4.5. Thanks to the conditions above, one easily establishes that
$\max_k \max_S \left| \frac{m_S^k}{m_S^{k+1}} - 1 \right| \le C\,\tau$, and the $2-$norm

$$\left\| \left(A_{p_i,sym}^{k+1}\right)^{1/2} \left(A_{p_i,sym}^k\right)^{\dagger} \left(A_{p_i,sym}^{k+1}\right)^{1/2} - \left(\left(A_{p_i,sym}^{k+1}\right)^{1/2}\right)^{\dagger} \left(A_{p_i,sym}^{k+1}\right)^{1/2} \right\|_2 \le C\tau.$$

Theorem 51 $\left(\textit{Discrete } \mathbb{L}^\infty(\mathbb{L}^2), \mathbb{L}^2(\mathbb{H}^1) \textit{ energy estimate}\right)$. *Let $\{U^k\}_{k=1,\cdots,k_{max}}$ be the discrete solution of (12) for a given discrete initial data $U^0 \in \mathcal{V}_h^0$ and the homogenous boundary condition $\{U_{\partial\Gamma}^k\}_{k=1,\cdots,k_{max}} \equiv 0$, then there exists a constant C depending solely on t_{max} such that*

$$\max_{k=1,\cdots,k_{max}} \|U^k\|_{\mathbb{L}^2(\Gamma_h^k)}^2 + \sum_{k=1}^{k_{max}} \tau \|U^k\|_{1,\Gamma_h^k}^2 \le C \left(\|U^0\|_{\mathbb{L}^2(\Gamma_h^0)}^2 + \tau \sum_{k=1}^{k_{max}} \|G^k\|_{\mathbb{L}^2(\Gamma_h^k)}^2 \right). \tag{24}$$

Proof As in the proof of Proposition 47, we multiply each equation of (12) by the corresponding cell center value unknown U_S^{k+1} and sum up the resulting equations. Thanks to (17), we obtain

$$\sum_S \left(m_S^{k+1} \left(U_S^{k+1}\right)^2 - m_S^k U_S^k U_S^{k+1} \right) + \tau \|U^{k+1}\|_{1,\Gamma_h^{k+1}}^2 = \sum_S m_S^{k+1} G_S^{k+1} U_S^{k+1}, \tag{25}$$

and using Young's inequality and the estimate $\max_k \max_S \left|\frac{m_S^k}{m_S^{k+1}} - 1\right| \leq C\tau$, one obtains

$$\begin{aligned}&\frac{1}{2}\|U^{k+1}\|^2_{\mathbb{L}^2(\Gamma_h^{k+1})} + \tau\|U^{k+1}\|^2_{1,\Gamma_h^{k+1}}\\ &\leq \frac{1}{2}\|U^k\|^2_{\mathbb{L}^2(\Gamma_h^k)} + \frac{C}{2}\tau\|U^{k+1}\|^2_{\mathbb{L}^2(\Gamma_h^{k+1})} + \frac{1}{2}\tau\|G^{k+1}\|^2_{\mathbb{L}^2(\Gamma_h^{k+1})}.\end{aligned} \tag{26}$$

Using the notation $a_k := \|U^k\|^2_{\mathbb{L}^2(\Gamma_h^k)}$ and $b_k := \|G^k\|^2_{\mathbb{L}^2(\Gamma_h^k)}$, one can deduce from $a_k \leq a_{k-1} + C\tau a_k + \tau b_k$ that

$$a_k \;\leq\; (1-C\tau)^{-1}(a_{k-1}+\tau b_k) \;\leq\; \cdots \;\leq\; (1-C\tau)^{-k}(a_0 + \tau\sum_{j=1}^{k} b_j)$$

Since

$$(1-C\tau)^{-k} = \left(\left(1-\frac{Ct_k}{k}\right)^{-\frac{k}{Ct_k}}\right)^{Ct_k}$$

is bounded by $2e^{Ct_k}$ for sufficiently small τ, we immediately get the desired bound for $\|U^k\|^2_{\mathbb{L}^2(\Gamma_h^k)}$:

$$\|U^k\|^2_{\mathbb{L}^2(\Gamma_h^k)} \;\leq\; 2e^{Ct_k}\left(\|U^0\|^2_{\mathbb{L}^2(\Gamma_h^0)} + \tau\sum_{j=1}^{k}\|G^k\|^2_{\mathbb{L}^2(\Gamma_h^k)}\right).$$

We sum (26) over $k = 0, \cdots, k_{max}-1$ and compensate the terms $\|U^k\|^2_{\mathbb{L}^2(\Gamma_h^k)}$ on the right hand side for $k = 1, \cdots, k_{max}-1$ with those on the left, and using the already established estimate for the $\mathbb{L}^2$ norm gives the bound for $\sum_{k=1}^{k_{max}} \tau\|U^k\|^2_{1,\Gamma_h^k}$.

□

Theorem 52 $\left(\textit{Discrete } \mathbb{H}^1(\mathbb{L}^2), \mathbb{L}^\infty(\mathbb{H}^1) \textit{ energy estimate}\right)$. *Let us assume the submatrices $A^k_{p_i}$ around regular vertices to be symmetric. We also consider $\{U^k\}_{k=1,\cdots,k_{max}}$, the discrete solution of (12) for given discrete initial data $U^0 \in \mathcal{V}_h^0$ and the homogenous boundary condition*
$\{U^k_{\partial\Gamma}\}_{k=1,\cdots,k_{max}} \equiv 0$, then there exists a constant C depending solely on t_{max} such that

$$\begin{aligned}&\sum_{k=1}^{k_{max}} \tau\|\partial_t^\tau U^k\|^2_{\mathbb{L}^2(\Gamma_h^k)} + \max_{k=1,\cdots,k_{max}}\|U^k\|^2_{1,\Gamma_h^k}\\ &\leq C\left(\|U^0\|^2_{\mathbb{L}^2(\Gamma_h^0)} + \|U^0\|^2_{1,\Gamma_h^0} + \tau\sum_{k=1}^{k_{max}}\|G^k\|^2_{\mathbb{L}^2(\Gamma_h^k)}\right),\end{aligned} \tag{27}$$

where $\partial_t^\tau U^k = \frac{U^k - U^{k-1}}{\tau}$ is defined as a difference quotient in time.

Proof We multiply each equation of (12) by the corresponding cell center difference quotient value $\partial_t^\tau U_S^{k+1} \equiv \partial_t^\tau U^{k+1}|_S$, each equation of (3) by the corresponding subedge difference quotient value $\frac{U^{k+1}_{p_i,j+1/2} - \left(U^k_{p_i,j+1/2}\right)'}{\tau}$, where the values $\left(U^k_{p_i,j+1/2}\right)'$, components of the vector $\left(\widetilde{U}^k_{p_i,\sigma}\right)'$, are interpolation of the components of $\widetilde{U}^k_{p_i}$ on subedges $\sigma^{k+1}_{p_i,j+1/2}$ around p_i^{k+1} through formula (7) (i.e. $\left(\widetilde{U}^k_{p_i,\sigma}\right)' = \mathbf{Coef}^{k+1}_{p_i}\widetilde{U}^k_{p_i}$). Next, we sum the resulting equations over all cells and subedges to obtain

$$\begin{aligned}
&\tau \sum_{S^{k+1}} m_S^{k+1} \left(\frac{U_S^{k+1} - U_S^k}{\tau}\right)^2 + \sum_{p_i^k} \left(\widetilde{U}^{k+1}_{p_i}\right)^\top A^{k+1}_{p_i} \widetilde{U}^{k+1} - \left(\widetilde{U}^{k+1}_{p_i}\right)^\top A^{k+1}_{p_i} \widetilde{U}^k \\
&= \sum_S \left(m_S^k - m_S^{k+1}\right) U_S^k \frac{U_S^{k+1} - U_S^k}{\tau} + \tau \sum_S m_S^{k+1} G_S^{k+1} \frac{U_S^{k+1} - U_S^k}{\tau}. \qquad (28)
\end{aligned}$$

Since the matrices $A^k_{p_i} (k = 0, 1, 2, \cdots)$ are symmetric and have the same kernel,

$$A^{k+1}_{p_i} = A^{k+1}_{p_i} \left(\left(A^k_{p_i}\right)^{1/2}\right)^\dagger \left(A^k_{p_i}\right)^{1/2},$$

where $\left(A^k_{p_i}\right)^{1/2}$ is the symmetric matrix satisfying $A^k_{p_i} = \left(A^k_{p_i}\right)^{1/2} \left(A^k_{p_i}\right)^{1/2}$. Now, applying Young's inequality to equation (28) gives

$$\begin{aligned}
&\tau \sum_{S^{k+1}} m_S^{k+1} \left(\frac{U_S^{k+1} - U_S^k}{\tau}\right)^2 + \|U^{k+1}\|^2_{1,\Gamma_h^{k+1}} \\
&\le \frac{1}{2}\|U^k\|^2_{1,\Gamma_h^k} + \frac{1}{2} \sum_{p_i^k} \left(\widetilde{U}^{k+1}_{p_i}\right)^\top A^{k+1}_{p_i} \left(A^k_{p_i}\right)^\dagger A^{k+1}_{p_i} \widetilde{U}^{k+1} \\
&\quad + \sum_{p_i^k} \sum_S \left(m_S^k - m_S^{k+1}\right) U_S^k \frac{U_S^{k+1} - U_S^k}{\tau} + \tau \sum_S m_S^{k+1} G_S^{k+1} \frac{U_S^{k+1} - U_S^k}{\tau}.
\end{aligned}$$

Taking into account that

$$\begin{aligned}
&A^{k+1}_{p_i} \left(A^k_{p_i}\right)^\dagger A^{k+1}_{p_i} - A^{k+1}_{p_i} \\
&= \left(A^{k+1}_{p_i}\right)^{1/2} \left[\left(A^{k+1}_{p_i}\right)^{1/2} \left(A^k_{p_i}\right)^\dagger \left(A^{k+1}_{p_i}\right)^{1/2} - \left(\left(A^{k+1}_{p_i}\right)^{1/2}\right)^\dagger \left(A^{k+1}_{p_i}\right)^{1/2}\right] \left(A^{k+1}_{p_i}\right)^{1/2},
\end{aligned}$$

the $2-$norm $\left\|\left(A^{k+1}_{p_i}\right)^{1/2} \left(A^k_{p_i}\right)^\dagger \left(A^{k+1}_{p_i}\right)^{1/2} - \left(\left(A^{k+1}_{p_i}\right)^{1/2}\right)^\dagger \left(A^{k+1}_{p_i}\right)^{1/2}\right\|_2 \le C\tau,$

and

$\left|\frac{m_S^k}{m^{k+1}} - 1\right| \frac{\sqrt{m_S^{k+1}}}{\sqrt{m_S^k}} \le C\tau$, we deduce the inequality

$$\begin{aligned}
&\tau \frac{1}{2}\|\partial_t^\tau U^{k+1}\|^2 + \frac{1}{2}\|U^{k+1}\|^2_{1,\Gamma_h^{k+1}} \\
&\le \frac{1}{2}\|U^k\|^2_{1,\Gamma_h^k} + \frac{C}{2}\tau \left(\|U^{k+1}\|^2_{1,\Gamma_h^{k+1}} + \|U^k\|^2_{\Gamma_h^k} + \|G^{k+1}\|^2_{\Gamma_h^{k+1}}\right)
\end{aligned}$$

Finally, summing over all time steps and using Theorem 51 gives the desired result.

□

6 Convergence

In this section, we prove an error estimate for the finite volume solution $U^k \in \mathcal{V}_h^k$. At first, we have to state how to compare a discrete solution defined on the sequence of polygonizations Γ_h^k and a continuous solution defined on the evolving family of smooth surfaces $\Gamma(t)$. Here, we will take into account the lifting operator from the discrete surfaces Γ_h^k onto the continuous surfaces $\Gamma(t_k)$ already introduced in Section 4.1. As for the error analysis in [1], we use the pull back from the continuous surface onto a corresponding polygonization to compare the continuous solution $u(t_k)$ at time t_k with the discrete solution $U^k = \sum_S U_S^k \chi_{S^k}$ where χ_{S^k} is the characteristic function of the cell S^k. To be explicit, we consider the pull back $u^{-l}(t_k, X_S^k)$ of the continuous solution u at time t_k and investigate the error $u^{-l}(t_k, X_S^k) - U_S^k$ at the cell node X_S^k. As already mentioned, the consistency of the scheme depends on the proper choice of center points, edge points and the behavior of the mesh during the evolution; therefore we assume (22), (23) and the following extra condition on X_S^k and $X_{p_i,j+1/2}^k$:

A3 There exists $\mathcal{C} > 0$ and $\theta \in]0, \pi/2]$ such that for two consecutive vertices p_i^k, p_{i+1}^k of any cell S^k
1) if $m([X_S^k, p_i^k, p_{i+1}^k]) \neq 0$, then there exist three points $x_{p_i,1}^k$, $x_{p_i,2}^k$, $x_{p_i,3}^k$ in the intersection of the convex hull of S^k and the plane generated by the points $\{X_S^k, p_i^k, p_{i+1}^k\}$ satisfying $\|x_{p_i,1}^k x_{p_i,2}^k\| \geq \mathcal{C}h$, $\|x_{p_i,1}^k x_{p_i,3}^k\| \geq \mathcal{C}h$ and $\theta \leq \sphericalangle(\overrightarrow{x_{p_i,1}^k x_{p_i,2}^k}, \overrightarrow{x_{p_i,1}^k x_{p_i,3}^k}) \leq \pi - \theta$. Here $\sphericalangle(\overrightarrow{x_{p_i,1}^k x_{p_i,2}^k}, \overrightarrow{x_{p_i,1}^k x_{p_i,3}^k})$ represents the oriented angle between the vectors $\overrightarrow{x_{p_i,1}^k x_{p_i,2}^k}$ and $\overrightarrow{x_{p_i,1}^k x_{p_i,3}^k}$, taken around the axis $(\overrightarrow{X_S^k p_i^k} \wedge \overrightarrow{X_S^k p_{i+1}^k})$.
2) there exists three points $y_{p_i,1}^k$, $y_{p_i,2}^k$, $y_{p_i,3}^k$ in the intersection of the convex hull of S^k and the plane generated by the points $(X_S^k, X_{\mathcal{J}(p_i,S)+1/2}^k, X_{\mathcal{J}(p_i,S)-1/2}^k)$ satisfying $\|y_{p_i,1}^k y_{p_i,2}^k\| \geq \mathcal{C}h$, $\|y_{p_i,1}^k y_{p_i,3}^k\| \geq \mathcal{C}h$, and $\theta \leq \sphericalangle(\overrightarrow{y_{p_i,1}^k y_{p_i,2}^k}, \overrightarrow{y_{p_i,1}^k y_{p_i,3}^k}) \leq \pi - \theta$. As above, $\sphericalangle(\overrightarrow{y_{p_i,1}^k y_{p_i,2}^k}, \overrightarrow{y_{p_i,1}^k y_{p_i,3}^k})$ represents the oriented angle between the vectors $\overrightarrow{y_{p_i,1}^k y_{p_i,2}^k}$ and $\overrightarrow{y_{p_i,1}^k y_{p_i,3}^k}$ taken around $(\overrightarrow{X_S^k X_{\mathcal{J}(p_i,S)+1/2}^k} \wedge \overrightarrow{X_S^k X_{\mathcal{J}(p_i,S)-1/2}^k})$.

We recall that $\mathcal{J}(p_i, S)$ is the local index of the cell S^k around the vertex p_i^k. We also assume that $\theta \leq \sphericalangle(\overrightarrow{X_S^k X_{\mathcal{J}(p_i,S)+1/2}^k}, \overrightarrow{X_S^k X_{\mathcal{J}(p_i,S)-1/2}^k}) \leq \pi - \theta$, and for closed cells S^k intersecting the boundary $\partial\Gamma_h^k$ and any edge unknown $x = X_{\mathcal{J}(p_i,S)+1/2}^k$ or $x = X_{\mathcal{J}(p_i,S)-1/2}^k$ in $S^k \cap \partial\Gamma_h^k$, $\|X_S^k - x\| \geq Ch$.

We shall precise here that the assumption **A3** part 1) aims at having cells whose surfaces approximate correctly (in the sense of Lemma 62) the surface of their lifted counterparts. If the vertices of S^k are coplanar, this assumption is true for any star-shaped point $x = X_S^k \in S^k$ (point whose any line connection to a vertex of S^k is entirely in S^k); but in general, on curved surface meshes, one must pay a careful attention. On the other hand, **A3** part 2) will guaranty the consistency of the approximations of surface normals and gradient operators. We refer to Section 4.5, for an example of an

algorithm enabling the choice of nodes X_S^k and the subedge virtual points $X^k_{p_i,j+1/2}$. Finally, the following convergence theorem holds:

Theorem 61 *(Error estimate). Suppose that the assumptions listed from Section 4 hold and define the piecewise constant error functional on Γ_h^k for $k = 1, \cdots, k_{max}$*

$$E^k := \sum_{S^k} \left(u^{-l}(t_k, X^k) - U_S^k \right) \chi_{S^k}$$

measuring the pull back $u^{-l}(t_k, \cdot)$ of the continuous solution $u(t_k, \cdot)$ of (1) at time t_k and the finite volume solution $U^k \in \mathcal{V}_h^k$ of (12). Furthermore, let us assume that $\|E^0\|_{\mathbb{L}^2(\Gamma_h^0)} \leq C\, h$, then the error estimate

$$\max_{k=1,\cdots,k_{max}} \left\| E^k \right\|^2_{\mathbb{L}^2(\Gamma_h^k)} + \tau \sum_{k=1}^{k_{max}} \left\| E^k \right\|^2_{1,\,\Gamma_h^k} \leq C\,(h+\tau)^2 \tag{29}$$

holds for a constant C depending on the regularity assumptions and the time t_{max}.

This error estimate generalizes the error estimate given in [1]. As already mentioned there, it depends on the consistency estimates of different terms which rely on geometric estimates; thus the proof of this theorem will follow the same procedure. The main difference here is that cells are not necessarily triangular and vertices are not necessarily bound to the surface, but we will always reformulate the results in order to use the gains of [1]. In what follows, we first establish the relevant geometric estimates, then prove the consistency of the scheme and finally establish the convergence result.

6.1 Geometric approximation estimates

Let us first extend the definition of $\mathcal{P}^k$ into a time continuous operator $\mathcal{P}(t, \cdot)$ which for each time $t \in [0,\, t_{max}]$, projects points orthogonally onto $\Gamma(t)$. This operator is well defined in a neighborhood of $\Gamma(t)$. We also introduce the time continuous lift operator

$$\Psi^k(t, \cdot) : S^k \;\longrightarrow\; S^{l,k}(t), \quad x \;\longmapsto\; \Psi^k(t, x) := \Phi(t, \Phi^{-1}(t_k, \mathcal{P}^k(x))) \tag{30}$$

which helps to follow the transported lifted cell $S^{l,k}(t) := \Psi^k(t, S^k)$. We then introduce an estimate for the distance between the continuous surface and the polygonization and for the ratio between cell areas and their lifted counterparts.

Lemma 62 *Let $d(t, x)$ be the signed distance from a point x to the surface $\Omega(t)$ taken to be positive in the direction of the surface normal ν, $\Gamma_h(t)$ an $(m, h)-$approximation of $\Gamma(t) \subset \Omega(t)$, and let $m_S^{l,k}$ denote the measure of the lifted cell $S^{l,k}$, $m^{l,k}_{p_i,j+1/2}$ the measure of the lifted subedge $\sigma^k_{p_i,j+1/2}$. The estimates*

$$\sup_{0\leq t\leq t_{max}} \|d(t,\cdot)\|_{\mathbb{L}^\infty(\Gamma_h(t))} \leq Ch^2, \qquad \sup_{k,\,S} \left| 1 - \frac{m_S^{l,k}}{m_S^k} \right| \leq Ch^2,$$

$$\sup_{i,\,j,\,k} \left| 1 - \frac{m^{l,k}_{p_i,j+1/2}}{m^k_{p_i,j+1/2}} \right| \leq Ch^2$$

hold for a constant C depending only on the regularity assumptions. Let us also consider the planes $T^k_{S_{\{i,i+1\}}}$ generated by the center point X_S^k, and the vertices p_i^k, p_{i+1}^k of S^k;

and the plane $T^k_{p_i,S}$ *generated by* X^k_S *and the virtual points* $X^k_{p_i,j-1/2}$ *and* $X^k_{p_i,j+1/2}$ *around* p^k_i. *There exists a constant* C *depending only on the regularity assumptions such that*

$$\max_{x\in S^k_{\{i,i+1\}}} \|\nabla_{T^k_{S_{\{i,i+1\}}}} d(t_k,x)\| \le Ch \quad \textit{and} \quad \max_{x\in S^k_{p_i,j}} \|\nabla_{T^k_{p_i,S}} d(t_k,x)\| \le Ch.$$

We recall that $S^k_{\{i,i+1\}}$ *is the triangle* $[X^k_S, p^k_i, p^k_{i+1}]$ *and* $S^k_{p_i,j}$ *is the virtual subcell of* S^k *containing* p^k_i.

Proof First notice that $d(t,\cdot)$ is a C^2 function. Let us consider a cell $S^k(t) := \Upsilon(t, S^k)$ with center $X^k_S(t)$ and vertices $\Psi^k(t,p^k_i)$, a point $x = \beta^k_S(x)X^k_S(t) + \beta^k_{S,i}(x)\Psi^k(t,p^k_i) + \beta^k_{S,i+1}(x)\Psi^k(t,p^k_{i+1})$ where $\beta^k_S(x)$, $\beta^k_{S,i}(x)$, and $\beta^k_{S,i+1}(x)$ are barycentric coordinates of x with respect to $X^k_S(t)$, $\Psi^k(t,p^k_i)$, and $\Psi^k(t,p^k_{i+1})$, respectively. The Taylor expression of $d(t,\cdot)$ at each vertex y of the triangle $[X^k_S(t), \Psi^k(t,p^k_i), \Psi^k(t,p^k_{i+1})]$ can be expressed in terms of $d(t,x)$ as

$$d(t,y) = d(t,x) + (y-x)\cdot\nabla d(t,x) + \mathcal{O}(\|y-x\|^2).$$

Finally, multiplying each of these equations by the corresponding barycentric coefficients and summing up all the equations, one obtains that $d(t,x) = \mathcal{O}(h^2)$ since the barycentric coefficients are bounded and we have assumed that $\Gamma_h(t)$ is an $(m,\, h)-$polygonization of $\Gamma(t)$. Next, the points $x^k_{p_i,j} \in T^k_{S_{\{i,i+1\}}}$ and $y^k_{p_i,j} \in T^k_{p_i,S}$ $(j \in \{1,2,3\})$ provided by assumption **A3** satisfy $\|\nabla_{T^k_{S_{\{i,i+1\}}}} d(t_k, x^k_{p_i,j})\| \le Ch$ and $\|\nabla_{T^k_{p_i,S}} d(t_k, y^k_{p_i,1})\| \le Ch$. Since these points are in the convex hull of S^k, one concludes that $\max_{S^k_{\{i,i+1\}}} \|\nabla_{T^k_{S_{\{i,i+1\}}}} d(t_k,x)\| \le Ch$ and $\max_{S^k_{p_i,j}} \|\nabla_{T^k_{p_i,S}} d(t_k,x)\| \le Ch$, where we recall that $S^k_{\{i,i+1\}}$ is the triangle $[X^k_S, p^k_i, p^k_{i+1}]$.

For the second estimate, we consider the triangle $S^k_{\{i,i+1\}}$ and assume without any restriction that $S^k_{\{i,i+1\}} \subset \{(\xi,0) | \xi \in \mathbb{R}^2\}$. Next, we define $\mathcal{P}^k_{ext}$ in a neighborhood of $S^k_{\{i,i+1\}}$ as follows

$$\mathcal{P}^k_{ext}(\xi,\zeta) = (\xi,0) + (\zeta - d(t_k,(\xi,0)))\nabla d^T(t_k,(\xi,0)).$$

Obviously, $\mathcal{P}^k_{ext} = \mathcal{P}^k$ on $S^k_{\{i,j\}}$ and from the results above, we deduce that

$$\Big|\Big|\det(D\mathcal{P}^k_{ext}(\xi,0))\Big| - 1\Big| \le Ch^2,$$

where $D\mathcal{P}^k_{ext}$ is the Jacobian of $\mathcal{P}^k_{ext}$. We can clearly see that $\big|\det(D\mathcal{P}^k_{ext}(\xi,0))\big|$ controls the transformation of the area under the projection $\mathcal{P}^k$ from $S^k_{\{i,i+1\}}$ to $S^{l,k}_{\{i,i+1\}} := \mathcal{P}^k(S^k_{\{i,i+1\}})$; since the third column of the Jacobian $\partial_\zeta \mathcal{P}^k_{ext}(\xi,0) = \nabla d^T(t_k,(\xi,0))$ has length 1 and is normal to $\Gamma(t_k)$ at $\mathcal{P}^k(\xi,0)$. The claim is therefore proven since the subcells $S^{l,k}_{\{i,i+1\}}$ as well as $S^k_{\{i,i+1\}}$ form a partition of $S^{l,k}$ and S^k, respectively.
The third estimate is obtained via an adaptation of arguments of the second estimate.

□

Let us also give the following lemma which states the consistency of the approximation of conormals to curved boundaries.

Lemma 63 *Let p_i^k and p_{i+1}^k be two consecutive vertices of a cell S^k, X_S^k its center and $\sigma_{p_i,j-1/2}^k$ the subedge around p_i^k satisfying $\sigma_{p_i,j-1/2}^k \subset [p_i^k, p_{i+1}^k]$. We also consider $\sigma_{p_i,j-1/2}^{l,k}$ the coresponding curved boundary on $\Gamma(t_k)$ and $X_{p_i,j-1/2}^k$, $X_{p_i,j+1/2}^k$ the subedge points of S^k around p_i^k. Finally, we assume $X_{p_i,j-1/2}^k \in \sigma_{p_i,j-1/2}^k$, then the conormal to $\sigma_{p_i,j-1/2}^{l,k}$ outward from $S^{l,k} \cap \Gamma^k$ is given by*

$$n_{p_i,j|j-1/2}^{l,k}(x) = n_{p_i,j|j-1/2}^k + \epsilon(x)$$

where $n_{p_i,j|j-1/2}^k := \left(\frac{p_{i+1}^k - p_i^k}{\|p_{i+1}^k - p_i^k\|} \wedge \nu_{p_i,j}^k \right) / \left\| \frac{p_{i+1}^k - p_i^k}{\|p_{i+1}^k - p_i^k\|} \wedge \nu_{p_i,j}^k \right\|$ *and $\epsilon(x)$ is a vector satisfying*
$\|\epsilon(x)\| \leq Ch$.

Proof We will distinguish the case where $\sigma_{p_i,j-1/2}^k$ is a boundary subedge ($\sigma_{p_i,j-1/2}^k \subset \partial\Gamma_h^k$) and the case where $\sigma_{p_i,j-1/2}^k$ is an interior subedge
($\sigma_{p_i,j-1/2}^k \subset \Gamma_h^k \backslash \partial\Gamma_h^k$). Let us consider the first case where $\sigma_{p_i,j-1/2}^k \subset \partial\Gamma_h^k$. We define the following map

$$\eta_{S,i|i+1}^k : \quad x := p_i^k + \alpha \frac{p_{i+1}^k - p_i^k}{\|p_{i+1}^k - p_i^k\|} \longmapsto \quad \eta_{S,i|i+1}^k(x) := x \; - \; d(t_k, x) \nabla d^T(t_k, x) \\ - \; d(\mathcal{P}^k(x), \Gamma^k) \nabla d^T(\mathcal{P}^k(x), \Gamma^k),$$

where $\alpha \in [0, \|p_{i+1}^k - p_i^k\|]$. Since this map transforms $\sigma_{p_i,j-1/2}^k$ to $\sigma_{p_i,j-1/2}^{l,k}$, a tangent vector to $\sigma_{p_i,j-1/2}^{l,k}$ is given by

$$\begin{aligned} \varpi_{S,i|i+1}^k(\eta_{S,i|i+1}^k(x)) = & \frac{p_{i+1}^k - p_i^k}{\|p_{i+1}^k - p_i^k\|} - \left(\nabla d^T(t_k, x) \cdot \frac{p_{i+1}^k - p_i^k}{\|p_{i+1}^k - p_i^k\|} \right) \nabla d^T(t_k, x) \\ & - d(t_k, x) \nabla \left(\nabla d^T(t_k, x) \right) \frac{p_{i+1}^k - p_i^k}{\|p_{i+1}^k - p_i^k\|} \\ & - \left(\nabla d^T(\mathcal{P}^k(x), \Gamma^k) \cdot \frac{p_{i+1}^k - p_i^k}{\|p_{i+1}^k - p_i^k\|} \right) \nabla d^T(\mathcal{P}^k(x), \Gamma^k) \\ & - d(\mathcal{P}^k(x), \Gamma^k) \nabla \left(\nabla d^T(\mathcal{P}^k(x), \Gamma^k) \right) \frac{p_{i+1}^k - p_i^k}{\|p_{i+1}^k - p_i^k\|} \end{aligned}$$

for points x where $\eta_{S,i|i+1}^k$ has enough regularity. Since $\eta_{S,i|i+1}^k$ is regular enough almost everywhere and referring to the assumption (v) and (vi) on the surface approximation in Definition 35 as well as to Lemma 62, one concludes that

$$\varpi_{S,i|i+1}^k(\eta_{S,i|i+1}^k(x)) = \frac{p_{i+1}^k - p_i^k}{\|p_{i+1}^k - p_i^k\|} + \epsilon_1(x),$$

where $\epsilon_1(x)$ is a vector satisfying $\|\epsilon_1(x)\| \leq Ch$. Next, one deduces from the last two inequalities of Lemma 62 that

$$\nu^k_{p_i,j} \cdot \frac{p^k_{i+1} - p^k_i}{\|p^k_{i+1} - p^k_i\|} = \mathcal{O}(h)$$

and the normal $\nu(\eta^k_{S,i|i+1}(x))$ to the surface Γ^k at $\eta^k_{S,i|i+1}(x)$ is given by

$$\nu(\eta^k_{S,i|i+1}(x)) = \nu^k_{p_i,j} + \epsilon_2(x),$$

where $\epsilon_2(x)$ is a vector satisfying $\|\epsilon_2(x)\| \leq Ch$. Finally, one deduces that the unit normal to $\sigma^{l,k}_{p_i,j+1/2}$ outward from $S^{l,k} \cap \Gamma^k$ is given by

$$\varpi^k_{S,i|i+1}(\eta^k_{S,i|i+1}(x)) \wedge \nu(\eta^k_{S,i|i+1}(x)) = n^k_{p_i,j|j-1/2} + \epsilon(x).$$

where $\epsilon(x)$ is a vector satisfying $\|\epsilon(x)\| \leq Ch$.
For the second case, $\eta^k_{S,i|i+1}(\cdot)$ is merely $\mathcal{P}(\cdot)$ and the above proof remains valid.

□

Next we control the area defect between the transported lifted versus a lifted transported cell.

Lemma 64 *For each cell S^k on Γ^k_h, and all x in S^k, the estimate*

$$\|\mathcal{P}(t, \Upsilon^k(t,x)) - \Psi(t,x)\| \leq C\tau h^2$$

holds for a constant C depending only on the regularity assumptions. Furthermore, for the symmetric difference between $S^{l,k}$ and $S^{l,k+1}$, one obtains

$$\mathcal{H}^{n-1}(S^{l,k}(t_{k+1}) \Delta S^{l,k+1}) \leq C\tau h m^{k+1}_S$$

where $\mathcal{H}^{n-1}(\cdot)$ represents the $(n-1)$- dimensional Hausdorff measure. We recall that the symmetric difference between two sets A and B is defined by $A\Delta B = (A \backslash B) \cup (B \backslash A)$.

Proof We first notice that the function $\Psi^k(t,\cdot)$ defined in (30) parameterizes the lifted and then transported cell $S^{l,k}(t)$ over S^k, and $\mathcal{P}(t, \Upsilon^k(t,\cdot))$ with $\Upsilon^k(t,\cdot)$ defined in (21) parameterizes the transported and then lifted cell $\mathcal{P}(t, S^k(t))$ over S^k. Next, one restricts oneself on the triangle $S^k_{i,i+1} := [X^k_S, p^k_i, p^k_{i+1}]$ and uses the Taylor expansion of respective functions at its vertices considered as neighboring points of a point $x \in S^k_{i,i+1}$. It follows that

$$\|\mathcal{P}(t, \Upsilon^k(t,x)) - \Psi(t,x)\| \leq \beta(t) h^2,$$

where $\beta(\cdot)$ is a nonnegative and smooth function in time. One deduces from $S^{l,k}(t_k) = S^{l,k}$ that $\beta(\cdot)$ can be chosen such that $\beta(t) \leq C\,|t - t_k|$ holds. This result shows that the maximum norm of the displacement $\mathcal{P}(t, \Upsilon^k(t,\cdot)) - \Psi(t,\cdot)$ on the boundary σ^k is $C\tau h^2$. The second claim is then obvious.

□

Based on this estimate, we immediately obtain the following corollary:

Corollary 65 *For any cell S^k on Γ_h^k and any Lipschitz continuous function $\omega(t,\cdot)$ defined on $\Gamma(t)$ one obtains*

$$\left| \int_{S^{l,k}(t_{k+1})\cap\Gamma(t_{k+1})} \omega(t_{k+1},a)da - \int_{S^{l,k+1}\cap\Gamma(t_{k+1})} \omega(t_{k+1},a)da \right| \leq C\tau h m_S^{k+1}$$

for a constant C depending only on the regularity assumptions.

6.2 Consistency estimates.

With these geometric preliminaries at hand, we are now able to derive a-priori bounds for various consistency errors in conjunction with the finite volume approximation (12) of the continuous evolution (1).

Lemma 66 *Let S^k be a cell in Γ_h^k and $t \in [t_k, t_{k+1}]$, then for*

$$\begin{aligned}\mathcal{R}_1(S^{l,k}(t)\cap\Gamma(t)) := &\int_{S^{l,k}(t)\cap\Gamma(t)} \nabla_{\Gamma(t)}\cdot(\mathcal{D}\nabla_{\Gamma(t)}u(t,\cdot))da \\ &- \int_{S^{l,k+1}\cap\Gamma(t_{k+1})} \nabla_{\Gamma(t_{k+1})}\cdot(\mathcal{D}\nabla_{\Gamma(t_{k+1})}u(t_{k+1},\cdot))da\end{aligned}$$

we obtain the estimate $\left|\mathcal{R}_1(S^{l,k}(t)\cap\Gamma(t))\right| \leq C\tau(1+Ch)m_S^{k+1}$.

Proof Given a function $u(t,\cdot)\in \mathrm{C}^2(\Gamma(t))$, we first define a continuous extension still called $u(t,\cdot)$ in the neighborhood $\mathcal{N}(t)$ of $\Gamma(t)$ as mention in Section 4.1, by requiring $\nabla_{\Gamma(t)}u(x)\cdot\nabla_{\Gamma(t)}d(x,\Gamma^k)=0$. We recall that $\nabla_{\Gamma(t)}u(t,x) = \nabla u(t,x) - (\nabla u(t,x)\cdot\nu(t,x))\nu(t,x)$. Any continuous and differentiable vector field $v(t,\cdot)$ on $\Gamma(t)$ can be extended in the same way for each component. Then we obtain for the surface divergence of $v(t,\cdot)$, at a point x on $\Gamma(t)$ the representation
$\nabla_{\Gamma(t)}\cdot v(t,x) = \mathrm{tr}\left((Id-\nu(t,x)\times\nu(t,x))\nabla v(t,x)\right)$. Thus, we deduce from our regularity assumptions that the function $(t,x)\mapsto\nabla_{\Gamma(t)}\cdot(\mathcal{D}\nabla_{\Gamma(t)}u(t,x))$ is Lipschitz in time and space. Next, taking into account corollary 65 the estimate immediately follows since

$$\begin{aligned}\mathcal{R}_1(S^{l,k}(t)\cap\Gamma(t)) = &\left(\int_{S^{l,k}(t)\cap\Gamma(t)} \nabla_{\Gamma(t)}\cdot(\mathcal{D}\nabla_{\Gamma(t)}u(t,\cdot))da\right. \\ &\left.- \int_{S^{l,k}(t_{k+1})\cap\Gamma(t_{k+1})} \nabla_{\Gamma(t_{k+1})}\cdot(\mathcal{D}\nabla_{\Gamma(t_{k+1})}u(t_{k+1},\cdot))da\right) \\ &+\left(\int_{S^{l,k}(t_{k+1})\cap\Gamma(t_{k+1})} \nabla_{\Gamma(t_{k+1})}\cdot(\mathcal{D}\nabla_{\Gamma(t_{k+1})}u(t_{k+1},\cdot))da\right. \\ &\left.- \int_{S^{l,k+1}\cap\Gamma(t_{k+1})} \nabla_{\Gamma(t_{k+1})}\cdot(\mathcal{D}\nabla_{\Gamma(t_{k+1})}u(t_{k+1},\cdot))da\right)\end{aligned}$$

□

Lemma 67 *Let the subedge $\sigma^{l,k}_{p_i,j+1/2}$ be the intersection between two adjacent subcells $S^{l,k}_{p_i,j}$ and $S^{l,k}_{p_i,j+1}$ or, with a slight misuse of notation, the intersection between $S^{l,k}_{p_i,j}$ and the boundary $\partial\left(\mathcal{P}^k(\Gamma^k_h)\cap\Gamma^k\right)$ of $\mathcal{P}^k(\Gamma^k_h)\cap\Gamma^k$; the term*

$$\begin{aligned}\mathcal{R}_2(S^k_{p_i,j}|S^k_{p_i,j+1}) &:= \int_{\sigma^{l,k}_{p_i,j+1/2}} \left(\mathcal{D}\nabla_{\Gamma(t_k)}u\right)\cdot n^{l,k}_{p_i,j+1/2}(t_k,x)dx\\ &- m^k_{p_i,j+1/2}\left(u(t_k,\mathcal{P}^k(X^k_{p_i,j+1/2}))-u(t_k,\mathcal{P}^k(X^k_{p_i,j}))\right)\lambda^k_{p_i,j|j+1/2}\\ &- m^k_{p_i,j+1/2}\left(u(t_k,\mathcal{P}^k(X^k_{p_i,j-1/2}))-u(t_k,\mathcal{P}^k(X^k_{p_i,j}))\right)\lambda^k_{p_i,j-1/2|j|j+1/2},\end{aligned}$$

where $n^{l,k}_{p_i,j+1/2}(t_k,\cdot)$ is the function describing the outward pointing unit conormal of $S^{l,k}_{p_i,j}$ on the subedge $\sigma^{l,k}_{p_i,j|j+1/2}$ and the other terms are defined in Section 4.2, obeys the estimate

$$\left|\mathcal{R}_2(S^k_{p_i,i}|S^k_{p_i,i+1})\right| \le Cm^k_{i(S)+1/2}h.$$

Proof As in Lemma 66, we consider the continuous extension of $u(t,\cdot)$, still called $u(t,\cdot)$. Next, we write the surface gradient of $u(t_k,\cdot)$ at a point x on $S^{l,k}_{p_i,j}\cap\Gamma^k$ as follows:

$$\nabla_{\Gamma^k}u(x) = \nabla u = \nabla_{T^k_{p_i,S}}u(x) + \left(\nabla u(x)\cdot\nu^k_{p_i,S}\right)\nu^k_{p_i,S}.$$

Since $\nabla_{T^k_{p_i,S}}u(x) = (\nabla_{T^k_{p_i,S}}\cdot e^k_{p_i,j|j-1/2})\mu^k_{p_i,j|j-1/2} + (\nabla_{T^k_{p_i,S}}\cdot e^k_{p_i,j|j+1/2})\mu^k_{p_i,j|j+1/2}$ and
$\nu(x) = \nu^k_{p_i,S} + \vartheta_j(t_k,x)h$ with $\|\vartheta_j(t_k,x)\|\le C$ on $S^{l,k}_{p_i,j}\cap\Gamma^k$, we obtain using the Taylor expansion, Definition 35 and assumption **A3**.2 that

$$\begin{aligned}\nabla_{\Gamma^k}u(x) =& \left(u(t_k,X^k_{p_i,j-1/2})-u(t_k,X^k_{p_i,j})\right)\mu^k_{p_i,j|j-1/2}\\ &+\left(u(t_k,X^k_{p_i,j+1/2})-u(t_k,X^k_{p_i,j})\right)\mu^k_{p_i,j|j+1/2}-\epsilon(t_k,x),\end{aligned}$$

where $\epsilon(t_k,x)$ is a three dimensional vector satisfying $\|\epsilon(t_k,x)\|\le Ch$. Thus, using the regularity assumptions on $\mathcal{D}$, Lemma 63 and assumption **A3**.2 we obtain

$$\begin{aligned}&\int_{\sigma^{l,k}_{p_i,j+1/2}}(\mathcal{D}\nabla_{\Gamma^k}u)\cdot n^{l,k}_{p_i,j|j+1/2}dx\\ &= m^k_{p_i,j+1/2}\left(u(t_k,X^k_{p_i,j-1/2})-u(t_k,X^k_{p_i,j})\right)\lambda^k_{p_i,j-1/2|j|j+1/2}\\ &+ m^k_{p_i,j+1/2}\left(u(t_k,X^k_{p_i,j+1/2})-u(t_k,X^k_{p_i,j})\right)\lambda^k_{p_i,j|j+1/2}\\ &+ \mathcal{O}(m^k_{p_i,j+1/2}h).\end{aligned}\tag{31}$$

We now need to prove that the approximation of the subedge values $u(t_k,X^k_{p_i,j-1/2})$ are $\mathcal{O}(h^2)$ consistent. To this end, we apply the continuous version of Proposition 41 on the above relation which gives

$$M^k_{p_i}\overline{U}^k_{p_i,\sigma} = N^k_{p_i}\overline{U}^k_{p_i} + v_1,\tag{32}$$

where $\overline{U}^k_{p_i,\sigma} := \left(u(t_k, X^k_{p_i,1/2}), u(t_k, X^k_{p_i,3/2}), \cdots\right)^\top$, $\overline{U}^k_{p_i} := \left(u(t_k, X^k_{p_i,1}), u(t_k, X^k_{p_i,2}), \cdots\right)^\top$ and v_1 is a vector satisfying $\|v_1\| \leq Ch^2$. Also, the $\mathbb{H}^1$–norm of the continuous solution reads

$$\begin{aligned}
&\sum_j \int_{S^{l,k}_{p_i,j} \cap \Gamma^k} \|\nabla_{\Gamma^k} u\|^2 dx \\
&= \sum_j \int_{S^{l,k}_{p_i,j} \cap \Gamma^k} \left\| \left(u(t_k, X^k_{p_i,j-1/2}) - u(t_k, X^k_{p_i,j})\right) \mu^k_{p_i,j|j-1/2} \right. \\
&+ \left. \left(u(t_k, X^k_{p_i,j+1/2}) - u(t_k, X^k_{p_i,j})\right) \mu^k_{p_i,j|j+1/2} + \epsilon(t_k, x) \right\|^2 dx.
\end{aligned}$$

The continuous setup of problem (6) is formulated as

$$\left\{ \begin{array}{l}
\text{Find } \overline{U}^k_{p_i,\sigma} \text{ in } \bar{\mathcal{B}}^k_{p_i} := \left\{ \overline{V}^k_{p_i,\sigma} := (V^k_{p_i,1/2}, V^k_{p_i,3/2}, \cdots)^\top \mid \right. \\
\left. M^k_{p_i} \overline{V}^k_{p_i,\sigma} = N^k_{p_i} \overline{U}^k_{p_i} + v_1 \right\} \text{ such that} \\
\overline{U}^k_{p_i,\sigma} = \underset{\overline{V}^k_{p_i,\sigma} \in \mathcal{B}^k_{p_i}}{\operatorname{argmin}} \sum_j \int_{S^{l,k}_{p_i,j} \cap \Gamma^k} \left\| \left[V^k_{p_i,j-1/2} - \overline{U}^k_{p_i,j}\right] \mu^k_{p_i,j|j-1/2} \right. \\
\qquad\qquad \left. + \left[V^k_{p_i,j+1/2} - \overline{U}^k_{p_i,j}\right] \mu^k_{p_i,j|j+1/2} + \epsilon(t_k, x) \right\|^2 dx;
\end{array} \right.$$

which in a simplified setup reads

$$\left\{ \begin{array}{l}
\text{Find } \overline{U}^k_{p_i,\sigma} \text{ in } \bar{\mathcal{B}}^k_{p_i} := \left\{ \overline{V}^k_{p_i,\sigma} := (V^k_{p_i,1/2}, V^k_{p_i,3/2}, \cdots)^\top \mid \right. \\
\left. M^k_{p_i} \overline{V}^k_{p_i,\sigma} = N^k_{p_i} \overline{U}^k_{p_i} + v_1 \right\} \text{ such that} \\
\overline{U}^k_{p_i,\sigma} = \underset{\overline{V}^k_{p_i,\sigma} \in \mathcal{B}^k_{p_i}}{\operatorname{argmin}} \left\| \sqrt{\mathbf{B}^k_{p_i}}\, \overline{V}^k_{p_i,\sigma} - \left(\sqrt{\mathbf{B}^k_{p_i}}\right)^{-1} \left(\mathbf{C}^k_{p_i} \overline{U}^k_{p_i} + v_2\right) \right\|^2
\end{array} \right.$$

since the error $\epsilon(t_k, x)$ is assumed to be known. v_2 is a vector satisfying $\|v_2\| \leq Ch^2$. Following the same procedure as in Section 4.2, one obtains

$$\overline{U}^k_{p_i,\sigma} = \mathbf{Coef}^k_{p_i} \overline{U}^k_{p_i} + v_3,$$

where $v_3 = \left(\sqrt{B^k_{p_i}}\right)^{-1} \left(M^k_{p_i} \left(\sqrt{B^k_{p_i}}\right)^{-1}\right)^\dagger \left(v_1 - M^k_{p_i} \left(B^k_{p_i}\right)^{-1} v_2\right) + \left(B^k_{p_i}\right)^{-1} v_2$. It is clear that $\|v_3\| \leq Ch^2$. We have just proven that a perturbation on the equation leads to a consistent solution. It is left to prove that the solution is also consistent with the expected data (values of functions at virtual points). In the flat case, this is evident since the reconstruction of affine functions using this method is exact if the tensor $\mathcal{D}$ is constant on $\cup_j S^{l,k}_{p_i,j} \cap \Gamma^k$ and $\mathcal{O}(h^2)$ consistent in general. In the curved case we consider the closest plane to the center points around p_i. There exists h_0 such that this plane is included in $\mathcal{N}(t_k)$ for any $h \leq h_0$. Next we project on the defined plane, in the direction of the surface normal ν, the whole geometrical setup represented around p_i and adopt the new subcells as discrete subcells. Let us consider the function $f(x) = u(t_k, X^k_1) + (\nabla_{\Gamma^k} u(t_k, X^k_1)) \cdot (x - X^k_1)$ defined in a neighborhood of

$\cup_j S^{l,k}_{p_i,j} \cap \Gamma^k$ whose restriction on Γ^k is considered for the reconstruction. The above problem posed on the new discrete subcells gives an $\mathcal{O}(h^2)$ consistent value of f at projected virtual points; These values are in an $\mathcal{O}(h^2)$ neighborhood of the values of f at the corresponding surface points. Also, due to the consistency of the geometric approximation, the newly stated problem can be stated as the above problem with an $\mathcal{O}(h^2)$ perturbation of the right hand side which means that the solution is evidently the solution of problem (6) with an uncertainty of $\mathcal{O}(h^2)$. This concludes that the right values of a continuous function is in an $\mathcal{O}(h^2)$ neighborhood of the value proposed by this reconstruction's method. Now, including this result in equation (31) gives the desired estimate.

□

Lemma 68 *For a cell S^k and the residual error term*

$$\mathcal{R}_3(S^{l,k}|S^{l,k+1}) = \int_{S^{l,k}(t_{k+1})\cap\Gamma^{k+1}} u da - \int_{S^{l,k}(t_k)\cap\Gamma^k} u da - \left(m_S^{k+1}u^{-l}(t_{k+1}, X_S^{k+1}) - m_S^k u^{-l}(t_k, X_S^k)\right)$$

one obtains the estimate $|\mathcal{R}^3(S^{l,k}|S^{l,k+1})| \leq C\tau h m_S^{k+1}$.

Proof At first, let us recall that $\Psi^k(t,\cdot)$, and $\mathcal{P}(t_{k+1}, \Upsilon^k(t_{k+1},\cdot))$ respectively parameterize $S^{l,k}(t)$ and $S^{l,k+1}$ over S^k. Via standard quadratic error estimates and due to the regularity assumption on Φ and u given in the introduction, we obtain for the smooth quadrature error function

$$Q(t) := \int_{S^{l,k}(t)} u(t,a)da - u(t, \mathcal{P}(t, \Upsilon^k(t, X_S^k)))\mathcal{H}^{n-1}(S^{l,k}(t))$$

the estimate $|Q(t) - Q(t_k)| \leq \tilde{\beta}(t) h \mathcal{H}^{n-1}(\mathcal{P}(t, \Upsilon^k(t, S^k)))$, where $\tilde{\beta}$ is a smooth non-negative function in time. From $|Q(t_k) - Q(t_k)| = 0$, we deduce that $\tilde{\beta}(t) \leq C|t - t_k|$ (cf. also the proof of Lemma 64). Based on an analogous argument, we obtain for the continuity modulus of $\tilde{Q}_1(t) := \int_{S^{l,k}(t)\setminus\Gamma(t)} u(t,a)da$ and $\tilde{Q}_2(t) := \int_{\mathcal{P}(t,\Upsilon^k(t,S^k))} da - \int_{\Upsilon^k(t,S^k)} da$ respectively that

$$|\tilde{Q}_1(t_{k+1}) - \tilde{Q}_1(t_k)| \leq C\tau\, h^2\, m_S^k$$
$$|\tilde{Q}_2(t_{k+1}) - \tilde{Q}_2(t_k)| \leq C\tau\, h^2\, m_S^k\,.$$

Making use of our notation we observe that the left hand sides of these two inequalities equal respectively $\left|\int_{S^{l,k}(t_{k+1})\setminus\Gamma^{k+1}} u(t_{k+1},a)\,\mathrm{d}a - \int_{S^{l,k}\setminus\Gamma^k} u(t_k,a)\,\mathrm{d}a\right|$, and $\left|(m_S^{l,k+1} - m_S^{k+1}) - (m_S^{l,k} - m_S^k)\right|$. Finally, we split the residual as follows

$$\begin{aligned}\mathcal{R}_3(S^{l,k}|S^{l,k+1}) &= (Q(t_{k+1}) - Q(t_k)) - \left(\int_{S^{l,k}(t_{k+1})\setminus\Gamma^{k+1}} u(t,a)\,\mathrm{d}a - \int_{S^{l,k}\setminus\Gamma^k} u(t,a)\,\mathrm{d}a\right)\\ &+ u(t_{k+1}, \mathcal{P}(t_{k+1}, X_S^{k+1}))\left(\mathcal{H}^{n-1}(S^{l,k}(t_{k+1})) - m_S^{l,k+1}\right)\\ &+ u(t_{k+1}, \mathcal{P}(t_{k+1}, X_S^{k+1}))\left[\left(m_S^{l,k+1} - m_S^{k+1}\right) - \left(m_S^{l,k} - m_S^k\right)\right]\\ &+ \left(u(t_{k+1}, \mathcal{P}(t_{k+1}, X_S^{k+1})) - u(t_k, \mathcal{P}(t_k, X_S^k))\right)\left(m_S^{l,k} - m_S^k\right),\end{aligned}$$

and apply the above estimates, Lemma 62 and Corrolary 65 to have

$$\begin{aligned}\left|\mathcal{R}_3(S^{l,k}|S^{l,k+1})\right| &\leq C\left(\tau h m_S^k + \tau h^2 m_S^k + \tau h m_S^{k+1} + \tau h^2 m_S^k + \tau h^2 m_S^k\right)\\ &\leq C\tau h\, m_S^k.\end{aligned}$$

□

Lemma 69 *For a cell S^k and the residual error term*

$$\mathcal{R}_4\left(S^{l,k}|S^{l,k+1}\right) = \int_{t_k}^{t_{k+1}} \int_{S^{l,k}(t)\cap\Gamma(t)} g(t,a)\ da\,\mathrm{d}t - \tau m_S^{k+1} g^{-l}\left(t_{k+1}, X_S^{k+1}\right)$$

one achieves the estimate $\left|\mathcal{R}_4\left(S^{l,k}|S^{l,k+1}\right)\right| \leq C\tau(\tau+h)m_S^{k+1}$.

Proof We expand the residual and estimate it as follows:

$$\begin{aligned}&\mathcal{R}_4\left(S^{l,k}|S^{l,k+1}\right)\\ =&-\int_{t_k}^{t_{k+1}}\int_{S^{l,k}(t)\setminus\Gamma(t)} g(t,x)da + \int_{t_k}^{t_{k+1}}\left(\int_{S^{l,k}(t)} g(t,x)da - \int_{S^{l,k}(t_{k+1})} g(t_{k+1},x)da\right)dt\\ &+\tau\left(\int_{S^{l,k}(t_{k+1})} g(t_{k+1},x)da - \int_{S^{l,k+1}} g(t_{k+1},x)da\right)\\ &+\tau\left(\int_{S^{l,k+1}} g(t_k,x)da - g^{-l}(t_{k+1},X_S^{k+1})\, m_S^{l,k+1}\right) + \tau\left(m_S^{l,k+1} - m_S^{k+1}\right) g^{-l}(t_{k+1},X_S^{k+1})\\ \leq& C(\tau\, h\, m_S^{k+1} + \tau^2\mathcal{H}^{n-1}(S^{l,k}(t_{k+1})) + \tau^2\, h\, m_S^{k+1} + \tau\, h\, m_S^{k+1} + \tau\, h^2\, m_S^{k+1})\\ \leq& C\tau(\tau+h)m_S^{k+1}\end{aligned}$$

Here we have used a standard quadrature estimate, Lemma 62, Lemma 64 and Corrolary 65.

□

6.3 Proof of Theorem 61

As in Section 4.3 (cf. (9), (10) and (11)), let us consider the following cellwise flux formulation of the continuous problem (1):

$$\begin{aligned}&\int_{S^{l,k}(t_{k+1})\cap\Gamma^{k+1}} u\,\mathrm{d}a - \int_{S^{l,k}\cap\Gamma^k} u\,\mathrm{d}a - \int_{t_k}^{t_{k+1}}\int_{\partial\left(S^{l,k}(t)\cap\Gamma(t)\right)} \mathcal{D}\nabla_{\Gamma(t)}u\cdot\mu_{\partial S^{l,k}(t)}\,dl\,\mathrm{d}t\\ =&\int_{t_k}^{t_{k+1}}\int_{S^{l,k}(t)\cap\Gamma(t)} g\,\mathrm{d}a\,\mathrm{d}t.\end{aligned}$$

From this equation we subtract the discrete counterpart (12)

$$
\begin{aligned}
&m_S^{k+1}U_S^{k+1} - m_S^k U_S^k \\
&- \tau \sum_{p_i \in \partial S^k} \Big[m^{k+1}_{p_i,\mathcal{J}(p_i,S)-1/2} \left(U^{k+1}_{p_i,\mathcal{J}(p_i,S)-1/2} - U^{k+1}_{p_i,\mathcal{J}(p_i,S)} \right) \lambda^{k+1}_{p_i,\mathcal{J}(p_i,S)|\mathcal{J}(p_i,S)-1/2} \\
&+ m^{k+1}_{p_i,\mathcal{J}(p_i,S)-1/2} \left(U^{k+1}_{p_i,\mathcal{J}(p_i,S)+1/2} - U^{k+1}_{p_i,\mathcal{J}(p_i,S)} \right) \lambda^{k+1}_{p_i,\mathcal{J}(p_i,S)+1/2|\mathcal{J}(p_i,S)|\mathcal{J}(p_i,S)-1/2} \\
&+ m^{k+1}_{p_i,\mathcal{J}(p_i,S)+1/2} \left(U^{k+1}_{p_i,\mathcal{J}(p_i,S)-1/2} - U^{k+1}_{p_i,\mathcal{J}(p_i,S)} \right) \lambda^{k+1}_{p_i,\mathcal{J}(p_i,S)-1/2|\mathcal{J}(p_i,S)|\mathcal{J}(p_i,S)+1/2} \\
&+ m^{k+1}_{p_i,\mathcal{J}(p_i,S)+1/2} \left(U^{k+1}_{p_i,\mathcal{J}(p_i,S)+1/2} - U^{k+1}_{p_i,\mathcal{J}(p_i,S)} \right) \lambda^{k+1}_{p_i,\mathcal{J}(p_i,S)|\mathcal{J}(p_i,S)+1/2} \Big] \\
&= \tau\, m_S^{k+1} G_S^{k+1}.
\end{aligned}
$$

and multiply this with $E_S^{k+1} = u^{-l}\left(t_{k+1}, X_S^{k+1}\right) - U_S^{k+1}$ to obtain

$$
\begin{aligned}
&\mathcal{R}_3(S^{l,k}|S^{l,k+1}) E_S^{k+1} - \left(\int_{t_k}^{t_{k+1}} \mathcal{R}_1(S^{l,k}(t) \cap \Gamma(t)) dt \right) E_S^{k+1} \\
&- \tau \sum_{p_i^{k+1} \in S^{k+1}} \left[\mathcal{R}_2(S^{k+1}_{p_i,\mathcal{J}(p_i,S)}|S^{k+1}_{p_i,\mathcal{J}(p_i,S)+1}) + \mathcal{R}_2(S^{k+1}_{p_i,\mathcal{J}(p_i,S)}|S^{k+1}_{p_i,\mathcal{J}(p_i,S)-1}) \right] E^{k+1}_{p_i,\mathcal{J}(p_i,S)} \\
&+ (m_S^{k+1}\left(E_S^{k+1}\right)^2 - m_S^k E_S^k E_S^{k+1}) \\
&- \tau \sum_{p_i^{k+1} \in S^{k+1}} \Big[m^{k+1}_{p_i,\mathcal{J}(p_i,S)+1/2} \left(E^{k+1}_{p_i,\mathcal{J}(p_i,S)+1/2} - E^{k+1}_{p_i,\mathcal{J}(p_i,S)} \right) E^{k+1}_{p_i,\mathcal{J}(p_i,S)} \lambda^{k+1}_{p_i,\mathcal{J}(p_i,S)|\mathcal{J}(p_i,S)+1/2} \\
&+ m^{k+1}_{p_i,\mathcal{J}(p_i,S)+1/2} \left(E^{k+1}_{p_i,\mathcal{J}(p_i,S)-1/2} - E^{k+1}_{p_i,\mathcal{J}(p_i,S)} \right) E^{k+1}_{p_i,\mathcal{J}(p_i,S)} \lambda^{k+1}_{p_i,\mathcal{J}(p_i,S)-1/2|\mathcal{J}(p_i,S)|\mathcal{J}(p_i,S)+1/2} \\
&+ m^{k+1}_{p_i,\mathcal{J}(p_i,S)-1/2} \left(E^{k+1}_{p_i,\mathcal{J}(p_i,S)+1/2} - E^{k+1}_{p_i,\mathcal{J}(p_i,S)} \right) E^{k+1}_{p_i,\mathcal{J}(p_i,S)} \lambda^{k+1}_{p_i,\mathcal{J}(p_i,S)+1/2|\mathcal{J}(p_i,S)|\mathcal{J}(p_i,S)-1/2} \\
&+ m^{k+1}_{p_i,\mathcal{J}(p_i,S)-1/2} \left(E^{k+1}_{p_i,\mathcal{J}(p_i,S)-1/2} - E^{k+1}_{p_i,\mathcal{J}(p_i,S)} \right) E^{k+1}_{p_i,\mathcal{J}(p_i,S)} \lambda^{k+1}_{p_i,\mathcal{J}(p_i,S)|\mathcal{J}(p_i,S)-1/2} \Big] \\
&= \mathcal{R}_4\left(S^{l,k}|S^{l,k+1}\right) E_S^{k+1},
\end{aligned} \tag{33}
$$

where $E^{k+1}_{p_i,\mathcal{J}(p_i,S)-1/2} := \left(u^{-l}\left(t_{k+1}, X^{k+1}_{j-1/2}\right) - U^{k+1,i}_{j-1/2}\right)$ and $E^{k+1}_{p_i,\mathcal{J}(p_i,S)+1/2}$ is defined analogously. We recall that the summation is always done on regular vertices (cf. Definition 43). Next, we substract from the flux continuity equation on subedges between neighboring sub-cell $S^{l,k+1}_{p_i,\mathcal{J}(p_i,S)}$ and $S^{l,k+1}_{p_i,\mathcal{J}(p_i,S)+1}$

$$
\begin{aligned}
&\int_{\sigma^{l,k+1}_{p_i,\mathcal{J}(p_i,S)+1/2}} (\mathcal{D}\nabla_\Gamma u)\,|_{S^{l,k+1}_{p_i,\mathcal{J}(p_i,S)}(t)} \cdot \mu_{\partial S^{l,k+1}_{p_i,\mathcal{J}(p_i,S)}(t)}\, dl \\
&+ \int_{\sigma^{l,k+1}_{p_i,\mathcal{J}(p_i,S)+1/2}} (\mathcal{D}\nabla_\Gamma u)\,|_{S^{l,k+1}_{p_i,\mathcal{J}(p_i,S)+1}(t)} \cdot \mu_{\partial S^{l,k+1}_{p_i,\mathcal{J}(p_i,S)+1}(t)}\, dl = 0,
\end{aligned}
$$

its discrete counterpart

$$
\begin{aligned}
&m^{k+1}_{p_i,\mathcal{J}(p_i,S)+1/2} \Big[\left(U^{k+1}_{p_i,\mathcal{J}(p_i,S)+1/2} - U^{k+1}_{\mathcal{J}(p_i,S)} \right) \lambda^{k+1,i}_{\mathcal{J}(p_i,S)|\mathcal{J}(p_i,S)+1/2} \\
&+ \left(U^{k+1}_{p_i,\mathcal{J}(p_i,S)-1/2} - U^{k+1}_{p_i,\mathcal{J}(p_i,S)} \right) \lambda^{k+1,i}_{p_i,\mathcal{J}(p_i,S)-1/2|\mathcal{J}(p_i,S)|\mathcal{J}(p_i,S)+1/2} \Big] \\
&+ m^{k+1}_{p_i,\mathcal{J}(p_i,S)+1/2} \Big[\left(U^{k+1}_{p_i,\mathcal{J}(p_i,S)+3/2} - U^{k+1,i}_{\mathcal{J}(p_i,S)+1} \right) \lambda^{k+1,i}_{p_i,\mathcal{J}(p_i,S)+2|\mathcal{J}(p_i,S)+1|\mathcal{J}(p_i,S)} \\
&+ \left(U^{k+1}_{p_i,\mathcal{J}(p_i,S)+1/2} - U^{k+1,i}_{\mathcal{J}(p_i,S)+1} \right) \lambda^{k+1}_{p_i,\mathcal{J}(p_i,S)+1|\mathcal{J}(p_i,S)} \Big] = 0.
\end{aligned}
$$

Furthermore, we multiply the result by $\tau E^{k+1}_{p_i,\mathcal{J}(p_i,S)+1/2}$ and obtain

$$
\begin{aligned}
&\tau\, m^{k+1}_{p_i,\mathcal{J}(p_i,S)+1/2}\left(E^{k+1}_{p_i,\mathcal{J}(p_i,S)+1/2}-E^{k+1}_{p_i,\mathcal{J}(p_i,S)}\right)E^{k+1}_{p_i,\mathcal{J}(p_i,S)+1/2}\cdot\\
&\quad\cdot\lambda^{k+1}_{p_i,\mathcal{J}(p_i,S)|\mathcal{J}(p_i,S)+1/2}\\
&+\tau\, m^{k+1}_{p_i,\mathcal{J}(p_i,S)+1/2}\left(E^{k+1}_{p_i,\mathcal{J}(p_i,S)-1/2}-E^{k+1}_{p_i,\mathcal{J}(p_i,S)}\right)E^{k+1}_{p_i,\mathcal{J}(p_i,S)+1/2}\cdot\\
&\quad\cdot\lambda^{k+1}_{p_i,\mathcal{J}(p_i,S)-1/2|\mathcal{J}(p_i,S)|\mathcal{J}(p_i,S)+1/2}\\
&+\tau\, m^{k+1}_{p_i,\mathcal{J}(p_i,S)+1/2}\left(E^{k+1}_{p_i,\mathcal{J}(p_i,S)+1/2}-E^{k+1}_{p_i,\mathcal{J}(p_i,S)+1}\right)E^{k+1}_{p_i,\mathcal{J}(p_i,S)+1/2}\cdot\\
&\quad\cdot\lambda^{k+1}_{p_i,\mathcal{J}(p_i,S)+1|\mathcal{J}(p_i,S)+1/2}\\
&+\tau\, m^{k+1}_{p_i,\mathcal{J}(p_i,S)+1/2}\left(E^{k+1}_{p_i,\mathcal{J}(p_i,S)+3/2}-E^{k+1}_{p_i,\mathcal{J}(p_i,S)+1}\right)E^{k+1}_{p_i,\mathcal{J}(p_i,S)+1/2}\cdot\\
&\quad\cdot\lambda^{k+1}_{p_i,\mathcal{J}(p_i,S)+3/2|\mathcal{J}(p_i,S)+1|\mathcal{J}(p_i,S)+1/2}\\
&+\tau\,\mathcal{R}_2(S^{k+1}_{\mathcal{J}(p_i,S)}|S^{k+1}_{p_i,\mathcal{J}(p_i,S)+1})E^{k+1}_{p_i,\mathcal{J}(p_i,S)+1/2}\\
&\quad+\tau\,\mathcal{R}_2(S^{k+1}_{p_i,\mathcal{J}(p_i,S)+1}|S^{k+1}_{p_i,\mathcal{J}(p_i,S)})E^{k+1}_{p_i,\mathcal{J}(p_i,S)+1/2}=0.
\end{aligned}
\tag{34}
$$

Now, summing up (33) and (34) respectively over all cells and subedges leads to

$$
\begin{aligned}
&\|E^{k+1}\|^2_{\mathbb{L}^2(\Gamma_h^{k+1})}+\tau\|E^{k+1}\|^2_{1,\Gamma_h^{k+1}}\\
&=\sum_S m_S^k\,E_S^k\,E_S^{k+1}+\sum_S\mathcal{R}_4\left(S^{l,k}|S^{l,k+1}\right)E_S^{k+1}-\sum_S\mathcal{R}_3(S^{l,k}|S^{l,k+1})E_S^{k+1}\\
&+\sum_S\left(\int_{t_k}^{t_{k+1}}\mathcal{R}_1(S^{l,k}(t)\cap\Gamma(t))dt\right)E_S^{k+1}\\
&-\tau\sum_{S^{k+1}}\sum_{p_i^{k+1}\in S^{k+1}}\Big[\mathcal{R}_2(S^{k+1}_{p_i,\mathcal{J}(p_i,S)}|S^{k+1}_{p_i,\mathcal{J}(p_i,S)+1})\left(E^{k+1}_{p_i,\mathcal{J}(p_i,S)+1/2}-E^{k+1}_{p_i,\mathcal{J}(p_i,S)}\right)\\
&+\mathcal{R}_2(S^{k+1}_{p_i,\mathcal{J}(p_i,S)}|S^{k+1}_{\mathcal{J}(p_i,S)-1})\left(E^{k+1}_{p_i,\mathcal{J}(p_i,S)-1/2}-E^{k+1}_{p_i,\mathcal{J}(p_i,S)}\right)\Big].
\end{aligned}
$$

Let us denote by $E^k_{p_i}:=\left(\sum_{S^k_{p_i,j}}E^k_{p_i,j}\right)/n_{p_i}$ the mean value of $E^k_{p_i,j}$ around p_i^k. The last term on the right hand side can be written as follows

$$
\begin{aligned}
Z:=&-\tau\sum_{S^{k+1}}\sum_{p_i^{k+1}\in S^{k+1}}\Big[\mathcal{R}_2(S^{k+1}_{p_i,\mathcal{J}(p_i,S)}|S^{k+1}_{p_i,\mathcal{J}(p_i,S)+1})\left(E^{k+1}_{p_i,\mathcal{J}(p_i,S)+1/2}-E^{k+1}_{p_i,\mathcal{J}(p_i,S)}\right)\\
&+\mathcal{R}_2(S^{k+1}_{p_i,\mathcal{J}(p_i,S)}|S^{k+1}_{p_i,\mathcal{J}(p_i,S)-1})\left(E^{k+1}_{p_i,\mathcal{J}(p_i,S)-1/2}-E^{k+1}_{p_i,\mathcal{J}(p_i,S)}\right)\Big]\\
=&-\tau\sum_{S^{k+1}}\sum_{p_i^{k+1}\in S^{k+1}}\Big[\mathcal{R}_2(S^{k+1}_{p_i,\mathcal{J}(p_i,S)}|S^{k+1}_{p_i,\mathcal{J}(p_i,S)+1})\cdot\\
&\cdot\left((E^{k+1}_{p_i,\mathcal{J}(p_i,S)+1/2}-E^k_{p_i})-(E^{k+1}_{p_i,\mathcal{J}(p_i,S)}-E^k_{p_i})\right)\\
&+\mathcal{R}_2(S^{k+1}_{p_i,\mathcal{J}(p_i,S)}|S^{k+1}_{p_i,\mathcal{J}(p_i,S)-1})\left((E^{k+1}_{p_i,\mathcal{J}(p_i,S)-1/2}-E^k_{p_i})-(E^{k+1}_{p_i,\mathcal{J}(p_i,S)}-E^k_{p_i})\right)\Big]\\
=&-\tau\sum_{p_i^{k+1}\in\Gamma_h^{k+1}}\left(\left(\overline{\mathcal{R}}^{k+1}_{2,p_i|\sigma}\right)^\top\mathbf{Coef}^k_{p_i}-\left(\overline{\mathcal{R}}^{k+1}_{2,p_i}\right)^\top\right)^\top\left(\overline{E}^{k+1}_{p_i}-E^{k+1}_{p_i}\mathbf{1}_{p_i}\right),
\end{aligned}
\tag{35}
$$

where $\overline{\mathcal{R}}_{2,p_i|\sigma}^{k+1}$ is the vector with components $\left(\overline{\mathcal{R}}_{2,p_i|\sigma}^{k+1}\right)_j := \left(\mathcal{R}_2^{k+1}(S_{p_i,j}^{k+1}|S_{p_i,j-1}^{k+1}) + \mathcal{R}_2^{k+1}(S_{p_i,j-1}^{k+1}|S_{p_i,j}^{k+1})\right)$, $\overline{\mathcal{R}}_{2,p_i}^{k+1}$ is the vector with components $\left(\overline{\mathcal{R}}_{2,p_i}^{k+1}\right)_j := \left(\mathcal{R}_2^{k+1}(S_{p_i,j}^{k+1}|S_{p_i,j-1}^{k+1}) + \mathcal{R}_2^{k+1}(S_{p_i,j}^{k+1}|S_{p_i,j+1}^{k+1})\right)$ and $\overline{E}_{p_i}^{k+1} := \left(E_{p_i,1}^{k+1}, E_{p_i,2}^{k+1}, \cdots\right)$. Of course we have to readjust these vectors around boundary points according to the boundary condition in the similar way as in Section 4.4. Next we introduce the local gradient operator in expression 35 and derive the following estimate

$$
\begin{aligned}
Z &= -\tau \sum_{p_i^{k+1}\in\Gamma_h^{k+1}} \left(\left(\overline{\mathcal{R}}_{2,p_i|\sigma}^{k+1}\right)^\top \mathbf{Coef}_{p_i}^k - \left(\overline{\mathcal{R}}_{2,p_i}^{k+1}\right)^\top\right)^\top \left(\overline{E}_{p_i}^{k+1} - E_{p_i}^{k+1}\mathbf{1}_{p_i}\right) \\
&= -\tau \sum_{p_i^{k+1}\in\Gamma_h^{k+1}} \left(\left(\overline{\mathcal{R}}_{2,p_i|\sigma}^{k+1}\right)^\top \mathbf{Coef}_{p_i}^k - \left(\overline{\mathcal{R}}_{2,p_i}^{k+1}\right)^\top\right)^\top \left(\sqrt{A_{p_i}^{k+1} + (\mathbf{1}_{p_i}\otimes\mathbf{1}_{p_i})/n_{p_i}}\right)^{-1} \\
&\quad \left(\sqrt{A_{p_i}^{k+1} + (\mathbf{1}_{p_i}\otimes\mathbf{1}_{p_i})/n_{p_i}}\right)\left(\overline{E}_{p_i}^{k+1} - E_{p_i}^{k+1}\mathbf{1}_{p_i}\right) \\
&\le \tau\Bigg(\sum_{p_i^{k+1}\in\Gamma_h^{k+1}} \left(\left(\overline{\mathcal{R}}_{2,p_i|\sigma}^{k+1}\right)^\top \mathbf{Coef}_{p_i}^k - \left(\overline{\mathcal{R}}_{2,p_i}^{k+1}\right)^\top\right)^\top \left(A_{p_i}^{k+1} + (\mathbf{1}_{p_i}\otimes\mathbf{1}_{p_i})/n_{p_i}\right)^{-1} \\
&\quad \left(\left(\overline{\mathcal{R}}_{2,p_i|\sigma}^{k+1}\right)^\top \mathbf{Coef}_{p_i}^k - \left(\overline{\mathcal{R}}_{2,p_i}^{k+1}\right)^\top\right)\Bigg)^{-1/2} \left(\sum_{p_i^{k+1}\in\Gamma_h^{k+1}} \left(\overline{E}_{p_i}^{k+1}\right)^\top A_{p_i}^{k+1}\overline{E}_{p_i}^{k+1}\right)^{-1/2}
\end{aligned}
$$

since $A_{p_i}^{k+1}\mathbf{1}_{p_i} = 0\cdot\mathbf{1}_{p_i}$ and $(\mathbf{1}_{p_i})^\top A_{p_i}^{k+1} = 0\cdot(\mathbf{1}_{p_i})^\top$. Finally, using Lemma 67, the estimate $h^2 \le C m_S^{k+1}$, the fact that the number of cell's vertices is uniformly bounded and the submatrices $A_{p_i}^{k+1} + (\mathbf{1}_{p_i}\otimes\mathbf{1}_{p_i})/n_{p_i}$ are uniformly elliptic, we obtain

$$
\begin{aligned}
Z &\le \tau C\left(\sum_{S^{k+1}} m_S^{k+1}h^2\right)^{1/2} \|E_S^{k+1}\|_{1,\Gamma_h^{k+1}} \\
&\le \tau C h\left(\mathcal{H}^{n-1}(\Gamma_h^{k+1})\right)^{1/2} \|E_S^{k+1}\|_{1,\Gamma_h^{k+1}}.
\end{aligned}
$$

Now, we take into account the consistency results from Lemma 66, Lemma 68, Lemma 69, apply Young's and Cauchy's inequality and achieve the result

$$
\begin{aligned}
&\|E^{k+1}\|^2_{\mathbb{L}^2(\Gamma_h^{k+1})} + \tau\|E^{k+1}\|^2_{1,\Gamma_h^{k+1}} \\
&\le \frac{1}{2}\|E^{k+1}\|^2_{\mathbb{L}^2(\Gamma_h^{k+1})} + \frac{1}{2}\|E^k\|^2_{\mathbb{L}^2(\Gamma_h^k)} + \frac{1}{2}\max_S\max_k\left|1 - \frac{m_S^k}{m_S^{k+1}}\right|\|E^k\|^2_{\mathbb{L}^2(\Gamma_h^k)} \\
&+ C\left(\tau(\tau+h) + \tau h + \tau^2(1+Ch)\right)\left(\mathcal{H}^{n-1}(\Gamma_h^{k+1})\right)^{1/2}\|E^{k+1}\|_{\mathbb{L}^2(\Gamma_h^{k+1})} \\
&+ C\tau h\left(\mathcal{H}^{n-1}(\Gamma_h^{k+1})\right)^{1/2}\|E^{k+1}\|_{1,\Gamma_h^{k+1}}.
\end{aligned}
$$

Based on the fact that the center points X_S describe a C^1 continuous curve $X_S(t) := \gamma(t, X_S)$, one easily proves that $\left|1 - \frac{m_S^k}{m_S^{k+1}}\right| \le C\tau$ as already mentioned in Section 5.

Again, applying Young's inequality to the last two terms on the right side gives

$$
\begin{aligned}
&C\left(\tau(\tau+h)+\tau h+\tau^2(1+Ch)\right)\left(\mathcal{H}^{n-1}(\Gamma_h^{k+1})\right)^{1/2}\|E^{k+1}\|_{\mathbb{L}^2(\Gamma_h^{k+1})}\\
&\leq \frac{C}{2}\tau(\tau+h)^2\mathcal{H}^{n-1}(\Gamma_h^{k+1})+\frac{C}{2}\tau\|E^{k+1}\|^2_{\mathbb{L}^2(\Gamma_h^{k+1})},\\
&C\tau h\left(\mathcal{H}^{n-1}(\Gamma_h^{k+1})\right)^{1/2}\|E^{k+1}\|_{1,\Gamma_h^{k+1}}\leq \frac{C^2\tau}{2}h^2\mathcal{H}^{n-1}(\Gamma_h^{k+1})+\frac{\tau}{2}\|E^{k+1}\|^2_{1,\Gamma_h^{k+1}}.
\end{aligned}
$$

Now, taking into account that $\mathcal{H}^{n-1}(\Gamma_h^{k+1})$ is uniformly bounded, we obtain the estimate

$$
\begin{aligned}
&(1-C\tau)\|E^{k+1}\|^2_{\mathbb{L}^2(\Gamma_h^{k+1})}+\frac{\tau}{2}\|E^{k+1}\|^2_{1,\Gamma_h^{k+1}}\\
&\leq (1+C\tau)\frac{1}{2}\|E^{k}\|^2_{\mathbb{L}^2(\Gamma_h^{k})}+C\tau(\tau+h)^2\mathcal{H}^{n-1}(\Gamma_h^{k+1}).
\end{aligned}
\tag{36}
$$

Next, we first skip the second term on the left hand side, use the inequality $\frac{1+C\tau}{1-C\tau}\leq (1+c\tau)$ for sufficiently small τ and a constant $c>0$ and obtain via iteration

$$
\begin{aligned}
\|E^{k+1}\|^2_{\mathbb{L}^2(\Gamma_h^{k+1})}&\leq (1+c\tau)\|E^{k}\|^2_{\mathbb{L}^2(\Gamma_h^{k})}+C\tau(\tau+h)^2\\
&\quad\cdots\cdots\\
&\leq (1+c\tau)^{k+1}\|E^{0}\|^2_{\mathbb{L}^2(\Gamma_h^{0})}+C\sum_{i=1}^{k}(1+c\tau)^{i-1}\tau(\tau+h)^2\\
&\leq Ce^{ct_k}(\tau+h)^2
\end{aligned}
$$

since $\|E^0\|^2_{\mathbb{L}^2(\Gamma_h^0)}\leq Ch$. This implies the first claim of the theorem

$$
\max_{k=1,\cdots,k_{max}}\|E^k\|^2_{\mathbb{L}^2(\Gamma_h^k)}\leq C(\tau+h)^2.
$$

Finally, taking into account this estimate and summing over $k=1,\cdots,k_{max}$ in (36), we also obtain the claim for the discrete $\mathbb{H}^1_0-$norm of the error

$$
\sum_{k=1,\cdots,k_{max}}\tau\|E^{k+1}\|^2_{1,\Gamma_h^{k+1}}\leq C(\tau+h)^2.
$$

Remark 610 *It is worth mentioning here that the exact solution of Equation* (4) *did not intervene in the actual development; thus Theorem 51, Theorem 52 and Theorem 61 remain valid even when Equation* (4) *is not satisfied. In that case the solution will not be locally conservative in the usual sense of finite volumes anymore. This situation was already reported in [12] where they also use barycentric coefficients to approximate solution values on edges. An advantage of our approach is that we reduce the residual of the mentioned equation in a way to avoid any undesirable oscillation on the solution. Nevertheless, we have not found any experimental evidence where this situation happens but, we have also not deeply studied the local matrices to be able to know whether this worst case scenario is even plausible.*

7 Coupled reaction diffusion and advection model

In this part, we wish to extend our method to the more general case of reaction diffusion and advection problems. We then consider a source term g which depends on the solution and an additional tangential advection term $\nabla_\Gamma\cdot(wu)$. Here, w is an additional tangential transport velocity on the surface, which transports the density u along the moving interface Γ instead of just passively advecting it with the interface. We assume the mapping $(t,x)\to w(t,\Phi(t,x))$ to be in $\mathrm{C}^1([0,t_{max}],\ \mathrm{C}^1(\Gamma_0))$. Furthermore, we suppose g to be Lipschitz continuous. An extension to a reaction term which also explicitly depends on time and position is straightforward. Hence, we investigate the evolution problem

$$\dot{u}+u\nabla_\Gamma\cdot v-\nabla_\Gamma\cdot(\mathcal{D}\nabla_\Gamma u)+\nabla_\Gamma\cdot(wu)=g(u)\quad\text{on }\Gamma=\Gamma(t)\,. \tag{37}$$

In what follows, let us consider an appropriate discretization for both terms. For the reaction term, we consider the time explicit approximation

$$\int_{t_k}^{t_{k+1}}\int_{S^{l,k}(t)\cap\Gamma(t)} g(u(t,x))\,\mathrm{d}a\,\mathrm{d}t\approx\tau\, m_S^k\, g(u(t_k,\mathcal{P}^kX_S^k)) \tag{38}$$

and then replace $u(t_k,\mathcal{P}^k(X_S^k))$ by U_S^k in the actual numerical scheme. Furthermore, we take into account an upwind discretization of the additional transport term to ensure robustness also in a regime where the transport induced by w dominates the diffusion. Different from [1], we introduce here a second order slope limiting upwind discretization derived from the above described method. Thus, since the solution u of problem 37 is $\mathbb{H}^1$ on $\Gamma(t)$ and $\nabla_{\Gamma(t)}u$ has a weak divergence, we use the procedure described in Section 4.2 to construct the subgradients $\nabla^k_{p_i,\mathcal{J}(p_i,S)}u$ of u around the vertices p_i^k. In this last procedure, we keep the center points obtained for the discretization of the diffusion operator while the virtual subedge points might vary. Let us now consider a cell S^k, the pseudo unit normal

$$e^k_{3,S}:=\Big(\sum_{p_i^k\in S^k}(p_i^k-p_1^k)\wedge(p_{i+1}^k-p_1^k)\Big)\Big/\Big\|\sum_{p_i^k\in S^k}(p_i^k-p_1^k)\wedge(p_{i+1}^k-p_1^k)\Big\|$$

of S^k, the vectors

$$e^k_{1,S}:=\Big((p_1^k-X_S^k)-\Big((p_1^k-X_S^k)\cdot e^k_{3,S}\Big)\,e^k_{3,S}\Big)\Big/\Big\|(p_1^k-X_S^k)-\Big((p_1^k-X_S^k)\cdot e^k_{3,S}\Big)\,e^k_{3,S}\Big\|$$

and $e^k_{2,S}:=e^k_{3,S}\wedge e^k_{1,S}$. We define

$$\nabla_S^k u:=\Big((\nabla_S^k u)\cdot e^k_{1,S}\Big)\,e^k_{1,S}+\Big((\nabla_S^k u)\cdot e^k_{2,S}\Big)\,e^k_{2,S}+\Big((\nabla_S^k u)\cdot e^k_{3,S}\Big)\,e^k_{3,S},$$

the slope limited gradient on S^k as follows: $\forall\ j=1,2,3$

$$\begin{cases}(\nabla_S^k u)\cdot e^k_{j,S} & :=\operatorname{sign}\Big((\nabla^k_{p_1,\mathcal{J}(p_1,S)}u)\cdot e^k_{j,S}\Big)\min_{p_i^k\in S^k}\Big|(\nabla^k_{p_i,\mathcal{J}(p_i,S)}u)\cdot e^k_{j,S}\Big|\\ & \qquad\text{if }\operatorname{sign}\Big((\nabla^k_{p_i,\mathcal{J}(p_i,S)}u)\cdot e^k_{j,S}\Big)=\text{const }\forall\ p_i,\\ (\nabla_S^k u)\cdot e^k_{j,S} & :=0\quad\text{ else.}\end{cases}$$

This gradient reconstruction is similar to the minmod gradient reconstruction method (cf. [29; 30; 31]). Let us now consider an edge σ^k common boundary of two cells S^k and L^k (i.e. $\sigma^k = S^k \cap L^k$). We assume σ^k being delimited by the points p_i^k and p_{i+1}^k (i.e. $\sigma^k = [p_i^k, p_{i+1}^k]$); we call $S_{p_i,j}^k$, $S_{p_i,j+1}^k$ the respective subcells of S^k and L^k around p_i^k and $S_{p_{i+1},m}^k$, $S_{p_{i+1},m-1}^k$ the respective subcells of S^k and L^k around p_{i+1}^k. We refer to Figure 11 for the illustration of this setup.

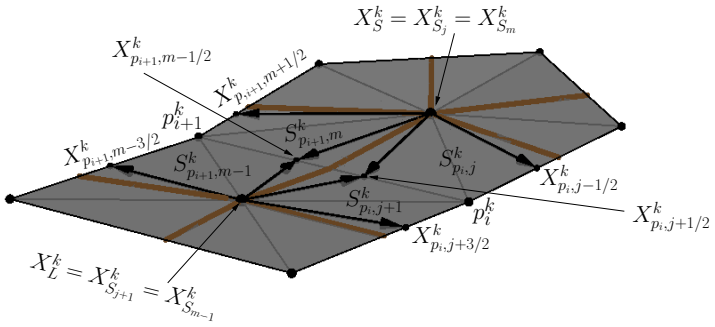

Fig. 11 Subcells across the edge $\sigma^k = [p_i^k, p_{i+1}^k]$ and virtual points around p_i^k and p_{i+1}^k.

We also denote by

$$n_{S|L}^k := n_{S,\sigma}^k = \frac{n_{p_i,j|j+1/2}^k + n_{p_i,m|m-1/2}^k - n_{p_i,j+1|j+1/2}^k - n_{p_i,m-1|m-1/2}^k}{\| n_{p_i,j|j+1/2}^k + n_{p_i,m|m-1/2}^k - n_{p_i,j+1|j+1/2}^k - n_{p_i,m-1|m-1/2}^k \|}$$

the average unit outward pointing conormal vectors of S^k on σ^k and by $p_\sigma^k := \dfrac{p_i^k + p_{i+1}^k}{2}$ the middle of σ^k. Here $n_{S,\sigma}^k = -n_{L,\sigma}^k$ holds. We will later denote by $n_{S,\sigma}^{l,k}(a)$ the unit conormal at $a \in \sigma^{l,k}$ pointing outward from $S^{l,k}$. Now if $n_{S,\sigma}^k \cdot w(t_k, p_\sigma^k) \geq 0$, the upwind direction is pointing inward and we define $u^+(t_k, p_\sigma^k) := u^{-l}(t_k, X_S^k) + (\nabla_S^k u) \cdot (p_\sigma^k - X_S^k)$, otherwise $u^+(t_k, p_\sigma^k) := u^{-l}(t_k, X_L^k) + (\nabla_L^k u) \cdot (p_\sigma^k - X_L^k)$. If σ^k is a boundary segment, the average unit outward pointing conormal of S^k on σ^k is defined by

$$n_{S,\sigma}^k = \frac{n_{p_i,j|j+1/2}^k + n_{p_i,m|m-1/2}^k}{\| n_{p_i,j|j+1/2}^k + n_{p_i,m|m-1/2}^k \|}.$$

In this case too, if $n_{S,\sigma}^k \cdot w(t_k, p_\sigma^k) \geq 0$, the upwind direction is pointing inward and we define $u^+(t_k, p_\sigma^k) := u^{-l}(t_k, X_S^k) + (\nabla_S^k u) \cdot (p_\sigma^k - X_S^k)$, but $u^+(t_k, p_\sigma^k) := u^{-l}(t_k, p_\sigma^k)$ if $n_{S,\sigma}^k \cdot w(t_k, p_\sigma^k) < 0$. Once, the upwind direction is identified, we take into account the classical approach by Engquist and Osher [32] and obtain the approximation:

$$\int_{t_k}^{t_{k+1}} \int_{S^{l,k}(t) \cap \Gamma(t)} \nabla_\Gamma \cdot (wu) \, \mathrm{d}a \, \mathrm{d}t \approx \tau \sum_{\sigma^k \subset \partial S^k} m_\sigma^k \left(n_{S,\sigma}^k \cdot w^{-l}(t_k, p_\sigma^k) \right) u^+(t_k, p_\sigma^k). \tag{39}$$

Finally, we again replace $u^{-l}(t_k, X_S^k)$ by the discrete nodal values U_S^k and denote the edge values $u^+(t_k, p_\sigma^k)$ by $U_\sigma^{k,+}$. For the sake of completeness let us resume the resulting scheme:

$$
\begin{aligned}
& m_S^{k+1} U_S^{k+1} - m_S^k U_S^k \\
& - \tau \sum_{p_i \in \partial S^k} \Big[m^{k+1}_{p_i, \mathcal{J}(p_i,S)-1/2} \left(U^{k+1}_{p_i,\mathcal{J}(p_i,S)-1/2} - U^{k+1}_{p_i,\mathcal{J}(p_i,S)} \right) \lambda^{k+1}_{p_i,\mathcal{J}(p_i,S)|\mathcal{J}(p_i,S)-1/2} \\
& + m^{k+1}_{p_i, \mathcal{J}(p_i,S)-1/2} \left(U^{k+1}_{p_i,\mathcal{J}(p_i,S)+1/2} - U^{k+1}_{p_i,\mathcal{J}(p_i,S)} \right) \lambda^{k+1}_{p_i,\mathcal{J}(p_i,S)+1/2|\mathcal{J}(p_i,S)|\mathcal{J}(p_i,S)-1/2} \\
& + m^{k+1}_{p_i, \mathcal{J}(p_i,S)+1/2} \left(U^{k+1}_{p_i,\mathcal{J}(p_i,S)-1/2} - U^{k+1}_{p_i,\mathcal{J}(p_i,S)} \right) \lambda^{k+1}_{p_i,\mathcal{J}(p_i,S)-1/2|\mathcal{J}(p_i,S)|\mathcal{J}(p_i,S)+1/2} \\
& + m^{k+1}_{p_i, \mathcal{J}(p_i,S)+1/2} \left(U^{k+1}_{p_i,\mathcal{J}(p_i,S)+1/2} - U^{k+1}_{p_i,\mathcal{J}(p_i,S)} \right) \lambda^{k+1}_{p_i,\mathcal{J}(p_i,S)|\mathcal{J}(p_i,S)+1/2} \Big] \\
& + \tau \sum_{\sigma^k \subset \partial S^k} m_\sigma^k \left(n^k_{S,\sigma} \cdot w^{-l}(t_k, p_\sigma^k) \right) U_\sigma^+ \\
& = \tau\, m_S^k\, g(U_S^k). \qquad (40)
\end{aligned}
$$

Obviously, due to the fully explicit discretization of the additional terms, Proposition 47 still applies and guarantees existence and uniqueness of a discrete solution. Furthermore, the convergence result can be adapted and the error estimate postulated in Theorem 61 holds. To see this, let us first consider the nonlinear source term $g(u)$ and the following estimate already presented in [1] for the triangular mesh;

$$
\begin{aligned}
& \int_{t_k}^{t_{k+1}} \int_{S^{l,k}(t) \cap \Gamma(t)} g(u(t,x))\, \mathrm{d}a\, \mathrm{d}t - \tau m_S^k\, g(U_S^k) \\
= & - \int_{t_k}^{t_{k+1}} \int_{S^{l,k}(t) \setminus \Gamma(t)} g(u(t,x)) da \\
& + \int_{t_k}^{t_{k+1}} \left(\int_{S^{l,k}(t)} g(u(t,x)) da - \int_{S^{l,k}} g(u(t_k,x)) da \right) dt \\
& + \tau \left(\int_{S^{l,k}} g(t_k,x) da - \int_{S^{l,k}} g(u(t_k, X_S^k)) da \right) + \tau \left(m_S^{l,k} - m_S^k \right) g(u(t_k, X_S^k)) \\
& + \tau\, m_S^k \left(g^{-l}(u(t_k, X_S^k)) - g(U_S^k) \right) \\
\leq & C(\tau\, h\, m_S^k + \tau^2 \mathcal{H}^{n-1}(S^{l,k}) + \tau\, h\, m_S^k + \tau\, h^2\, m_S^k + C_{Lip}(g)\, \tau\, m_S^k E_S^k),
\end{aligned}
$$

where $C_{Lip}(g)$ denotes the Lipschitz constant of g. In the proof of Theorem 61 we already have treated terms identical to the first four on the right hand side. For the last term we obtain after multiplication with the nodal error E_S^{k+1} and summation over all cells S

$$
\begin{aligned}
& C_{Lip}(g)\, \tau \sum_S m_S^k E_S^k E_S^{k+1} \\
\leq\ & C_{Lip}(g)\, \tau \max_S \left(\frac{m_S^k}{m_S^{k+1}} \right)^{\frac{1}{2}} \|E^k\|_{\mathbb{L}^2(\Gamma_h(t_k))} \|E^{k+1}\|_{\mathbb{L}^2(\Gamma_h(t_k))} \\
\leq\ & C\, \tau \left(\|E^k\|^2_{\mathbb{L}^2(\Gamma_h(t_k))} + \|E^{k+1}\|^2_{\mathbb{L}^2(\Gamma_h(t_{k+1}))} \right).
\end{aligned}
$$

Taking into account these additional error terms the estimate (36) remains unaltered. Next, we investigate the error due to the additional advection term and rewrite

$$\begin{aligned}
&\int_{t_k}^{t_{k+1}}\int_{S^{l,k}(t)\cap\Gamma(t)} \nabla_\Gamma\cdot(wu)\,\mathrm{d}a\,\mathrm{d}t - \tau\sum_{\sigma^k\subset\partial S^k} m_\sigma^k\left(\mu_{\sigma,S}^k\cdot w^{-l}(t_k,X_\sigma^k)\right)U_\sigma^{k,+}\\
&=\int_{t_k}^{t_{k+1}}\int_{S^{l,k}(t)\cap\Gamma(t)} \nabla_\Gamma\cdot(wu)\,\mathrm{d}a\,\mathrm{d}t - \tau\int_{S^{l,k}\cap\Gamma(t_k)}\nabla_\Gamma\cdot(wu)\,\mathrm{d}a\\
&\quad+\sum_{\substack{\sigma^k\subset\partial S^k\\ \sigma^k=S^k\cap L^k}}\left(\tau\mathcal{R}_5\left(S^{l,k}|L^{l,k}\right)+\tau\mathcal{F}\left(S^{l,k}|L^{l,k}\right)E_\sigma^{k,+}\right),
\end{aligned}$$

where $\mathcal{R}_5\left(S^{l,k}|L^{l,k}\right)=\int_{\sigma^{l,k}} n_{S,\sigma}^{l,k}\cdot w\,u\;\mathrm{d}l - m_\sigma^k w^{-l}(t_k,p_\sigma^k)\cdot n_{S,\sigma}^k u^+(t_k,p_\sigma^k)$ is an edge residual,
$\mathcal{F}\left(S^{l,k}|L^{l,k}\right)=m_\sigma^k w^l(t_k,p_\sigma^k)\cdot n_{S,\sigma}^k$ a flux term on the edge $\sigma^{l,k}=S^{l,k}\cap L^{l,k}$ and $E_\sigma^{k,+}=u^+(t_k,p_\sigma^k)-U_\sigma^{k,+}$ a piecewise constant upwind error function on the discrete surface Γ_h^k. For the sake of consistency in the notation, we have assumed here as in the following any curved boundary segment $\sigma^{l,k}$ being the intersection of a curved cell $S^{l,k}\subset\Gamma^k$ and the curved cell $L^{l,k}:=\sigma^{l,k}$ of measure 0. In this case, the cell's center value as well as any error comming from $L^{l,k}$ are taken to be 0 and the subedges values are known from the boundary condition. Now the first term in the above error representation can again be estimated by $C\,\tau^2\mathcal{H}^{n-1}(S^{l,k})$. From $|u^+(t_k,p_\sigma^k)-u^{-l}(t_k,p_\sigma^k)|\le C\,h^2$, we deduce by similar arguments as in the proof of Lemma 67 that $|\mathcal{R}_5\left(S^{l,k}|L^{l,k}\right)|\le C\,hm_\sigma^k$. Furthermore, the antisymmetry relations $\mathcal{R}_5\left(S^{l,k}|L^{l,k}\right)=-\mathcal{R}_5\left(L^{l,k}|S^{l,k}\right)$ and $\mathcal{F}\left(S^{l,k}|L^{l,k}\right)=-\mathcal{F}\left(L^{l,k}|S^{l,k}\right)$ hold. After multiplication with the nodal error E_S^{k+1} and summation over all cells S we obtain

$$\begin{aligned}
Z&=\tau\sum_S\sum_{\substack{\sigma^k\subset\partial S^k\\ \sigma^k=S^k\cap L^k}}\left(\mathcal{R}_5\left(S^{l,k}|L^{l,k}\right)+\tau\mathcal{F}\left(S^{l,k}|L^{l,k}\right)E_\sigma^{k,+}\right)E_S^{k+1}\\
&=\tau\sum_{\sigma^k=S^k\cap L^k}\left[\mathcal{R}_5\left(S^{l,k}|L^{l,k}\right)+\mathcal{F}\left(S^{l,k}|L^{l,k}\right)E_\sigma^{k,+}\right](E_S^{k+1}-E_L^{k+1})\\
&=\tau\sum_{p_i^k\in\Gamma_h^k}\left(\overline{\mathcal{R}}_{5,p_i}^k\right)^\top(\overline{E}_{p_i}^{k+1}-E_{p_i}^{k+1}\mathbf{1}_{p_i})+\left(\overline{\mathcal{R}}_{6,p_i}^k\right)^\top(\overline{E}_{p_i}^{k+1}-E_{p_i}^{k+1}\mathbf{1}_{p_i}),
\end{aligned}$$

where $\overline{\mathcal{R}}_{5,p_i}^k$ and $\overline{\mathcal{R}}_{6,p_i}^k$ are vectors with entries

$$\left(\overline{\mathcal{R}}_{5,p_i}^k\right)_j:=(m_{p_i,j-1/2}^k/\overline{m}_{p_i,j-1/2}^k)\left(\mathcal{R}_5\left(S_{p_i,j}^{l,k}|S_{p_i,j-1}^{l,k}\right)+\mathcal{R}_5\left(S_{p_i,j}^{l,k}|S_{p_i,j+1}^{l,k}\right)\right)$$

and $\left(\overline{\mathcal{R}}_{6,p_i}^k\right)_j:=(m_{p_i,j-1/2}^k/\overline{m}_{p_i,j-1/2}^k)\left(\overline{\mathcal{F}}\left(S_{p_i,j}^{l,k}|S_{p_i,j-1}^{l,k}\right)E_{\sigma_{p_i,j-1/2}}^{k,+}+\overline{\mathcal{F}}\left(S_{p_i,j}^{l,k}|S_{p_i,j+1}^{l,k}\right)E_{\sigma_{p_i,j+1/2}}^{k,+}\right)$

respectively; $\overline{m}_{p_i,j-1/2}^k$ being the length of the entire edge σ containing $\sigma_{p_i,j-1/2}^k$ and $E_{\sigma_{p_i,j+1/2}}^{k,+}:=E_\sigma^{k,+}$. Using similar arguments as in the proof of Theorem 61 and the

definition of upwind values on edges, one deduces that

$$
\begin{aligned}
Z \leq \tau \Big[\sum_{p_i^k \in \Gamma_h^k} \big(\overline{\mathcal{R}}^k_{5,p_i}\big)^\top \big(A^{k+1}_{p_i} + (\mathbf{1}_{p_i} \otimes \mathbf{1}_{p_i})/n_{p_i}\big)^{-1} \overline{\mathcal{R}}^k_{5,p_i} \Big]^{1/2} \cdot \\
\cdot \Big[\sum_{p_i^k \in \Gamma_h^k} \big(\overline{E}^{k+1}_{p_i}\big)^\top A^{k+1}_{p_i} \overline{E}^{k+1}_{p_i} \Big]^{1/2} \\
+ \tau \Big[\sum_{p_i^k \in \Gamma_h^k} \big(\overline{\mathcal{R}}^k_{6,p_i}\big)^\top \big(A^{k+1}_{p_i} + (\mathbf{1}_{p_i} \otimes \mathbf{1}_{p_i})/n_{p_i}\big)^{-1} \overline{\mathcal{R}}^k_{6,p_i} \Big]^{1/2} \cdot \\
\cdot \Big[\sum_{p_i^k \in \Gamma_h^k} \big(\overline{E}^{k+1}_{p_i}\big)^\top A^{k+1}_{p_i} \overline{E}^{k+1}_{p_i} \Big]^{1/2} \\
\leq C\,\tau \bigg(h\,\mathcal{H}^{n-1}(\Gamma_h^k)^{\frac{1}{2}} + \Big(\sum_{p_i \in \Gamma_h^k} \big(\overline{\mathcal{R}}^k_{6,p_i}\big)^\top \overline{\mathcal{R}}^k_{6,p_i} \Big)^{\frac{1}{2}} \bigg) \|E^{k+1}\|_{1,\Gamma_h^{k+1}} \\
\leq \frac{\tau}{4} \|E^{k+1}\|^2_{1,\Gamma_h^{k+1}} + C\,\tau\,h^2 + C\,\tau\,\|E^k\|^2_{\mathbb{L}^2(\Gamma_h^k)}\,.
\end{aligned}
$$

Again, taking into account these error terms due to the added advection in the original error estimate (36) solely the constant in front of the term $\|E^{k+1}\|^2_{1,\Gamma_h^{k+1}}$ on the left hand side of (36) is slightly reduced. Thus, both the explicit discretization of a nonlinear reaction term and the upwind discretization of the additional tangential advection still allow us to establish the error estimate postulated in Theorem 61.

8 Numerical results

In this paragraph, we present several simulation results. To begin with, we consider the time evolving parametric surface $\Gamma(t)$ described by the evolution of the material point $M(t,x,y) = (x,y,h(t,x,y))^\top$, where $(x,y) \in [-0.6, 0.6] \times [-0.5, 0.5]$, $h(t,x,y) = x^2 f_1(t) + y^3 f_2(t)$ with $f_1(t) = \sin(\pi t/t_{max})^2 \sin(2\pi t/t_{max})$ and $f_2(t) = \sin(\pi t/t_{max})^2 \cos(2\pi t/t_{max})$; t_{max} being the maximum time. We define on $\Gamma(t)$ the surface tangential matrix

$$
\begin{aligned}
\mathcal{D}_0(t,x,y) := \frac{1 + 4x^2 f_1(t)^2 + 9y^4 f_2(t)^2}{1 + 4 f_1(t)^2 + 9 f_2(t)^2} \cdot \\
\cdot \Big[e_1(t,x,y), e_2(t,x,y) \Big] \begin{pmatrix} 5 & 0 \\ 0 & 1 \end{pmatrix} \Big[\mu_1(t,x,y), \mu_2(t,x,y) \Big]^\top
\end{aligned}
$$

and the tangential vector $w(t,x,y) := 10\, e_1(t,x,y)$, where
$e_1(t,x,y) := (1, 0, 2x f_1(t))^\top$, $e_2(t,x,y) := (0, 1, 3y^2 f_2(t))^\top$ are tangential vectors of $\Gamma(t)$ and $\mu_1(t)$, $\mu_2(t)$ their corresponding contravariant counterparts defined through the four equations $e_1(t,x,y) \cdot \mu_1(t,x,y) = 1$, $e_1(t,x,y) \cdot \mu_2(t,x,y) = 0$, $e_2(t,x,y) \cdot \mu_1(t,x,y) = 0$ and $e_2(t,x,y) \cdot \mu_2(t,x,y) = 1$. We approximate on successive refined polygonal meshes (cf. Figure 12), the solution $u := h(t,x,y) + 0.5$ of Problem 37 for $\mathcal{D} := (\mathcal{D}_0 + \mathcal{D}_0^\top)/2$, w defined above and g computed from the data. The Dirichlet boundary condition is considered. On Figure 12 we present the successively refined

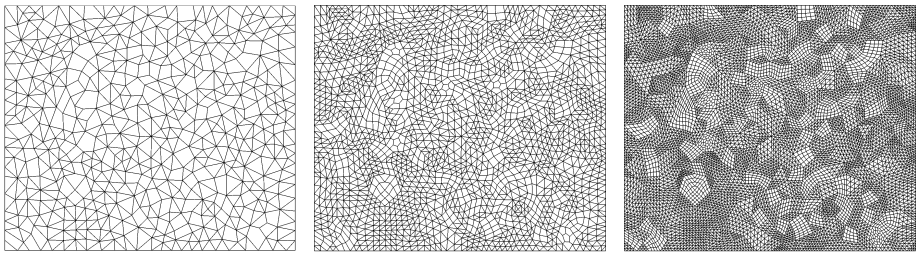

820 polygons, 508 points. 3292 polygons, 1959 points. 13240 polygons, 7765 points.

Fig. 12 Successively refined polygonal mesh used for the convergence test. At each refined step, sizes of cells are divided into 2.

polygonal surfaces used for this simulation test case. At each refined step, edges of the previous step have been divided into two. The computation is done for $t \in [0,1]$ and we present in Figure 13 a sequence of frames from the simulation result. Here, as in the sequel, color shading range from blue to red representing minimum to maximum values. Finally, in Table 1, we display the errors in the discrete $\mathbb{L}^\infty(\mathbb{L}^2)$ norm and discrete energy seminorm (18), respectively. Indeed, the observed error decay is consistent with the convergence result in Theorem 61.

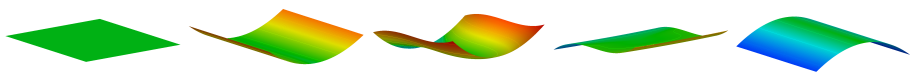

Fig. 13 Solution of the first simulation at different time steps.

$\min_{t\in[0,1]} h(t)$	$\max_{t\in[0,1]} h(t)$	norm of the error $\mathbb{L}^\infty(\mathbb{L}^2)$	norm of the error $\mathbb{L}^\infty(\mathbb{H}^1)$
0.0294	0.1168	$91.617 \cdot 10^{-5}$	$14.8 \cdot 10^{-3}$
0.0119	0.0595	$21.269 \cdot 10^{-5}$	$5.3 \cdot 10^{-3}$
0.0041	0.0302	$5.768 \cdot 10^{-5}$	$2.0 \cdot 10^{-3}$

Table 1 The table displays the numerical error on grids presented in Figure 12 in two different norms, when compared to the explicit solution. The time discretization was chosen as $\tau = 1/30000$ in all three computations.

Next, we compute a second example using the same successive initial surfaces and compare the result to the result of the refined surface. We consider the evolution of the surface material point described by $M(t,x,y) = (x,y,h(t,x,y))^\top$, where $h(t,x,y) = (f(t)/4.5)\sum_{i=1}^{12}\beta(i)\exp(-\alpha(i))$ with $f(t) = (\sin(\pi t - \pi/2)+1)/2$ and $\alpha(i) := [(x-P(i,1))^2/(2\,V(i,1)^2)] + [(y-P(i,2))^2/(2\,V($
The variables P, V and β are defined by

$$P = \begin{pmatrix} 3 & 22 & 4 & 8 & 12 & 18 & 21 & 0 & 8 & 14 & 10 & 8 \\ 3 & 6 & 16 & 16 & 16 & 12 & 21 & 24 & 24 & 5 & 8 & 2 \end{pmatrix}^\top /24,$$

$$V = \begin{pmatrix} 3 & 2 & 2 & 4 & 4 & 2 & 3 & 2 & 3 & 1.5 & 2 & 2 \\ 3 & 4 & 4 & 2 & 4 & 2 & 3 & 2 & 3 & 1.5 & 1.5 & 2 \end{pmatrix}^\top /24 \text{ and}$$

$$\beta = (3.5\ 4\ 4\ 2\ 6\ 5\ 3\ 1.75\ 4\ -2.5\ -3\ -2)^\top /6.$$

For $t = 1$, $f(t) = 1$ and we recover the surface presented on Figure 2; therefore the evolution considered here is obtained by continuously scaling the height of the given surface by $f(t)$ as time evolves. We also consider the advection vector w, tangential component of $w_0 = -50\,(0,0,1)^\top$ and the source term $g(t) = (1 - f(t))(1.5\exp(-\alpha_1) + \exp(-\alpha_2) + \exp(-\alpha_3))$, where

$$\begin{aligned} \alpha_1 &:= \|M(t,x,y) - (3/6, 4/6, 0)^\top\|^2/(0.035^2), \\ \alpha_2 &:= \|M(t,x,y) - (18/24, 12/24, 0)^\top\|^2/(0.035^2) \text{ and} \\ \alpha_3 &:= \|M(t,x,y) - (1/6, 4/6, 0)^\top\|^2/(0.035^2). \end{aligned}$$

The function $g(t)$ defines three localized sources (cf. Figure 14) whose density reduces as time evolves and vanishes at the end of the process. We depict on Figure 14 a sequence frame from the simulation result of problem 37 with homogeneous Dirichlet boundary condition in the time intervale $[0, 1]$; isolines are also drawn. We can clearly notice the dominance of the diffusion at the beginning of the process and progressively the dominance of the advection.

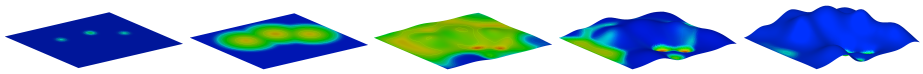

Fig. 14 The evolution of a density under diffusion and advection by gravity is investigated.

The results have been compared to the solution obtained on the refined mesh in $\mathbb{L}^\infty(\mathbb{L}^2)$ norm and discrete energy seminorm (18), respectively. The result is reported in Table 2. Comparing these results to the simulation results of [1], we notice the improvement

		norm of the error	
$\min_{t\in[0,1]} h(t)$	$\max_{t\in[0,1]} h(t)$	$\mathrm{L}^\infty(\mathbb{L}^2)$	$\mathbb{L}^\infty(\mathbb{H}^1)$
0.0294	0.1382	$4.85 \cdot 10^{-4}$	$5.4 \cdot 10^{-3}$
0.0119	0.0722	$1.28 \cdot 10^{-4}$	$1.9 \cdot 10^{-3}$

Table 2 The table displays the numerical error of the solution on the first two grids of Figure 12 in two different norms, when compared to the solution of the last grid (refined grid). The time discretization was chosen as $\tau = 1/60000$ in all three computations.

in the spatial convergence which is $\mathcal{O}(h^2)$ for the $\mathbb{L}^\infty(\mathbb{L}^2)$ norm. This is due to the use of barycenter of cells as presented in Section 4.5 and the slope limiting procedure introduced in Section 7.

As third example, we consider the fixed triangulated geometry of an elephant as presented in Figure 15 and solve Problem 1 in the time interval $[0,1]$, with the diffusion tensor $\mathcal{D}$ being the tangential component of the tensor $\mathcal{D}_0 := \begin{pmatrix} 25 & 0 & 0 \\ 0 & 0.1 & 0 \\ 0 & 0 & 0.001 \end{pmatrix}$; the $X-$direction points to the right and the $Z-$direction points up. Five sources are put in the $(Y,Z)-$plane around the front legs as can be noticed on the second picture of Figure 15 (two at the elephant front side, two at the elephant back side and one at symmetric upper point). We present on Figure 15 a sequence of frames from this simulation. One effectively observes a rapid diffusion in the $X-$direction and a very slow diffusion in the $Z-$direction.

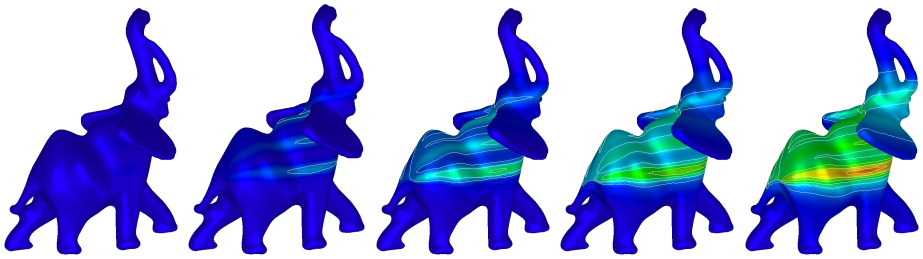

Fig. 15 Strong anisotropic diffusion of a density on a fixed elephant geometry. The polygonal mesh is made up of 83840 triangles and 41916 points.

Now in our fourth example, we consider a diffusion advection problem which involves the curvature tensor. In fact, we consider the advection vector $w = 13\,(\,\mathrm{Id} - 0.0015(\mathcal{K}\,\mathrm{Id} + 4\,K))\,(0,0,1)^\top$, where K the curvature tensor of the considered surface and $\mathcal{K} := \mathrm{tr}\,(K)$ (trace of K) is the mean curvature. We also consider a source term g made up of three localized sources as depicted on the first pictures of Figure 16 and Figure 17. The intensity of the source is a decreasing function in time $t \in [0,1]$ which vanishes at the end of the process. First we consider an evolution by mean curvature flow $\partial M(t,s_1,s_2)/\partial t = (\mathcal{K}/30)\nu(t,s_1,s_2)$, where $M(t,s_1,s_2)$ is the material point of the surface, $\nu(t,s_1,s_2)$ the normal at $M(t,s_1,s_2)$ and s_1, s_2 some parameters used to locally parameterize the surface. Here, we use an adaptive time step $\tau^{k+1} = \min(1/(\mathcal{K}_2^k + 10^{-8}), 13l^2)/10.2$, where $\mathcal{K}_2^k := \mathrm{tr}\,((K^k)^2)$ is the trace of the squared curvature tensor (K^2) at the time step t_k and l the smallest length of the polygons sides. Noticing that $(\nabla_\Gamma z) = (0,0,1)^\top$ (z being the third spatial coordinate), we evaluate $\mathcal{K}$ and K at cell centers using a weighted least square fitting and then use the procedure described in Section 4.2 to compute the flux of the advection vector on subedges while the flux on entire edges is obtained by summing the flux on subedges as for the diffusion operator. There is no need to compute conormal vectors anymore and our slope limiting procedure is applied using these fluxes. Since the evaluation of the curvature can only be consistent if one has a $(3,h)$-approximation of the surface, we solve the mean curvature flow equation for nodal points using a semi-implicit scheme. Figure 16 presents a sequence of frames from this simulation. Due to the advection process which is dominant where the tangential component of $(0,0,1)^\top$ is pronounced, the density would try to concentrate where the $Z-$coordinate of the material points presents a local maximum; but due

to the smoothening process,the local maxima of the $Z-$coordinate tends to disappear and the density moves and concentrates at the point of heighest $Z-$coordinate.

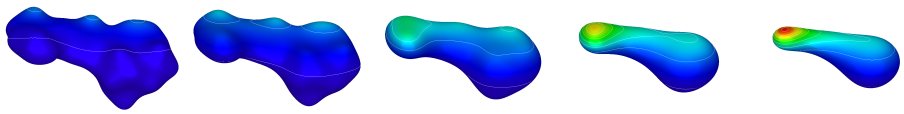

Fig. 16 Evolution of a density under diffusion and advection on a surface moving by mean curvature. The initial polygonal surface is made up of 26848 triangles and 13426 points.

Next the same simulation is done on the fixed initial surface. We effectively notice the concentation of density at points of local maximum on the $Z-$coordinate due to the advection process. Figure 17 presents a sequence of the result of this simulation.

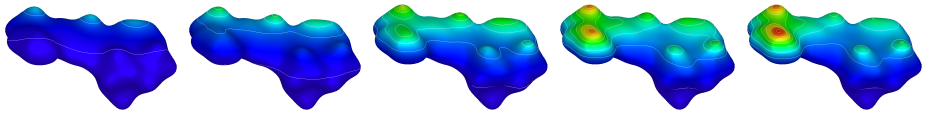

Fig. 17 Evolution of a density under diffusion and advection on a fixed surface.

Examples of practical use of reaction diffusion equations include texture generation [33; 34] and biological pattern formation [35; 36; 37]. In these fields, one uses a system of coupled reaction-diffusion equations introduced by A. Turing in 1952 [37] to explain the formation of patterns on animals. He assumed the existence of two kinds of morphogenes diffusing on a surface and interacting with each other and showed that the presence of diffusion could drive a system instability leading to the formation of spatial patterns by the morphogenes distribution. Here we consider the Turing system

$$\begin{aligned}\frac{\partial u}{\partial t} &= c\delta\Delta_\Gamma u + \alpha u(1 - r_1 v^2) + v(1 - r_2 u)\\ \frac{\partial v}{\partial t} &= \delta\Delta_\Gamma v + \beta v(1 + \frac{\alpha r_1}{\beta} uv) + u(\gamma + r_2 v)\end{aligned}$$

presented by R. A. Barrio et al. in [35] and describing the interaction between two morphogenes u and v. The coefficient c is the ratio of diffusion coefficients, δ is a parameter that can be viewed either as a relative strength of the diffusion compared to the interaction terms or the measure of length scale and α, β, γ, r_1, r_2 are some coefficients. We refer to [35] for how these coefficients are chosen to generate particular patterns. We should nevertheless mention that cubic interaction favors stripes and quadratic interaction produces spot patterns. We simulate this system on the closed triangulated surface using the coefficients provided in [17] for the simulation on a sphere. As in this reference, we chose as initial condition for u and v random values between $-1/2$ and $1/2$. Figure 18 and Figure 19 show some sequence of the simulation result of the solution u which leads to the striped pattern and the spotted pattern respectively.

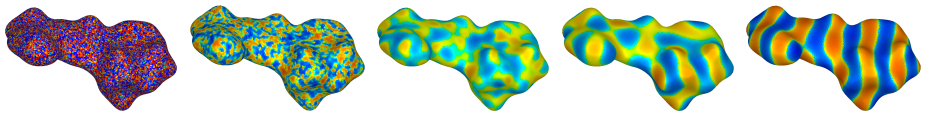

Fig. 18 Striped pattern formation from the Turing system.
$\delta = 0.0021$, $c = 0.516$, $r_1 = 3.5$, $r_2 = 0$, $\alpha = 0.899$, $\beta = -0.91$, $\gamma = -\alpha$.

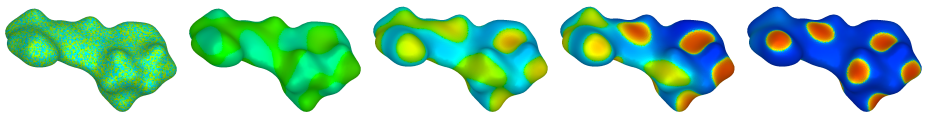

Fig. 19 Dotted pattern formation from the Turing system.
$\delta = 0.0045$, $c = 0.516$, $r_1 = 0.02$, $r_1 = 0.2$, $\alpha = 0.899$, $\beta = -0.91$, $\gamma = -\alpha$.

Acknowledgements This work has been developed at the university of Bonn and at the university of Eindhoven. We would therefore like to thank the institute of numerical simulation of the university of Bonn and particularly Prof. Dr. Martin Rumpf for it precious advises and supports. Many thanks go also to the CASA group of the mathematics department of the Eindhoven university of technology which has partly financed the work.

References

1. M. Lenz, S.F. Nemadjieu, M. Rumpf, SIAM J. Numer. Anal. **49**(1), 15 (2011)
2. R. Eymard, J.M. Hérard, *Finite Volume for Complex Application V: Problems & Perspectives:* (Wiley, 2008)
3. J. Fořt, J. Fürst, J. Halama, R. Herbin, F. Hubert, *Finite Volumes for Complex Applications VI: Problems & Perspectives* (Springer Proceedings in Mathematics, 2011)
4. R. Eymard, T. Gallouët, R. Herbin, in *Special Volume Foundation of Computational Mathematics, Handb. of numer. anal. VII* (P. G. Ciarlet, ed., North-Holland, Amsterdam, 2000), pp. 713–1020
5. K. Domelevo, P. Omnes, ESAIM, Math. Model. Numer. Anal. **39**(6), 1203 (2005)
6. F. Hermeline, J. Comput. Phys. **160**(2), 481 (2000)
7. A.J. Kinfack, A. Njifenjou, IJFV **5**(1) (2008)
8. I.M. Nguena, A. Njifenjou, IJFV **3**(2) (2006)
9. I. Aavatsmark, 9th International Forum on Reservoir Simulation, Abu Dhabi, 9–13 December pp. 1–44 (2007)
10. C. Le Potier, C.R. Acad. Sci. Paris Ser. I 340 pp. 921–926 (2005)
11. K. Lipnikov, M. Shashkov, I. Yotov, Numer. Math. **112**(1), 115 (2009)
12. R. Eymard, T. Gallouët, R. Herbin, IMA J. Numer. Anal. **30**(4), 1009 (2010)
13. M. Afif, B. Amaziane, in *Finite Volume for Complex Application V: Problems & Perspectives* (eds. R. Eymard and J. M. Hérard, 2008), pp. 693–704
14. C. Ollivier-Gooch, M.V. Altena, J. Comput. Phys. **181**(2), 729 (2002)
15. Q. Du, L. Ju, L. Tian, IMA J. Numer. Anal. **29**(2), 376 (2009)
16. L. Ju, Q. Du, J. Math. Anal. Appl. **352**, 645 (2009)
17. D.A. Calhoun, C. Helzel, R.J. LeVeque, SIAM Rev. **50**, 723 (2008)
18. G. Dziuk, C.M. Elliott, IMA J. Numer. Anal. **27**(2), 262 (2007)
19. L. Eldén, Numer. Math. **22**(4), 487 (1982)
20. S.L. Campbell, Linear Algebra and its Applications pp. 53–57 (1977)
21. G. Corach, A. Maestripieri, Numerical Functional Analysis and Optimization **26**, 659 (2005)
22. T. Damm, H.K. Wimmer, J. Aust. Math. Soc. **86**, 33 (2009)
23. L. Eldén, SIAM J. Numer. Anal. **17**(3), 338 (1980)
24. J.J. Koliha, Math. Scand. **88**, 154 (2001)
25. V. Rakocevic, MATEMATIQKI VESNIK **49**, 163 (1997)

26. Y. Takane, Y. Tian, H. Yanai, Ann. Inst. Stat. Math. **59**(4), 807 (2007)
27. M. Rao, J. Sokolowskit, Math. Meth. Appl. Sci. **14**, 281 (1991)
28. G. Still, University of Twente pp. 1–19 (2006)
29. T. Barth, M. Ohlberger, *Finite volume methods: Foundation and analysis* (In E. Stein, R. de Borst, and T.J.R. Hughes, ed., Enc. Comput. Mech. John Wiley & Sons, 2004)
30. E. Goncalvès, *Resolution numérique des équatons d'Euler monodimensionnelles* (Lecture notes, Institut National Polytechnique de Grenoble, 2004)
31. B. Perthame, *Equations de transport non linéaires et systèmes hyperboliques: Théorie et méthodes numériques* (Lecture notes, 2003-2004)
32. B. Engquist, S. Osher, Math. Comp. **31**, 321 (1981)
33. G. Turk, ACM SIGGRAPH Comput. Graphics **25**(4), 289 (1991)
34. A. Witkin, M. Kass, in *Computer Graphics* (1991), pp. 299–308
35. R.A. Barrio, C. rea, J.L. Aragón, P.K. Maini, Bull. Math. Biol. **61**(3), 483 (1999)
36. R.T. Liu, S.S. Liaw, M.P. K., Phys. Rev. E 74, 011914 pp. 011,914(1)–011,914(8) (2006)
37. A.M. Turing, Philosophical Transactions of the Royal Society of London. B 327 pp. 37–72 (1952)

PREVIOUS PUBLICATIONS IN THIS SERIES:

Number	Author(s)	Title	Month
14-17	S.W. Rienstra D.K. Singh	Hard wall – soft wall – vorticity scattering in shear slow	May '14
14-18	D.K. Singh S.W. Rienstra	Nonlinear asymptotic impedance model for a Helmholtz resonator liner	May '14
14-19	O. Krehel A. Muntean	Error control for the FEM approximation of an upscaled thermo-diffusion system with Smoluchowski interactions	June '14
14-20	J.H.M. Evers R.C. Fetecau L. Ryzhik	Anisotropic interactions in a first-order aggregation model: a proof of concept	June '14
14-21	S.F. Nemadjieu	A stable and convergent O-method for general moving hypersurfaces	July '14

Ontwerp: de Tantes,
Tobias Baanders, CWI